SEISMIC BASE ISOLATOR FOR ADOBE DWELLINGS IN CHILE

A THESIS

SUBMITTED TO

THE FACULTY OF

UNIVERSITY OF MINNESOTA

BY

SEBASTIAN MERY

IN PARTIAL FULFILLMENT OF THE REQUIREMENTS

FOR THE DEGREE OF

MASTER OF SCIENCE

BLAINE BROWNELL

June 2013

COPYRIGHT

ACKNOWLEDGEMENTS

I would like to express my deepest appreciation to my thesis adviser Blaine Brownell. It was a great pleasure for me to work with him and receive his guidance throughout this research. The motivation for developing this study was highly strengthened by the course he taught on preliminary formation of material studies.

I would also like to thank to Arturo Schultz for his support, encouragement, criticism, and insight throughout the research, determining the baseline design of this project from the engineering view. The support of the specialist in Conservation and Restoration of Built Heritage, Mr. Benjamin Ibarra, is also kindly acknowledged here.

I would like to thank to Estudios Estructurales and my project friends the graduate in engineering Rodrigo Bravo, for their precious assistance and help throughout seismic analytical studies. I am also grateful to the Chilean Historian, Mr José Bengoa and the graduate in architecture, Ms Bianca Cabellos for their help through the content of the adobe history in Chile. Also, I could not have been able to accomplish this research without support of my friend Natalia Serna, Dane McLain, and Elliot Surber.

Finally, I would like to thank my mother, Cecilia, her partner Alejandro, and my dear brother Nicolas, who encouraged me through my Master of Science Program.

DEDICATION

To all those who believe the adobe architecture will continue providing significant value in approaching affordable design with low environmental impact to those territories where it is used.

ABSTRACT

SEISMIC BASE ISOLATOR FOR ADOBE DWELLINGS IN CHILE

Sebastian Mery

MS Sustainable Design

School of Architecture

University of Minnesota

Adviser: Blaine Brownell

May 2013

This thesis explores the effects of employing an affordable seismic base isolator (SBI) in adobe dwellings in Chile. The SBI is formed by two components located between the footing and the foundation wall of the adobe housing unit, acting together during the seismic event. These components are (1) the frictional interface layer, which diffuses horizontal forces by employing 6 to 8 mm pebbles and (2) the re-centering piece, which limits lateral displacements and relocates the adobe structure in the center of gravity by employing scrap tire lock-donuts. The SBI was seismically analyzed in a 650 ft^2 one story adobe dwelling with 18″ wall thickness.

The seismic analysis uses the package SAP 2000 and the static analysis method required by Chilean seismic design code. Results show that the SBI case C1 reduces seismic forces in about 17.5%. The differences between the maximum seismic stresses and the admissible wall stresses is 5 [lb/in2] shorter than by using polymer mesh, diminishing damaged areas generated in the wall in about 11.4%, which is 2% less of affected area if the adobe dwellings is protected with polymer mesh. This system also augments the total cost in 2%, which is almost half of employing polymer mesh.

Keywords: Earthquake, seismic base isolator, adobe, earth block.

AISLADOR SISMICO DE BASE PARA VIVENDAS DE ADOBE EN CHILE

Sebastian Mery

MS Sustainable Design

School of Architecture

University of Minnesota

Tutor: Blaine Brownell

Mayo 2013

Esta tesis explora los effectos de utilizar un aislador sísmico de base (ASB) económico para viviendas de adobe en Chile. El ASB está formado por dos componentes ubicados entre la fudación y el sobre-cimieto de una vivenda de adobe, actuando juntos durante un evento sísmico. Estos componetes son (1) una capa interface que difusa las fuerzas horizontales utilizando piedras de 6 a 8mm y (2) la pieza de recentrado, que limita los dezplazamientos laterales y reubica la superestructura en el centro de gravedad, usando una dona tope de caucho neumático reciclado. El SBI se analizó en una vivendad de adobe de un piso de 60 m2 con muros de 45 cm de espesor.

El análisis sismico empleó el simulador SAP 2000 siguiendo el metodo estatico requerido por el codigo de diseño sísmico Chileno. Resul-tados de este analisis muestran que el ASB caso C1 reduce la fuerza sísmica en 17,5%. La differencia entre la fuerza máxima admisible de corte y la fuerza máxima sismica solicitante es 5 [lb/in^2] menor que la producida en viviendas protegida con geomalla, disminuyendo el area de daños en el muro en 11.4%, lo que es 2% menor que si se ocupa geomalla. También, el SBI aumeta el costo total en 2%, lo que corresponde a la mitad del costo de utilizar geomalla.

Palabras clave: Terremoto, aislador sísmico de base, adobe.

TABLE OF CONTENTS

LIST OF TABLES

Chapter I

Chapter II

Chapter III

LIST OF FIGURES

Chapter I

Chapter II

Chapter III

Chapter IV

LIST OF SYMBOLS

AS: Adobe structure

AD: Anno Domini

A: Area

A_o: Effective ground acceleration peak [m/s2]

b_{kx} and b_{ky}: Largest dimension of the structure

BC: Before Christ

C: Seismic coefficient

CB: Cut earth block

cm²: Square centimeter

dl: Daylight factor

DL: Dead loads

EUI: Energy use intencity

EB: Elastomeric bearing

E: Modulus of elasticity

EEB: Extruded earth block

F2010: Earthquake in Cobquecura on February 27th, 2010

FVDB: Fluid viscous damper bearing

FSV: Fondo solidario de la Vivienda

fc: Foot candle

F: Force

FB: Friction bearing

FDSMB: Friction dry-staked masonry bearing

Ff: Friction force

FLB: Friction layer bearing

FPB: Friction pendulum bearing

Fdf: Friction dynamic force

Fsf: friction static force

FRB: Friction roller bearing

f'_0: Untamate, and admissible compressive stregnh [MPa]

g: Gravitational acceleration

HDRB: High-dumping rubber bearing

H or h: Structure height

Hf: Horizontal force

I: Building importance class. Structural failure risks and use. [no unit]

IES VE: Integrated enviromental solutions software

k: Thermal conductivity

k_s: Story level

km^2: Square kilometer

L: Rubber thickness

LPRB: Lead-plug rubber bearing

LL: Live loads

MLL: Material Liquid limit

m: Mass

MINVU: Ministry of Housings and Urbanism in Chile

MINPLA: Ministry of Planing in Chile

MCEB: Manual compressed earth block

MMEB: Manual molded earth block

MPa: Mega pascal

M_w: Richter magnitude

NRB: Natural rubber bearing

N: Normal force

OGUC: Ordenanza general de urbanismo y construccion

P: Total weight of the superstructure n.

PL: Plastic limit

Pt: Soil type parameter [s]

PRTM: Plan de reconstruction terremoto y maremoto

PCEB: Powered compressed earth block

R: Seismic response reduction factor

R value: Thermal resistance [m^2K/W]

R*: The reduction factor of spectral acceleration factor (security factor) used to estimate mode period with highest traslacional weight ecquivalent on the analysis direction. [without unit]

R_o: The global reduction factor of the structure, given by the Chilean design code

S_a: Design spectrum aceleration [m/sw^2]

SCSB: Self-centering strut bearing

Sf: Seismic force

SAM: Static analysis method

SM: Sebastián Mery

SMAM: Spectral modal analysis method

SBI: Seismic base isolator

SDC: The seismic design code in Chile

SL: Semisolid limit

SL: Solid limit

SMAM: Spectral analysis method

T': Parameters depending on the foundation soil TDC: Thermal de sign code

T_n: n mode period vibration [s]

T_o, p: Parameters depending on the type of foundation soil

T^*: Mode vibration period with the highest translational equiva lent mass in the direction of analysis

USGS: United States Geological Survey

U value: Thermal Transmittance [W/m^2K]

Vf: Vertical force

V_m: Stress strength [MPa]

w: Wall thickness

Z_k: Distance from floor k to the base of the building

δ : Delta of deformation

ε : Epsilon for unitarian streching

σ : Axial object stress

Δ, Δ_s: Horizontal displacement

γ: Shear strain

σ: Compressive stress

Φ: Diameter of circular elastomer isolatior

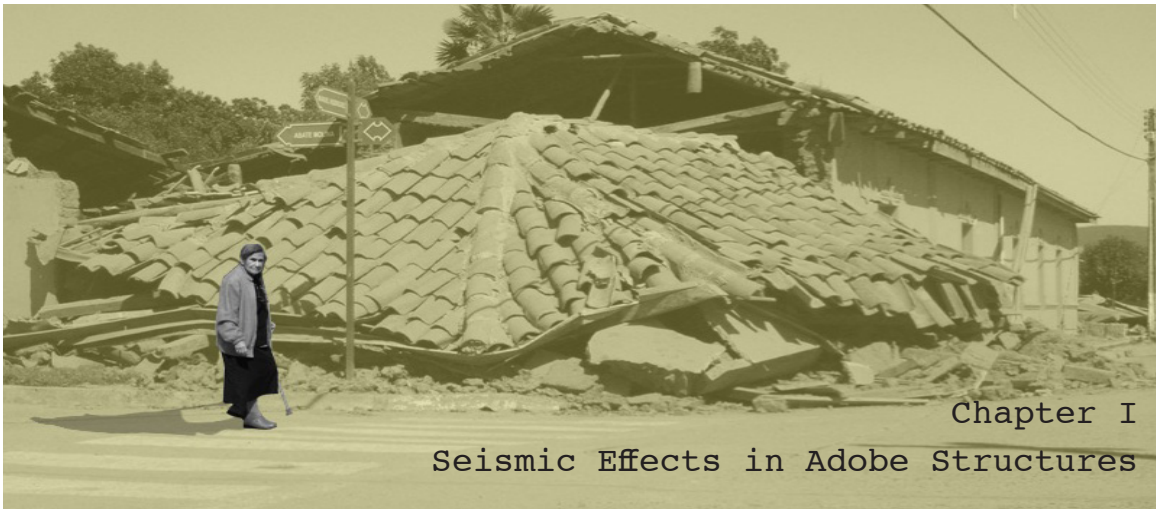

Chapter I
Seismic Effects in Adobe Structures

Image: Adobe dewelling destroyed by earthquke in Chile F2010
Source:http://panoramio.cl

An earthquake is one of the most destructive natural events to occur. In an instant a large-scale seismic quake can transform topography and large cities, causing nations to suffer both economically and socially, losing infrastructure and lives. Evison (1987) mentions that earthquakes are unpredictable and the knowledge about them is still limited since two earthquakes with similar magnitudes do not necessarily have the same characteristics. He adds that an earthquake's impact depends on many factors such as the building soil composition and how close a structure is located to an earthquake's epicenter. Consequently, seismic regulation is not interchangeable between two nations that have earthquake activity. This is one of the main fac-

tors that makes designing earthquake resistant buildings a challenge for architects and structural

1.1 Adobe construction's vulnerability to earthquakes in Chile

Chile is one of the most seismically active areas in the world. According to the United States Geological Survey (USGS), every ten years Chile is afflicted by a destructive seismic upheaval. USGS also mentions that Chile has had two of the largest earthquakes in the world since 1900; the M_w = 9.5 with epicenter in Valdivia on May 22nd, 1960, and the M_w = 8.8 in Cobquecura on February 27th, 2010, as shown in Figure 1.1.1.

The Chilean government report PRTM (2010) "Plan de reconstruction terremoto y maremoto del 27 de February del 2010" reviewed these catastrophic events. In this document the 1960 earthquake is reviewed to compare damage records. This seismic event caused damages in 66,623 ml^2 [166,220 km^2] of the southern territory was affected. This earthquake was responsible for the death of 6,000 inhabitants, it left 2,000,000 homeless, damaged 45,000 dwellings, and

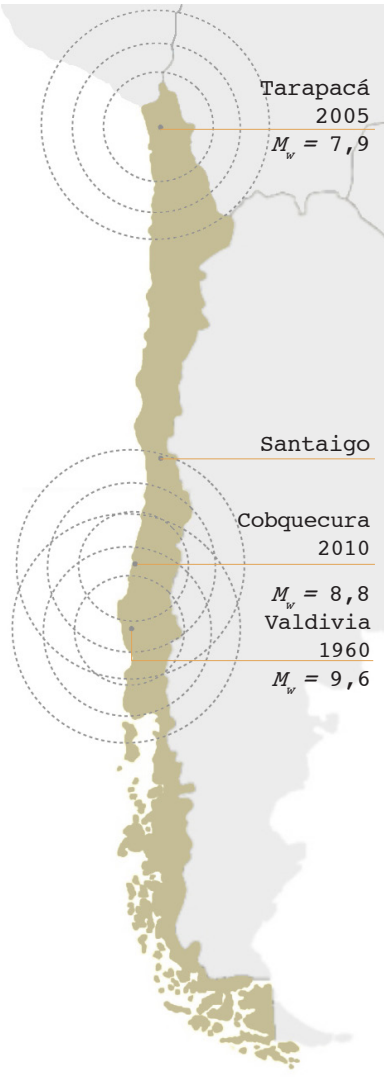

Figure 1.1.1: Three largest earthquakes in Chile since 1900.
Source: SM creation based on OSGS.

caused US$3,089 million in destruction to infrastructure and properties. Regarding the 2010 earthquake, this event not only badly damaged a vast national territory, but it also affected the whole planet, changing the world axis by an astounding 2 inches. This accelerated the planet's rotation and subsequently made our days 0.025 seconds shorter than they were before. The survey of damage illustrates that 50,582 ml^2 [131,006 km^2] of Chile's southern region was affected. This quake caused the death of about 521 inhabitants, it left 2,000,000 homeless, damaged 370,000 dwellings, and caused US$30,000 million in destruction to infrastructure and properties.

Dwelling Tipology	Total destruction	Major damages	Minor damages	Total
Costal	7,931	8,607	15,384	31,922
Urban adobe	26,038	28,153	14,869	69,060
Rural adobe	24,538	19,783	22,052	66,373
SERVIU	5,489	15,015	50,955	71,459
Privated	17,448	37,356	76,433	131,237
total	81,444	108,914	179,693	370,051

dwellings		people
135,433	x	3.4

460,472
Total affected residents

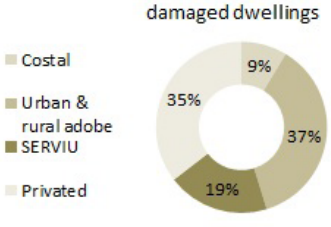

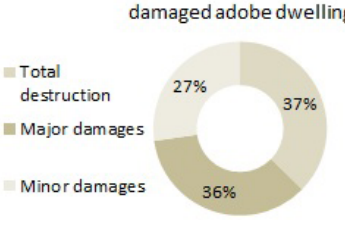

Table 1.1.2: Seismic damages in dwellings in F2010
Source: SM creation based on PRTM (2010) and CASEN survey 2009.

The breakdown of the affected dwellings reveals that out of the 370,000 damaged properties 135,433 were built out of adobe, 460,472 households, which represents almost 40% of the total number of affected housings as demostrated in Table 1.1.2. Out of this amount, 50,536 adobe constructions were completely destroyed, representing more than 50% of the total adobe dwellings. The remaining units suffered medium and lower damages that were able to be repaired. Adobe dwellings were the most affected type of construction, confirming the poor seismic resistance of the material.

Image: Earthquake 2010 destruction in adobe dwelling.
Source: www.solidarity-us.org

Blondet, Villa, Brzev, and Rubiños (2011) extend this matter by saying that earthen architecture have poor seismic resistance because they are heavy structures, have little material ductility or low tensile strength. This content is reviewed in detail in section 1.7 of this investigation.

Unfortunately, De Sensi (2003) notes that earth construction will continually be shaken by seismic

events due to their location within seismically active territories as shown in Figure 1.1.3. Sadly, the most common places where earth architecture is used happens to be in the world's most seismically active regions. Chile is one of the nations that portrays this relation. With regard to the first condition, according to PRTM (2010), 20% of Chile's urban population and 60% of its rural inhabitants live in adobe masonry buildings. On the other hand, the USGS explains that the collisional boundary between the continental South American Plate and the oceanic Nazca Plate coincides with the location of the Chilean territory.

Figure 1.1.3: Earth architecture v/s seismic hazards.
Source: De Sensi (2003).

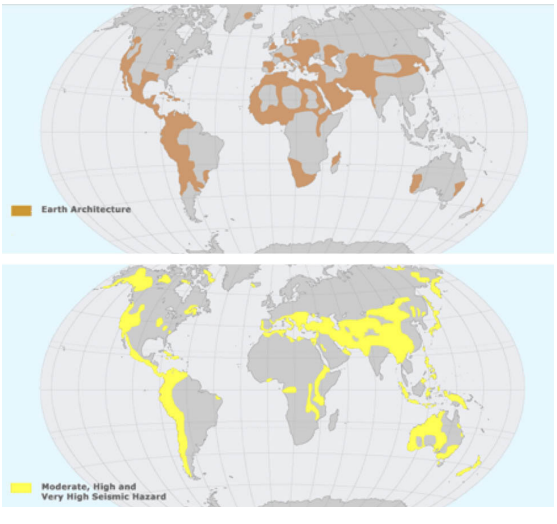

Image: Valdivia earthquake 1960
Source: http://www.cbsnews.com/2300-202_162-10007015-17.html

1.2 Earthquake nature and seismic measuring systems

1.2.1 Earthquake definition.

USGS defines an earthquake as a sudden release of energy from the earth's core in the form of seismic waves. The wave is the motion perceived when an event occurs.

Small seismic events that are not perceived by people are called micro-seismic events. Seismic events that cause moderate to high destruction are most commonly called earthquakes but they are also known as macro-seismic, or mega-seismic events, causing moderate to high destruction. An earthquake's origin is directly related to the dynamic earth composition, being that this is where the wave is propa-

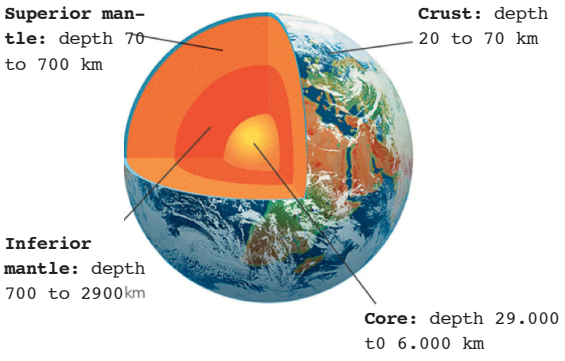

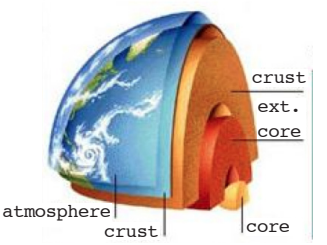

Layer	thickness		Composition
	Miles	Km	
Crust	397	640	Silicea rock
Mantle	1490	2400	Rock
Esterior mantle	1430	2300	Melted iron and nickel
Interior mantle	745	1200	Solid iron and nickel

Figure 1.2.1: Dynamic earth composition.
Source: www.kalipedia.com/Estructura y composición de la tierra

gated. As Figure 1.2.1 shows, three layers form the dynamic earth composition: Core, mantle, and crust. The crust is formed by plates as show in Figure 1.2.2, which are constantly interacting with each other, accumulating energy that is later released by the seismic event.

1.2.2 Seismic types

According to Comte (2012) a seismic event can be produced by three sources:

- Tectonic: This seismic event is caused by the crushing of crust boundaries, as this occurs between the Nazca and South America plates, generating the seismic activity in the Chilean territory, shown in Figure 1.2.2.
- Volcanic: This seismic event occurs before or af-

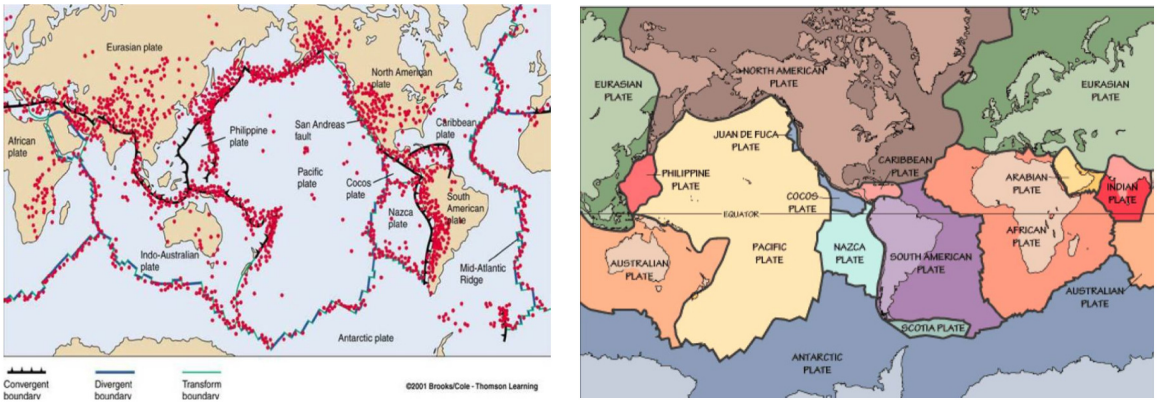

Figure 1.2.2: Seismic plates.
Soruce: www.usgs. gov

ter volcanic activity.

• Collapse: Is generally produced by ground depression or human caused explosions. This seismic event is of a low intensity magnitude.

The author describe that in tectonic seismic events plate boundaries push against each other generating in the region force accumulation (stress), associated deformation (strain), and later energy release (crush). As with any elastic object during seismic events, plates can exceed their elastic limit, adopting permanent deformation and displacement from their original location. This is known as elastic bouncing, which is the result of the released energy.

1.2.3 Interaction between plate boundaries in tec-

tonic seismic events.

This content was fully sourced from Comte (2012).

• Divergent plate boundaries: As Figure 1.2.3.A shows, these boundaries are located between either two adjacent oceanic plates or two continental plates that are moving away from the seismic source. In both cases a rift valley is formed, which has a much thinner crust than the tectonic plates due to the separation between them. The outcome of this separation results in the formation of lakes and oceans.

• Convergent plate boundaries: As Figure 1.2.3.B shows, these are territories in which there is a collision between litopheric plates. The collision can occur between two continental plates, one oceanic and one continental plate, and two oceanic plates. Subduction of the oceanic lithosphere into the mantle occurs in the last two cases.

• Transforming plate boundaries: As Figure 1.2.3.C, shows these are zones that move in parallel but opposite directions, generating energy and accumulating energy.

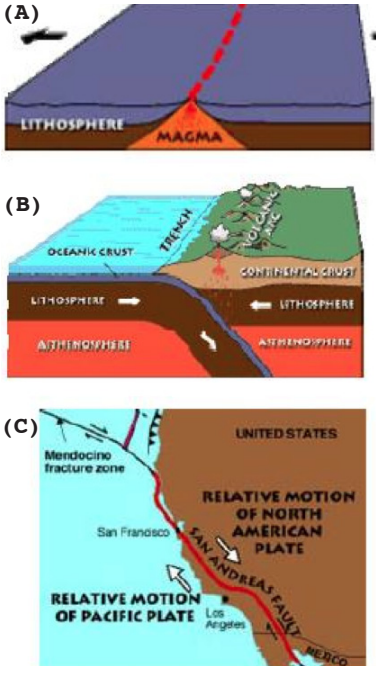

Figure 1.2.3: Interaction between plates.
Source: Comte (2012)

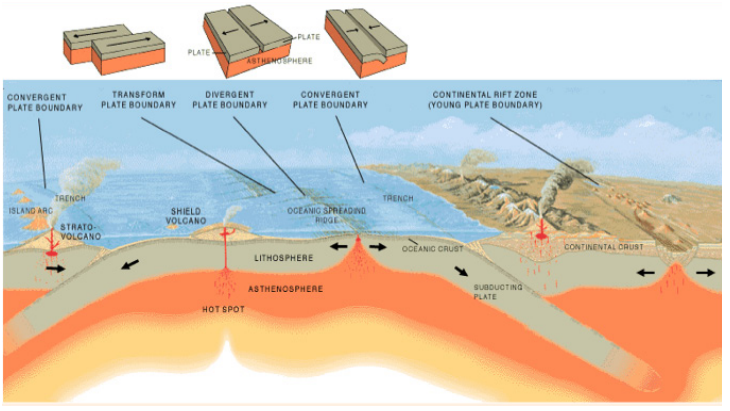

Figure 1.2.4: Failure depth representation.
Source: www.usgs. gov

1.2.4 Classification of tectonic seismic events depend on the distance from the plate failure.

Seismic events are different depending on the depth of the failure as shown in Figure 1.2.4. Comte explains that a superficial and low magnitude quake can produce the same impact as a deep and high magnitude seismic event.

- **Superficials** (6.2 to 13 miles or 10 to 20 km): This is produced by the plane extension and strechning after cold down, friction like this happens between transforming plate boundaries. Superficial seismic events also occur close to mountains and volcanos due to the compression and traction between these surfaces.

- **Intermediates** (19 to 62 miles or 30 to 100 km): Subduction is the cause of this tectonic phenomenon, occurring where the plate is still rigid.

Thus, this is associated to inter plate and their hypocentre allows to determinate the subduction angle.

• **Deepth** (43 to 62 Miles or 70 to 100 km): Change periods in the oceanic rock are mainly associated with this quake type, because at this level the rock is not solid and can be fractured.

1.2.5 Seismic cycle and Seismic waves.

USGS describes that the seismic cycle is the time period between two main seismic events as figure 1.2.5.1 illustrates. A low intensity seismic event occurs before and after the seismic cycle, however, they are perceived slightly. In a seismic cycle, energy is accumulated and released and the relation between the first and second earthquake is exponential. The earthquake that occurred in Chile in 1960 is prime example of this situation. Before the second earthquake occurred, it was thought that the seismic wave cycle had reached its peak on May 21st when M_w = 7.8 earthquake was

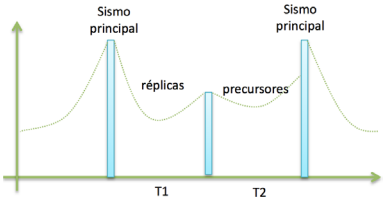

Figure 1.2.5.1: Seismic cylces.
Source: Comte (2012).

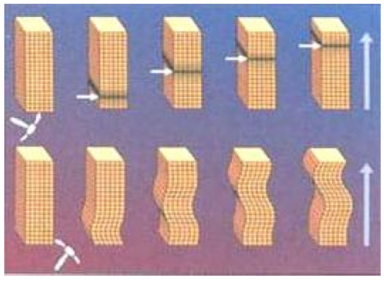

Figure 1.2.5.2: Seismic waves P ans S.
Source: www.usgs. gov

recorded, but the M_w = 9.5 earthquake that occurred the day after far exceeded the former quake, and it happens to be the world's strongest earthquake ever registered.

In regards to seismic waves, two types exist: "P" and "S" waves. P waves are longitudinal whereas S are transversal. In P waves, particles move in the same direction as the wave propagation. In S waves particles move perpendicular to the wave propagation. In addition, P waves are the first to reach the ground surface because their propagation speed is higher than the S waves and are allowed to cross solid and fluid layers as shown in Figure 1.2.5.2.

1.2.6 Land seismic frequency

Comte (2012) sites that waves that are active close to the rock may involve high frequencies and high energy.

A wave's amplitude is amplified and reduced by its

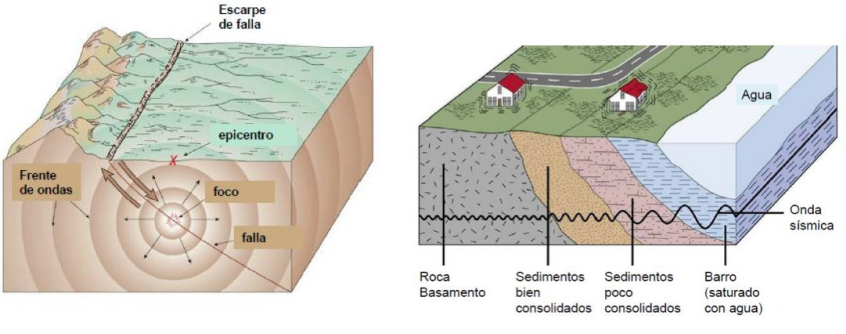

Figure 1.2.6: Type of grounds.
Source: www.usgs.gov

frequency once the over deposits are reached because the energy tends to be conserved, as shown in figure 1.2.6.

Un-consolidated fields can increase the seismic intensity by one degree, whereas phereatic (water contect) levels that are located lower that 32'(10 meters) ground level can increase in seismic intensity by a half degree.

1.2.7 Seismic scale measuring systems

Mokrovic (1982) explains that seismic measurements began in 132 A.D, using the first seismoscope designed by Chang Heng. The author explains that this seismic estimator was able to identify the oscillation of major earthquakes as shown in Figure 1.2.7.1. However, Reitherman (2012) notes that the first earthquake was fully recorded only a few decades ago, which would in turn help in designing buildings with accurate resistance capacity. He also mentions that this occurred due to the development of advanced technologies based on reliable softwares, physical tests using shaking tables, and the precise estimation of site-specific earthquake

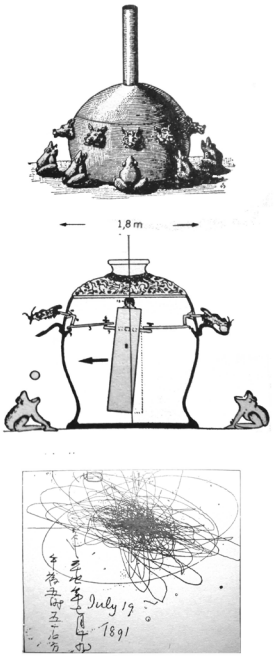

Figure 1.2.7.1: Chang Heng's seismoscopio.
Source: Skoko and Mokrovic (1982)

motion.

According to Comte (2012), two reference magnitude scales are used to measure quakes in Chile; The Mercalli and Richter magnitude scale as Figure 1.2.7.2 shows. Mercalli magnitude scale was developed by the Italian Guiseppe Mercalli to evaluate effects or damage in structures subjected to quakes. This measuring system posseesses twelve degrees. On the other hand, the Richter magnitude scale (M_w) was developed by the US physics Charles Richter to determinate energy released during quake events. This system measures lineal magnitudes between 2.0 to 6.9, from 0 to 240 Miles (0 to 400 Km). Quakes that exceed this magnitud are calculated using logarithmic forms.

Table 1.2.7.2: Mercally v/s Richter magnitude scale. **Source:** Thomson(2005).

Richter Magnitude (M_L)	Mercalli Intensity (Approx.) at Epicenter	Effect on People and Buildings	Max. Acceleration (Approx. % of g)[a]	Maximum Velocity of Back-and-Forth Shaking (cm/sec.)	Time of Shaking[a] Near Source (sec.)	Displacement or Offset	Surface Rupture Length (km)
<2	I–II	Not felt by most people.	0.1–0.2				
~3	III	Felt indoors by some people.	<1.4	<1	0–2		
~4	IV–V	Felt by most people; dishes rattle, some break.	1.4–9	1–8	0–2		
~5	VI–VII[b]	Felt by all; many windows and some masonry cracks or falls.	9–34	8–31	2–5	~1 cm	1
~6	VIII–IX[c]	People frightened; most chimneys fall; major damage to poorly built structures.	34–124	31–116	10–15	60–140? cm	~8
~7	X–XI	People panic; most masonry structures and bridges destroyed.	>124	<116	20–30	~2 m	50–80
~8	XII	Nearly total damage to masonry structures; major damage to bridges, dams; rails bent.	>124	>150	>30	4.1 m	200–400
~9+	>XII	Nearly total destruction; people see ground surface move in waves; objects thrown into air.	>124		>80	13 m	>1,200

Image source: http://tunza.mobi/articles/house-of-bricks/

1.3 Adobe classification and origins

For centuries earth buildings have provided environmental friendly shelter to communities from diverse cultures all over the world located in dry and moderate cold areas. Rael (2009) highlights that earth constructions have accompanied humanity since 8,000 BC as shown in Figure 1.3.1, becoming one of the most widely used building material. Furthermore, the US Earth Architecture blog and studies done by Houben and Guillard (1994) note that currently between 30% to 50% of the world's population lives in earth-based structures.

Material	Period
Mud, stones, wood/thatch	Prior 8000 BC
Sun dried bricks	6000 BC
Pottery products	4000 - 8000 BC
Burnt bricks	4000 BC
Lime	3000 BC
Glass	1300 BC
Iron products	1350 BC
Lime-pozzolana cement	300 BC - 476 AD
Aluminum	1808 AD
Portland cement	1824 AD
Plastic	1862 AD

Table 1.3.1: Earth construction origin period.
Source: Reddy (2004)

Several publications related to earth con-

structions discuss the classification of adobe constructions. For example, the UNESCO Chair Earth Architecture categorizes the earth architecture in types of techniques depending on the fabrication process, whereas other publications like Housben and Guillaud (1994) group earth structures based on the final construction specimen. These techniques are shown in Figure 1.3.2.

The adobe block, also called “mud bricks”, or “sun dried mud bricks”, has a rich heritage in diverse cultures. Adobe materials are been found in ancient civilization ruins on almost every continent, and these are the foundation of many ancient buildings still in occupation. Reddy (2004) notes that adobe

Figure 1.3.2: Classification of earth architecture.
Image source: www.aurovile.com

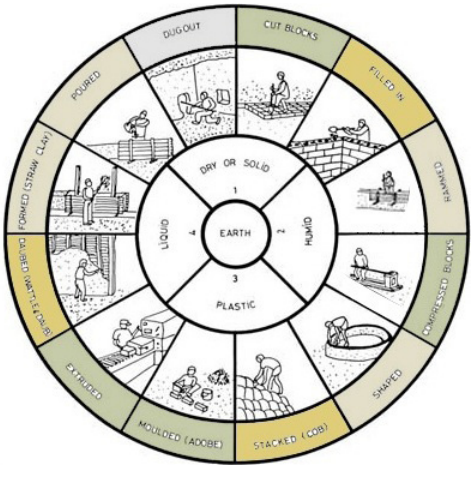

- Monolithic or Massive Earth: Formed (straw and clay), poured, shaped, and rammed earth (pisé)
- Excavaded or dug out of soil: Excavaded foundations, dwellings, and chambers made in volcanic tuff.
- Structural components: Covered, Filled in, daubed (wattle and daud), and staked earth (cob on posts).
- Masonry: Cut blocks and adobe blocks (fabricated by moulding mud and sun dried couring) such as the manual moulded, moulded process, extruded blocks, and compressed blocks.

appeared as the natural industrialization of rammed earth construction (Monolithic or Massive Earth type), playing a significant role in the urban planning of many different societies.

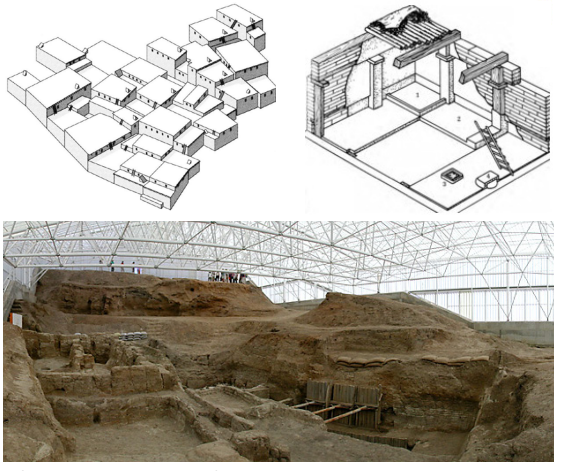

Figure 1.3.3: Diagrams of Çatal Hüyük town (above left), town house (above right), and excavation ruins (below).
Source: www.catalhoyuk.com

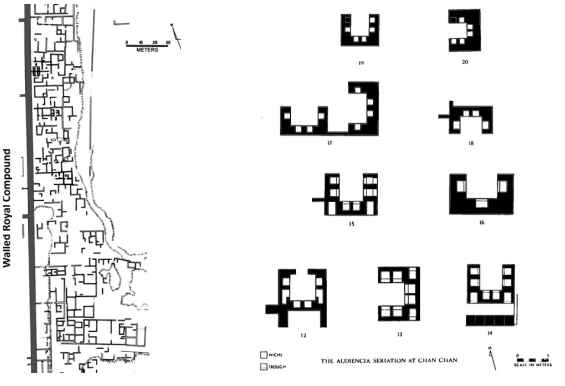

Figure 1.3.4: Plan Chin Chon city (above left), town house (above right), and excavation ruins (below).
Source: www.catalhoyuk.com

Overviewing the ancestral examples of this natural building method, Jerome (2000) notes that 10,000 year-old adobe ruins have been excavated in Jericho and in Çatal Hüyuk, Turkey, dating back from the Neolithic period around 7,000 BC, as shown in Figure 1.3.3. Pumpelly (1908) also reviews the history of this natural construction technique. He highlights adobe ruin excavations in Russian Turkestan, dating from 8,000 BC to 6,000 BC, in the Jordan Valley, and in Mesopotamia, dating back from 8,000 BC. Adobe ruins also have been found in South America. Moseley and Mackey (1974) documents the colossal adobe ruins of

Chan Chan, the capital city of Kingdom of Cimmor, which covered more than 12 miles [20 km] of the central costal and northern areas of Peru between 1000 AD and 1400 A.D, as shown Figure 1.3.4.

Examples of adobe constructions that have been continually inhabited over centuries can be found in dry areas of several different territories. Mehta (2007) in his study about the role of traditional mud bricks in the Hadhramaut Valley, Yemen, and Western Asia, explain that sun dried mud blocks have steadily been used to develop the urban territory of these locations since the seventh century BC. In 1982 all of these areas adopted conservation initiatives by their citizens in which 300 adobe towns were declared heritage sites by UNESCO World Heritage Centre. This episode did not only strengthen their legacy of using adobe, but it also built a solid micro economy based on mud brick production in these countries. Houben and Guillaud (1989) and Minke (2008) have also documented other examples of ancestral adobe architecture in Asia, Africa, and the Middle East, which continue to use

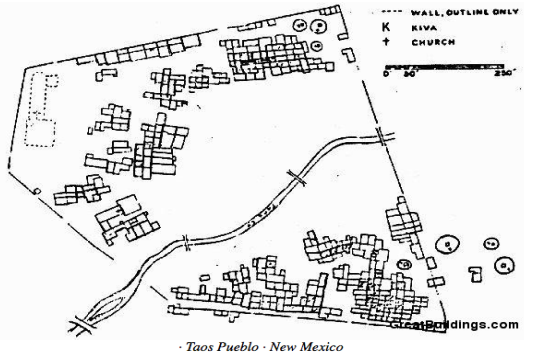

Figure 1.3.5: Taos Pueblo, New Mexico. US ancient adobe town occupied since late 13th century.
Source: www.taospueblo.com

adobe to this days.

Jerome (2000) mentions that the warm dry southern regions of Europe possess an extensive area of centennial adobe settlements with permanent occupation thanks to earth construction technologies migrated from the Middle East with. Thus, the author notes that this architecture type was mainly established in Spain by Moorish, Persian, and Turkish settlers. In America, newer examples of adobe constructions with permanent occupation over generations can be found. The UNESCO World Heritage Centre highlights the multi-storied adobe structure Taos pueblo in New Mexico, located in the drier climate southwestern states of the US, as shown in Figure 1.3.5. As mentioned in the official website of Taos Pueblo, this village, settled by the Grande River, has has been permanently occupied since the late 13th and early 14th century.

Image: Curepto, VII Maule Region.
Source: http://patrimoniochilenoadobe.blogspot.com

1.4 Adobe tradition in Chile

Jorquera (2010) mentions that in Chile earth architecture is massively used in urban and rural areas, between the dry and temperate latitudes, from the north I Region, border with Peru, to south VIII Bio-Bio Region as shown in Figure 1.4.1. The poor humidity resistance of the adobe, reviewed in section 1.7 of this research, limits the extension of this material in regions south of VIII Bio-Bio Region. In these regions rain and cold are predominant, and the wooden culture dominates the building construction.

Regarding adobe architecture, Karmelic (2009) study reveals that 47% of the Chilean heritage buildings are made out of earth material, 41% is adobe and 6%

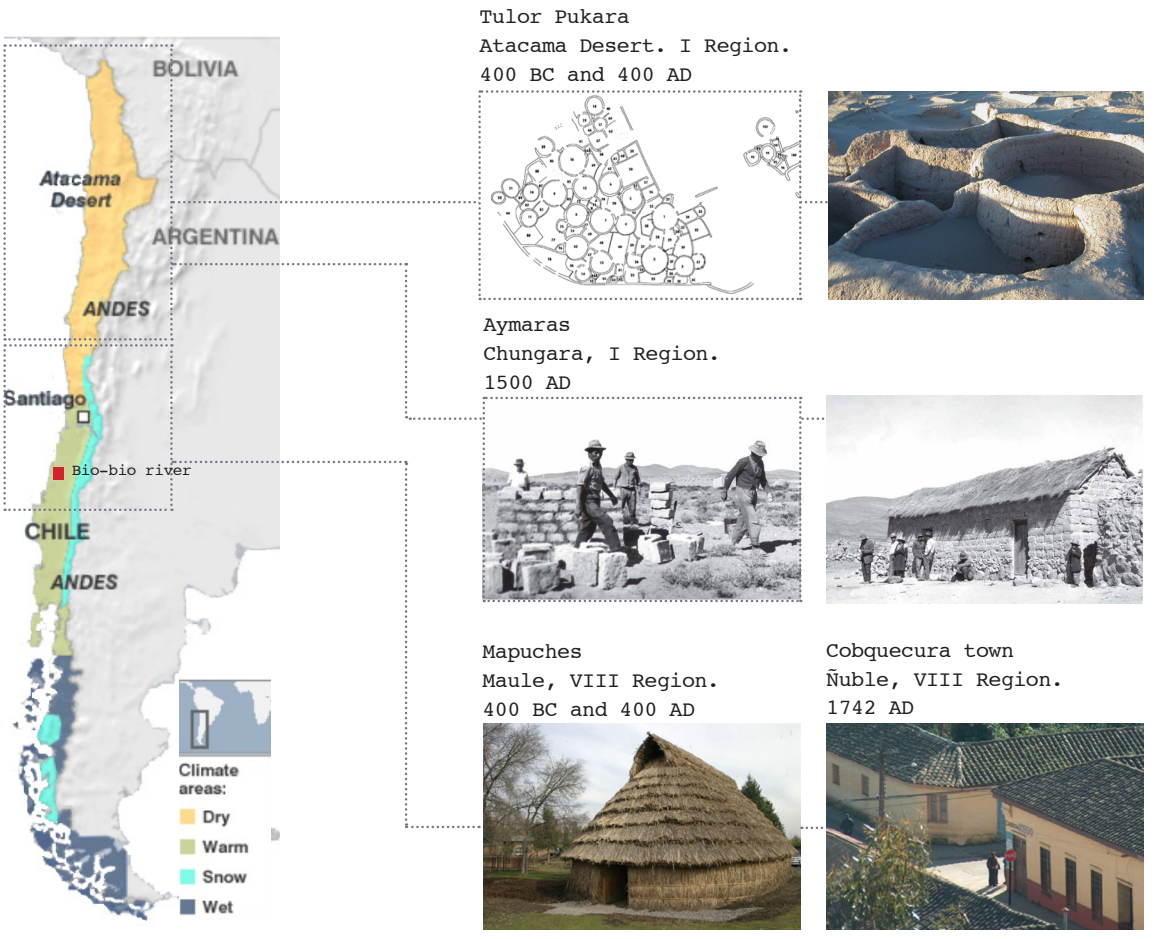

Figure 1.4.1: Adobe distribution in Chile
Chile map: www.geology.about.com
Tulor Pukara images: Adan, L., and Urbina, S. (2007)
Aymara images: Václav šolc. (2011)
Mapuche images: www.comunidadecologicapenalolen.bligoo.com

is earth-timber based structures such as the "quincha" technique.

North regions: Barón (1982) mentions that excavations from the Tulor ruins confirmed the presence of an adobe culture in the North of Chile since 400 BC to 400 AC. Tulor was occupied by the Aymares who incorporated the adobe designs from Inca cul-

Images: San Pedro, Atacama Region.
Source image: http://serendipitoussenderos.blogspot.com/

ture, the largest pre-columbian civilization established in South America since 13th century. Concha (1966) describes that from that empire the Atacameños, the Aymaras, and the Diaguitas have continuously inhabited adobe constructions spread out from the Andes Mountains in the north territory of Peru to the II region of Chile. Their housing units consist of one circular or square big room, thick adobe walls, and vegetable fiber roof.

Center regions: Bengoa (1985) explains that beginning in the 16th century Spanish colonizers made their presence felt in the North and Center territories of Chile until the Maule river using adobe construction. However, the Mapuche natives, located in the

Images: Pisco, Coqumbo Region.
Source image: http://serendipitoussenderos.blogspot.com/

Southern territories of this river, confronted the colonial expansion through continuous wars that lasted over 200 years. This river became not only the boundary between the colonizers and the natives, but it also limited adobe designs to extend further into southern territories. Nowadays, Mapuches still inhabitant the Bio-Bio region in villages formed by "ruka" housing units. As shown in bottom image of Figure 1.4.1 ruka is a circular residential unit covered by vegetable fibers with a center fireplace.

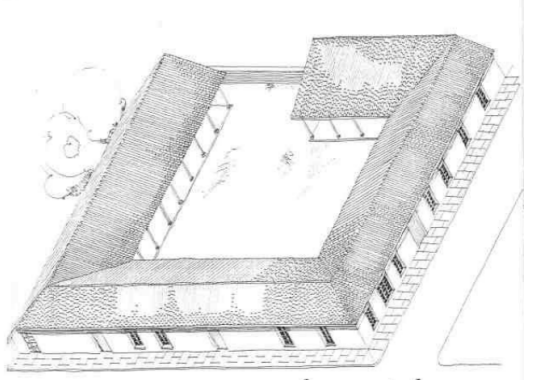

Image above: Typical Colonial housing unit. Cauquenes, VII Region.
Source: http://patrimoniochilenoadobe.blogspot.com/
Image below: Patronal house diagram.
Source: technical team, www.cobquecura.wordpress.com

South regions: Machin (2010) notes that in the 17th century, Spain crushed the Mapuche rebellion and finally crossed the Maule river to inhabit the VII Los Lagos Region and VIII Bio-Bio Region with adobe-based settlements. An example of this colonization can be found in the town of Cobquecura, Ñuble province. The frequent earthquakes

in Chile eventually forced Spanish colonizers to modify their adobe patterns brought from European architecture, characterized by thin, tall, and decorated walls. In response new adobe settlements in Chile incorporated robust walls, lower ceilings, big roof, and no wall decorations.

The difference between urban and rural adobe designs are presented in the following content fully sourced in Cabrizo (2010).

• **Urban adobe:** In the second half of the 17th century, adobe was adopted as the main building material in Chile. It was used for isolated constructions, strip configuration buildings, and places of worship. The adobe tradition is based on the Spain Andaluza influence portryed by the corner post design, the front facades, zaguan or hall, exterior corridors, and courtyards.

• **Rural adobe:** Early in the 17th century, migration from urban to rural areas began, occupying central valleys with three types of adobe housung units:

Image above: Urban adobe. Colonial center in Rancagua. VI Region.
Source: www.diarioviregion.cl / Museo Regional de Rancagua
Image below: Rural adobe. Maule Region.
Source: http://patrimoniochilenoadobe.blogspot.com

farm houses, landlord's houses, and houses of rural villagers.

Decay

The introduction of the new cultural movements such as Absolutism, the Reform, and later the Jeusitas expulsion after Chilean independence in 1810, forced the decay of Spanish traditions. Thus, the adobe construction and housing units adopted new building trends such as the French neoclasic style, making interior courtyard, which prevailed in spain housing units, as a thing of the past.

In the early 9th century, Jorquera (2010) explains that the adobe tradition gradually was abandoned and replaced by more industrialized and efficient construction techniques such as the "Quincha", composed of timber framed walls and filled with adobe blocks. In the 20th century, the rural -city migra-

Image: Rural quincha dwelling.
Source: http://patrimoniochilenoadobe.blogspot.com

tion started. Clay bricks and cement became the main materials for building residential and public constructions, and the Modernism fashion from Germany, Spain, Italy and France was introduced. The replacemt of adobe construction did not only change building layouts, but it also involved the looseness of adobe building technique by those who used to carry the earth construction tradition generation to generations.

Nowadays, adobe construction is acknowledged as being very poor in regards to seismic resistance. The introduction of industrial construction material is often time preferred, and the absence of regulation for adobe construction has significantly reduced the acceptation of earth architecture. However, in Chile many highlights its advantages and importance to the national cultural identity. Thus, the adobe seismic design code “Anteporyecto de Norma NTM 002” (2010) appeared as the first introductory document regulating this material for construction. This

document, still in development, will provide the design criteria and minimum mechanical properties of adobe structures as shown in Table 1.4.2.

Table 1.4.2: NTM 002 (2010) Material properties for Adobe construction.

E:	200MPa
f'_0:	1.2MPa
f'_m:	0.6 MPa
f_b:	1.25f'm
V_m:	0.025MPa

The Technological development corporation CDP (2012) developed the "Manual de Terreno" in earth construction. This is the most updated guide on how to repair adobe units affected by humidity, insects, and seismic events. There are also many organizations that have helped make adobe more accessible and popular. One of these organizations is Fundacion Jofre which is a collective that trains local communities construction techniques in adobe, timber, and stone, and also rehabilitates abode villages and heritage properties affected by seismic events. The 2012 National Architecture Award recipient, Marcelo Cortes, is another example of current adobe expressions. He has steadily developed adobe projects with contemporary innovations.

Image above: Huatacondo church. Tarapaca Region. Surce: Fundacion Jofre. www.culturasdetierra.cl
Image below: Casa lo Arcaya. VI Region.
Source: Marcelo Cortés architect- www.marcelocortes.cl

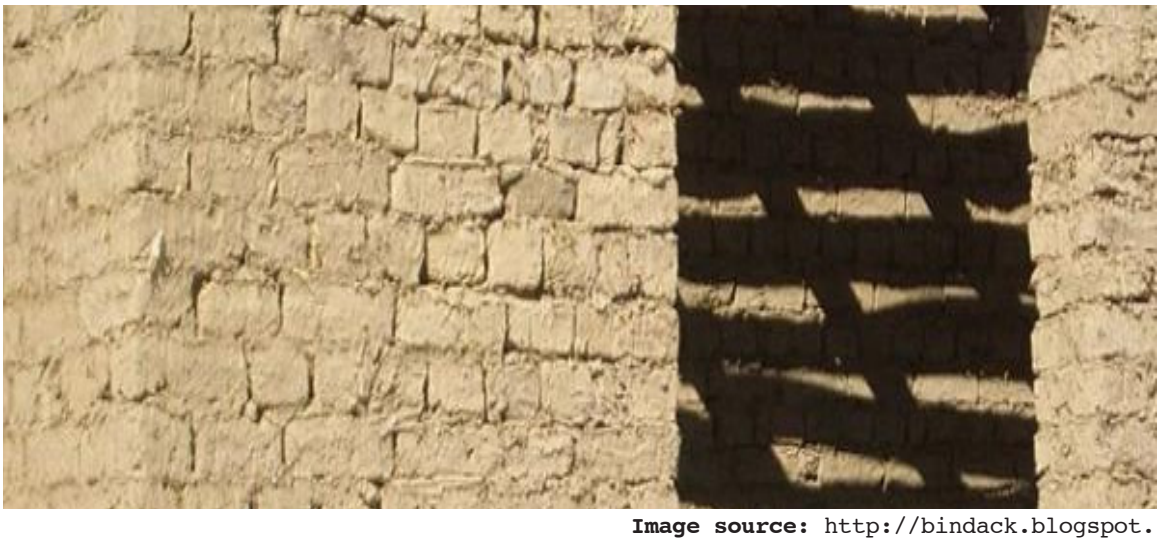

Image source: http://bindack.blogspot.com/2012/06/ventajas-y-desventajas-de-la.html

1.5 Advantages and limitations

Advantages

It is not a simple coincidence that adobe is one of the oldest and widely used building materials in the world. Numerous studies have revealed the historical advantages of using adobe masonry construction system.

• **Economic:** Rael (2009) notes that adobe is one of the most inexpensive building resources that is readily available as an onsite construction material. This makes earth bricks a relatively cost free, convenient endeavor, which makes it a widely used component in most developing nations.

• **Thermal and acoustic comfort:** Choksiriwanna and Lertwattanaruk (2011) mention that as with other mass materials, not only does adobe absorb and store energy, but it also gradually releases this energy. This helps to delay the heat energy being transferred through the wall into the interior surface. Adobe structures keep dwellings about 40% warmer in winter and 50% colder in summer than concrete brick housing units, as reviwed in section 1.8.2.

• **Ease of construction:** Housben and Guillaud (1994) note that adobe is a very simple construction technology. It can be easily manufactured by local communities without professional assistance or skilled technicians such as architects and engineers allowing the community, grouped or as individuals to contribute.

Image source: http://tunza.mobi/articles/house-of-bricks/

• **Endurance:** Studies conducted by Blondet et al. (2011) indicate that adobe can withstand enough to last centuries without corroding in territories that have a low risk for haz-

ardous natural disasters and buildings are provided with appropriate water protection, as reviewed in section 1.3 of this research.

• **Ecology:** Choksiriwanna and Lertwattanaruk (2011) highlight that basic manual molded earth brick without unorganic component is 100% recycled, it has renewable content, and does not have any toxic components. Also, reviewed literature shows that clay concrete blocks and concrete blocks are of good quality but are energy intensive in production. By contrast, in general, adobe blocks (with organic aggregates) are low energy intensive production.

Limitations

The common failures that affect adobe buildings have been overviewed in multiple articles during the last four decades. Researchers mainly focus on moisture infiltration, termite intrusion, and the low seismic resistance.

• **Moisture infiltration:** Adobe masonry, like other

earth-based structures, can easily be damaged by moisture, which leads to the vertical collapse of the adobe design as shown in Figure 1.5.1. Chok-siriwanna and Lertwattanaruk (2011) note that this condition is the reason why earth architecture is mostly used in drier territories. Torraca (1970) published a study about the deterioration process of mud brick structures caused by moisture damage. The author explains that mud bricks contain acid or alkali salt additives, thereby, during moisture infiltration by absorption or capillarity the tem-perature of these components change, corroding and cracking the mud brick. Minke (2006) recommends controlling fungus growth using lime or borax. Nev-ertheless, it can lead to some disadvantages such as a decrease in binding forces and the compressive strength between soil components used in the adobe fabri-cation.

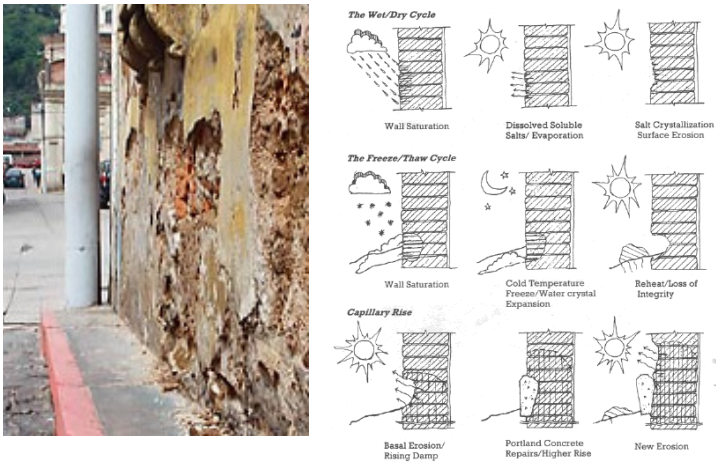

Image: Adobe wall with humidify effects after rain storm. in Agath. Mexico.
Source: http://elquetzaltecocom.gt

Figure 1.5.1: Moisture infiltration.
Source: Uviña Contreras (1998)

Image: Adobe dewelling affected by earthquke in Chile 2010
Source:http://panoramio.cl

Image: Adobe dewelling affected by earthquke in Guatemala 2012
Source:http://sipse.com

• **Termite effects:** Choksiriwanna and Lertwattanaruk (2011) mention that adobe bricks can also be corroded and cracked by termites because the earth is the natural home of these insects. Thus, they argue that termita prevention starts by maintaining the stucco layer without cracks as well as by controlling pest infiltrations over time.

• **Low seismic capacity or tensile strength:** Blondet et al. (2011), Tolles, Leroy, Edna, and William (2002), and Dowling and Samali (2005), among others, highlight that adobe bricks do have high compressive strenght and low tensile strength capacity (little material ductility). This aspect has been extensively discussed in several studies, evaluating alternatives and recommended strategies to artificially improve this limitation as reviewed in section 1.7 of this Chapter. Previously presenting this aspect, section 1.6 describes main adobe architecture features focus on the block composition (soil, water, and aggregates), manufacturing, and building patterns.

Image: Dry adobe blocks.
Source: www.todoarquitectura.com

1.6 Material Composition

Studies done by Oates (1990) and Minke (2006) describe that adobe components are soil, water, and organic or inorganic aggregates. Aggregates can improve moisture resistance, thermal isolation or mechanical properties to resist seismic hazard events. However, Avrami, Guillaud, and Hardy (2008) cite that there is not a real consensus about the proportion of components in adobe bricks. Often times, it depends on site material resources and local construction practices. Even, the add, grain size distribution in soils for adobe fabrication varies from site to site, thereby, soil test are suggested to determine the loam composition for adobe fabrication.

Figure 1.6.1: Soil grain size distribution.
Source: Minke, G (2006).

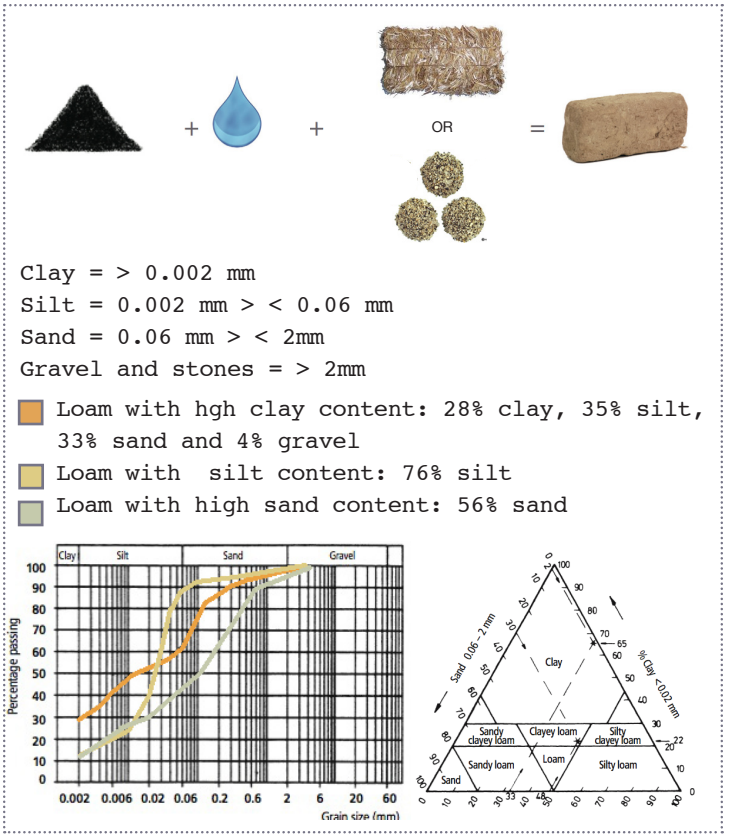

1.6.1 Soil

Minke (2006) specifies that the loam composition of adobe usually contains clay, silt, sand, gravel, and stones as illustrated in Figure 1.6.1. Avrami et al. (2008) explain that clay is the loam component that acts as a natural binder for the no-clay components (silt, sand, and gravels and stone), providing homogeneous and compact mass to the adobe block. Loam without clay tends to have less cohesion between its grains. Same authors agree that in earth structures clay gives to aggregated grains with stability. This in turn affects the overall stability of the final masonry wall.

Soil tests: Blondet at al. (2011) argue that loam types are classified according to their component

proportion. They can be clayey loam, silty loam, and sandy or gravelly loam. The following content summarizes common field tests to estimate soil composition employed in adobe fabrication. This information was collected from Minke (2006), Avrami et al. (2008), and Blondet at al. (2011).

- **Smell test**

This test helps to obtain the amount of organic content in soil. Loam is odorless, thereby if it contains any organic matter, it should have a strong musty smell.

- **Nibble test**

The nibbling sensation using nibbling on a pinch of soil helps to estimate the predominance of components and dominant ingredients. Thus, floury sensations are related to clayey soil, smooth to silty soil, and a more objectionable sensation to sandy or gravelly soil.

- **Wash test**

In this test, the predominance of a component is

estimated and can be found by rubbing a humid soil sample example between one's hands. Thus, a claycy soil sample can be identified when water is needed to clean one's hands of sticky soil. A silty soil can be recognized if one's hands do not need water to clean them and the adobe sample is still sticky. The soil is sandy or gravelly if perceived when one's hands are able to feel these components.

Images: Cutting test.
Source: Work Shop School GTZ, Cobquecura 2010. Chile. http://cobquecura.wordpress.com

- **Cutting test**

A clayey soil is identified when a humid sample of soil is cut and the surface is shiny. On the other hand, a silty soil is shown wh-when a dull cut is obtained.

Images: Sedimentation test.
Source: Work Shop School GTZ, Cobquecura 2010. Chile. http://cobquecura.wordpress.com

- **Sedimentation test**

In this test in a half glass jar, a sample of soil is mixed with a lot of water. The larger components will remain on the bottom of the jar, whereas fine sediments remain on the top. This test estimates soil constitu-ents by stratification.

Images: Ball dropping test.
Source: Work Shop School GTZ, Cobquecura 2010. Chile. http://cobquecura.wordpress.com

• Ball dropping test

In this test, 2" (5 cm) balls of soil samples are dropped from 5' (1.5 mt) to help to determine its loam composition. If the ball only shows a few cracks, the sample represents a clayey soil. By contrast, if the ball disintegrates once it reaches the ground, the sample might be more of a sandy or gravelly soil.

• Consistency test

In this test, a 1" (2.5 cm) ball is formed. If the ball reaches the diameter without breaking the sample, it represents a clayey or silty soil. If it is not possible to form a ball, the soil might be sandy or gravelly.

• Cohesion

By Making a 1/2" (12 mm) cigar-shaped roll, this test helps to measure the clay content in the soil. This is done by identifying the length at which the cigar breaks when this is rested on a table and is pushed towards the edge.

Images: cohesion test.
Source: Work Shop School GTZ, Cobquecura 2010. Chile. http://cobquecura.wordpress.com

- **Acid test**

In this test the lime content is estimated. 20% solution of hydrocloric acid is aggregated to the soil sample. If there is no efflorescence, the lime content is less than 1%. On the other hand, if the efflorescence is brief, the lime content is higher than 3%.

1.6.2 Water

Minke (2006) admitts that binding forces in loam are activated by water, affecting the four states of consistency: liquid, plastic, semisolid, and solid. The boundary between two states is called limit; Liquid limit (LL), plastic limit (PL), semisolid limit (SL), and solid limit (SL) as shown in Table 1.6.2. He adds that in loam, the water can be presented like crystallization (structural water), adsorbed water, and capillarity. Neverthelles, for adobe bricks 10% is the optimal water content, on which the maximum dry density is achieved after per-

Type of loam	LL [%]	PL [%]	PI = LL–PL
sandy	10 – 23	5 – 23	<5
silty	15 – 35	10 – 25	5 – 15
clayey	28 – 150	20 – 50	15 – 95
bentonite	40	8	32

Table 1.6.2: Loam types depending on water content.
Source: Minke (2006).

forming a proctor test. However, the suggested water content for abobe blocks is 10% higher than the optimal content because at that point the mud is workable and the binding forces act better.

1.6.3 Aggregates

Nwankwor (Terra 2008) and Burroughs (2001) coincide that aggregates, also called stabilizers, are components that enhance adobe composition to reach effective moisture resistance, minimizes shrinkage and swelling, increases thermal isolation, or improves compressive-tensile strengths. The same author adds that these aggregates are also used to meet the local building code, in which organic or inorganic components are used to achieve the desired resistances. However, Minke (2006) enphasizes that soil types that are highly organic, gravelly, or sandy are not suitable for stabilizing the adobe specimen. Section 1.8 shows the most common aggregates used to stabilize earth specimens.

Image: Mechotique, El Salvador
Source: http://www.hawkey.co.uk/site/blog/Entries/1996/3/15_How_to_build_with_adobe.html

1.7 Building process

1.7.1 Adobe fabrication process

As was mentioned earlier in this study, adobe, or the sun dried earth brick, can be obtained through four manufacturing processes: the manual molded brick, the extruded block, and the compressed blocks employing manual or powered machine. Although Reddy (1990) argues that adobe bricks were originated as the natural industrialization of monolithic earth walls like rammed walls, on the other hand, Avrami et al. (2008) imply that these two methods, adobe and rammed mud, are completely opposite in regards to the produced final earth specimen. They point out that in adobe fabrication water naturally shrinks the block into the final object,

reducing its volume by 20%, whereas in the rammed constructions water is expelled by earth compaction pressure or dynamic force, on which the final wall is nearly the same size as the produced object. The typical linear organization of adobe production is shown in Figure 1.7.1.1.

- **The manual molded earth block (MMEB)**

Content reviewed in Auriville, the UNESCO chair Earth Architecture, shows that the MMEB is employed all over the world. Minke (2006) asserts that hand

Figure 1.7.1.1: Typical linear organization of adobe production.
Diagram source: Auram press 3000. http://www.earth-auroville.com
Images source: http://altbuildblog.blogspot.com/2012/07/making-adobe-bricks.html

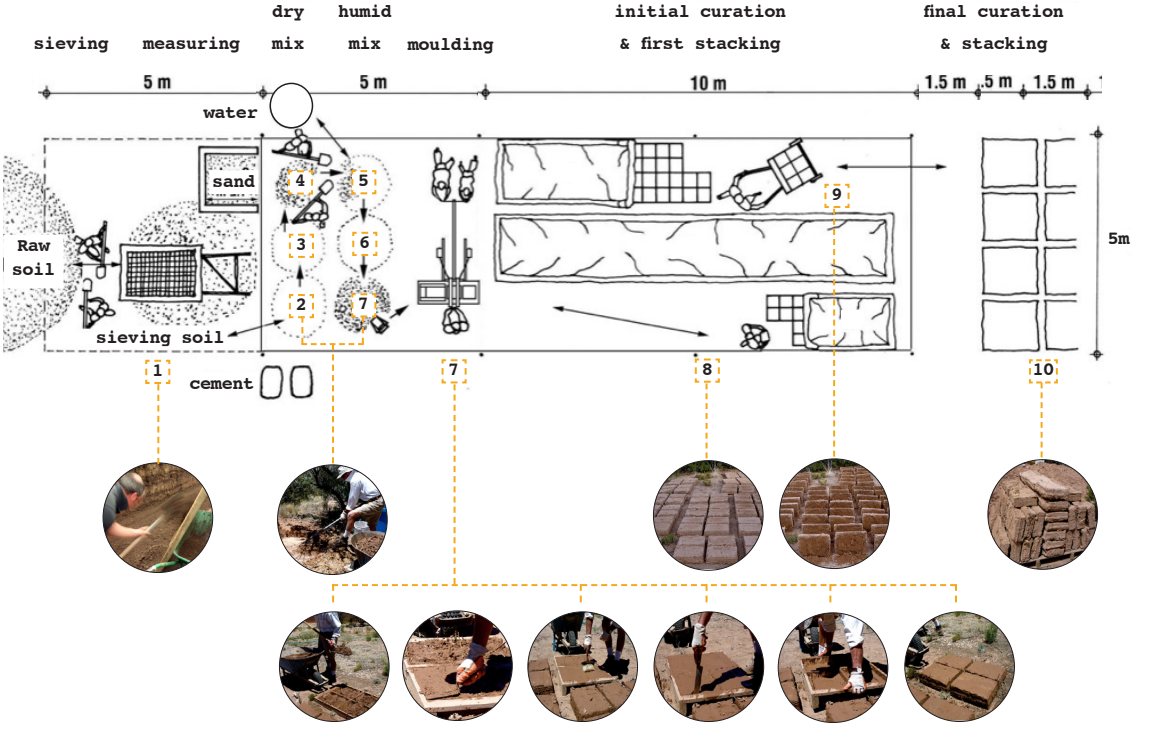

MMEB **EEB** **MCEB** **PCEB** **CB**

Images' source: Auram press 3000. http://www.earth-auroville.com

molding follows steps illustrated in the bottom image series of Figure 1.7.1. A variety of shapes are used to cast the mud as shown in Figure 1.7.2.2. For example, Haesebrouck (2011) mentions that common size used in Cuenca, Mexico, is 50x25x15 cm^2. In Chile, Fundación Jofre acknowledges that adobe blocks are commonly fabricated with dimensions 16"x16"(40x40cm), 16"x8" (40x20cm), or 10"x8" (30x20cm), and 3" or 4 1/2" (6 or 8 cm) high thickness.

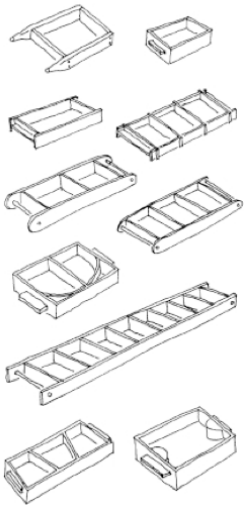

Figure 1.7.1.2: Mold types for making the manula molded earth block.
Image source: Minke (2006)

- **Extruded earth block (EEB)**

Content reviewed in Auriville, the UNESCO chair Earth Architecture, describes that in this fabrication technique power gives the desired shape and ejects the earthen specimen. The loam used in this process is often stabilized with sand, which makes

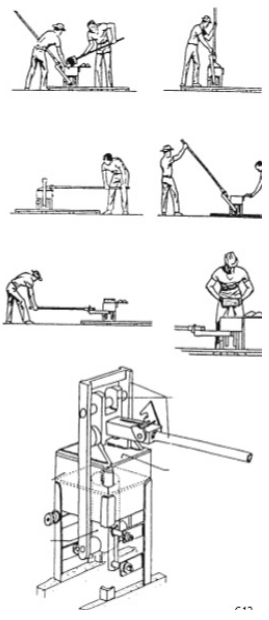

Figure 1.7.1.3: CINVA Ram, first MCEB developed by Ramirez
Source: Minke (2006)

the specimen more abrasive.

• Manual and powered compressed earth block (MCEB) (PCEB)

Minke (2006) sings that in the 1950' the firt MCEB press, shown in Figure 1.7.1.3, was developed by the Chilean engineer Ramirez at the Inter American Housing Centre in Columbia. Regarding PCEB, Rael (2008) notes that this press type was developed by Francois Cointeraux in 1803. The same author argues that this discovery represents the industrialization of the earth block for construction during the modern era. Rael also mentions that PCEB has the versatility of a brick, but also possesses the social, economic, and environmental potential of rammed earth walls. Asquith and Vellinga (2006) mention that PCEB are an improvised version of adobe bricks. He adds, the block is slightly moistened and generally is stabilized with cement or lime, achieving structural walls higher and thinner than molded adobe based-walls, better moisture resistance, compressive and telsile strength.

• **Cut earth block (CB)**

Although cut blocks is commonly classified as the masonry building types like MMEB, EEB, or PCEB, the UNESCO chair Earth Architecture points out that the fabrication process does not imply neither moulding or sun drying. Instead, in this process, the soil is cut with the block shape. This technique is prevalent in tropical territories with presence of lateric soil, possessing high cohesive and carbonate components. India and Africa possess territories where this block is in use for adobe structures.

1.7.2 Bonding patterns

Blondet (2001) comments that generally the adobe

Figure 1.7.2.1:
Bonding type in adobe construction
Source: Minke (2006)

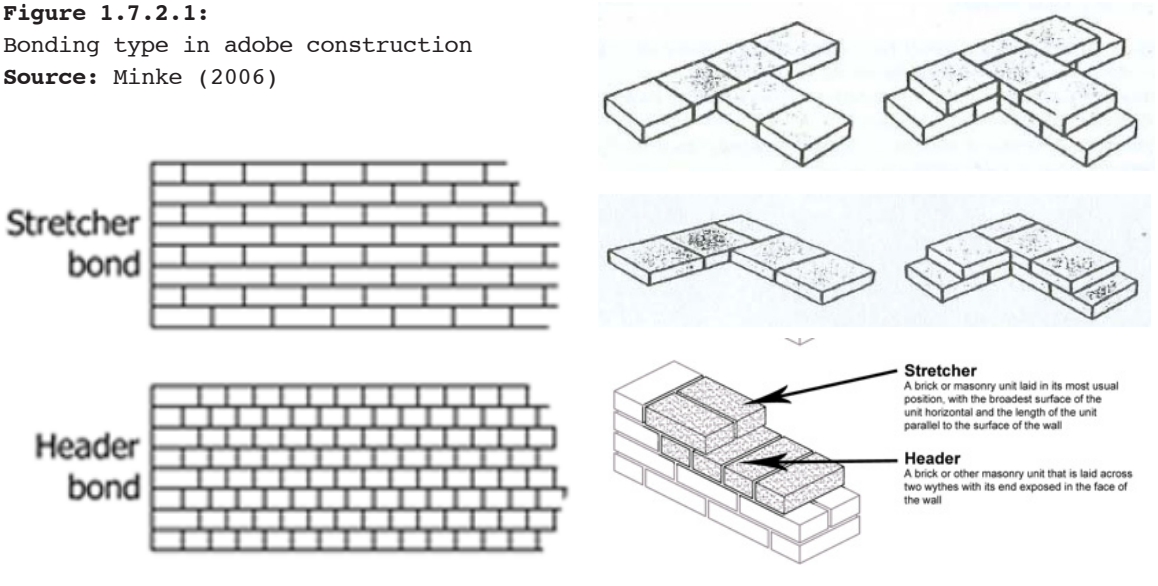

wall building commonly uses three types of boundings as shown in Figure 1.7.2.1: the stretcher bond, header, and the stretcher-header bond. These are represented with horizontal row of bricks that form a wall without posts. Thus the adobe blocks cover corners and other wall joints. In the building process the stretch or head is centered over the join below it. Thereby, all alternate stretchers or headers are aligned vertically and none of the vertical joints between the horizontal row of bricks should coincide. These bonding rules result in tying blocks between rows and in corners to provide monolithic walls.

1.7.3 Building layouts

The design of adobe walls is required to meet the stabilized wall shape concept and the wall openings design criteria.

A. Stabilized wall shapes

Minke (2006) explains that since adobe has a seismic vulnerability caused by its poor tensile strength, it's construction should employ robust

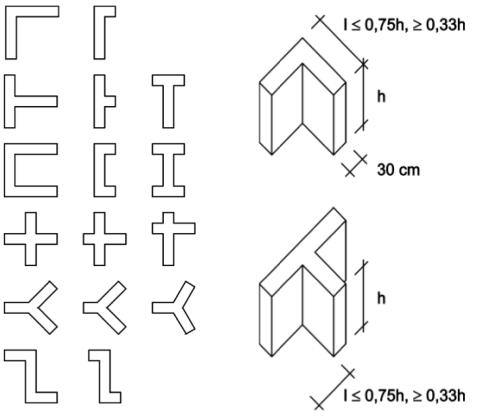

Figure 1.7.3.1: Stabilized wall shape concept.
Source: Minke (2005).

walls and compacted layouts in which the mass prevails over the wall openings for windows and doors. The common seismic failure in adobe is reviewed in detail in section 1.9. Adobe walls have to be designed according to the stabilized wall shape concept. This helps adobe walls to withstand without structural collaboration by using angular shapes like L, T,U,X,Y, or Z, illustrated in Figure 1.7.3.1. Minke (2006) describes the most important consideration for assigning dimensions to adobe walls:

• In one side attached wall designs, the wall thickness cannot be smaller than 12 inches [30 cm] and its length cannot be higher than 3/4 its height, and no smaller than 1/3 its height.

• Thickness-height ration cannot be bigger than 1/8 the thickness.

B. Openings

Minke (2006) illustrates that certain dimensional rules must be met when designing windows and doors

in adobe construction as these rules favor monolithic structures for better seismic resistance. Figure 1.8.3.2 summarizes some of the main design rules:

- (1) Lintels used for windows and doors and crown beams must keep the same horizontal line.
- (2) Window length (b) cannot be longer than 4'(1,2 m).
- (3) Window length cannot be bigger than 1/3 the wall length.
- (4) Wall length between windows or window and door should be not be smaller than 1/3 the height.

Figure 1.7.3.2: Design rules for opening in adobe construction.
Source: SM based on Minke (2005).
Image source: http://www.hawkey.co.uk/site/blog/Entries/1996/3/15_How_to_build_with_adobe.html

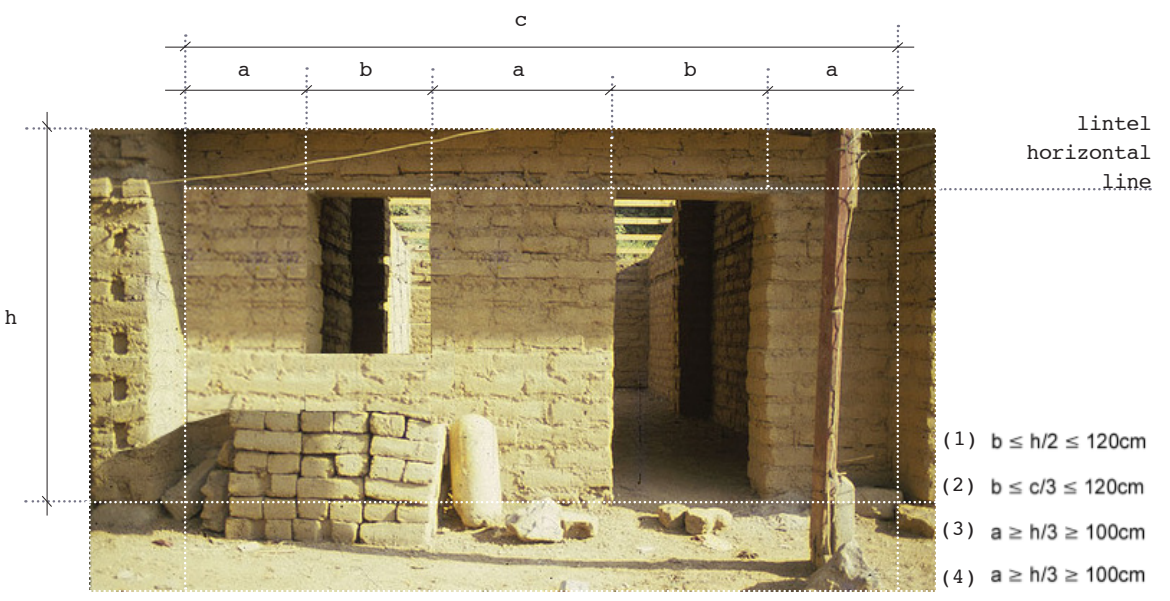

Image: Straw stabilization
Source: http://www.flickriver.com/photos/lararr/6911802702/

1.8 Stabilizers

As was mentioned in the previous section adobe blocks have low moisture resistance, thermic isolation, and seismic resistance. Strategies for enhancing this limitation are presented in this section.

1.8.1 Moisture resistance

Heredia, Bariola, Neumann, and Metha (1988) believe that increase moisture resistance to moisture permeation depends on the abobe block's ability to reduce number and size of cracks. Guettala (2006) explains that cement and resin generate the lowest total water absorption and total capillary absorption, compared to lime or cement-lime. Larbi (2004) documents that salt crystallization

is due to moisture infiltration. Two deteriorating effects are produced by salt crystallization. The first is caused by the cycle of wetting and drying. This leads to repeate crystallization of insoluble salts, which dislodges particles of the block. During rain, these dislodged particles are washed off from the surface, leading to the erosion of the earth block. The second decay of the adobe block is caused by salt infiltration from groundwater due to rising dampness during the dry process. Heredia et al. (1988) tested mud plasters to reduce moisture infiltration in adobe using the following mixtures: Plain soil, soil with banana stabilizer solution, soil with cactus stabilizer solution, soil with 2% asphalt emulsion, and soil with 4% asphalt emulsion.

Wetting and drying cycles that employed the water jet test were used in each sample. The asphalt emulsion had the best performance as stabilizer, showing the least amount of visual damage. Also, their test revealed that although banana and cactus stabilizers do aid in reducing crack sizes, they

are not enough to sufficiently prevent moisture permeation. Larbi (2004) mentions that an effective way to prevent moisture penetration in adobe structure is to allow water drops to slide off the surface instead of being absorbed into the wall before it has cured.

1.8.2 Thermal isolation

Heathcote (2010) comments that adobe has poor steady thermal resistance. Choksiriwanna and Lertwattanaruk (2011) state that an adobe brick containing reduced inorganic materials can reach thermal conductivity (k) of 0.71 W/m-K. This means that a typical 12 inch (300 mm) thick earth wall possesses a thermal resistance (R) of about 0.42 m^2K/W or thermal transmittance (U) of about of 2.38 W/m^2K. This value meets the minimum R value of 3.0 (U value of 0.33 W/m^2K) required for walls by Thermal regulation in Chile OGUC Artículo 4.1.10, for a Climate Zone 2, which includes the cities of Arica and Serena. However, this value does not meet the minimum R value of 0.53 (U value of 1.9 W/m^2K) required for walls by the Building Code in Chile for

Climate Zone 3 which includes the city of Santiago. This thermal resistance is also less than the R value of 1.9 m^2K/W (U value of 0.53 W/m^2K) required by the Building Code of Australia for a temperate climate such as found in the city of Sydney.

It is common knowledge that adobe houses are cool in summer and warm in the winter. Haglund and Rathman (no date) argues that this is caused by the thermal mass effect or the cyclic thermal resistance of earthen materials like adobe, explained by the theory of heat flow through mass specimen. Mass materials such as adobe, concrete, and stone can not only absorb and store energy, but they can also gradually release this energy. This dexterity delays the heat energy from being transferred through the wall into the interior surface. Thus, the magnitude of the internal temperature fluctuations is diminished. This condition can be seen using the example shown in Figure 1.8.2.1. which demonstrates that a dwelling that possesses a mean temperature of 25 °C in

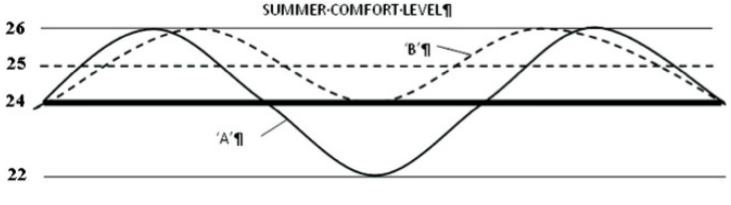

Figure 1.8.2.1 Adobe internal temperature fluctuations
Source: Heathcote (2010)

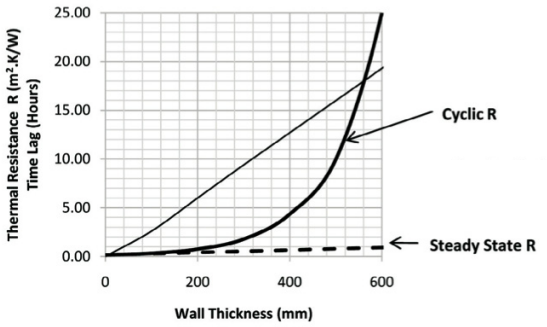

Figure 1.8.2.2: Cyclic R value.
Source: Heathcote (2010)

the summer with a swing of +/—1 °C provides the same maximum temperature as a mean temperature of 24 °C with a swing of +/—2 °C .

R cyclic = 1/(F x U)

Steady states that the thermal resistance of the wall including outside and inside surface re-substances (m^2K/W). Thus, following this line, Heathcote (2010) argues that the cyclic thermal resistance rapidly augments by using an earth wall that is 14 inches [450 mm] thick or greater, that is coupled by a time lag (delay in peak the thermal wave) greater than 12 hours. Thus, the heat flow through adobe walls is negligible when using wall thickness that is greater than 14 inches (450 mm) as shown in Figure 1.8.2.2.

Choksiriwanna and Lertwattanaruk (2011) claim that if there is a need to increase thermal isolation without incrementing the thickness of the walls, the porous content (air rooms) should be augmented. This means the more porous contained in the speci-

men the better the thermal insulation will be. However, the increase of porous content reduces the specimen mass (density), which diminishes the wall's cyclic thermal resistance.

Minke (2006) enphasizes that trapping air in the earth structure can be reached by using organic or inorganic components; foamed organic substances such as straw shoots, reeds, seaweed, cork, or inorganic aggregates such as foamed glass, pumice, lava, expanded clay, or expanded perlite. However, However, Blondet (2003) notes that soil and the porous aggregators should be homogeneously mixed to reach their estimated performance. In case straw is used, shoots should be rigid and completely covered by the slurry.

1.8.3 Compressive strength

Numerous studies on adobe blocks have explained how to increase compressive strength and reduce micro cracking caused by drying shrinkage. In general, De Jongh and Van Wijnendaele (2009) report that compressive strength in adobe elements is about 0.3 to

Image: Failure patterns of unstabilized block (top line) and stabilized block (bottom line)
Source: terra (2008)

0.5 MPa (3 to 5 kg/cm²), which is six times lower than the concrete compressive strength. Minke (2006) states that augmenting mechanical strength can be obtained by maintaining a sufficient amount of clay content andorganics (straw or rice husk) or inorganic aggregates (sand or gravels). In this process, Avrami et al. (2008) note that the final compressive strength of adobe is also affected by the adequate distribution and compaction during the mixing process, by manual or dynamic compaction. In case sand is employed, Blondet at al. (2011) mention that the proportion of this content can be obtained by performing either a field test, a “microcracking control test”, or a laboratory test like The Atterberg’s limit of sand ASTM D4318 (ASTM, 2006).

Regarding the microcracking control, Blondet at al. (2011) show that usually four block samples are tested, in which the soil-to-coarse sand proportion

will be 1:0 (no sand) in the first sample and a 1:3 (sandy sample) in the last sample.

Heredia et al. (1988) studied alternatives for reducing cracks by testing the dry effect on earth blocks with different proportions of sand. The test mixed 50% coarse sand and 2% straw. The block had adequate workability, effectively reduced microcracking, and increased the adherence between the adobe brick and the adobe plaster thanks to both the coarse and the straw content.

The following content compares the mechanical properties of five types of adobes: the manual molded earth brick (MMEB), the manual compressed earth brick (MCEB), and the powered compressed earth brick (PCEB). Figure 1.8.3.1 and Table 1.8.3.2 summarizes these cases showing compressive strengths [MPa] by comparing percentages of material composition.

Image: Compressive test
Source: terra (2008)

Image: 3 points bending test
Source: terra (2008)

Case 1

Manual molded earth block (MMEB) stabi-

lized with high sand content / Milani and Paradisco (2010):

This research was conducted after Peruvian M_w = 8.0 earthquake to verify adobe local construction process. One of the adobe structures tested in this analysis employed a sandy samples assigning following mechanical properties.

- Specimen composition: 23% clay, 5.6% silt, 64.5% sand, and 6.8% gravel.
- Density: 1600 [Kgf/m^3] or 99.8 [Kgf/m^3].
- Compressive strength: 0.75 [MPa].

Case 2

MMEB stabilized with straw or straw and rice husk / Nwankwor (Terra 2008):

This research explores the effects of stabilize adobe blocks in Africa with cement, lime, straw, and rice husk. The author performed a series of tests that meet the minimum local compressive strength standard of 2.07 [MPa] or 300 psi (NMSBBC 2003).

- Specimen composition 1: 5% Lime, 20% straw,

and 75% earth.

- Density: 97.5 [Kgf/m^3] or 1563 [Kgf/m^3].
- Compressive strength: 3.28 [MPa].

- Specimen composition 2: 5% Lime, 15% rice husk ash, 15% straw, 65% earth.
- Density:99.2 [lb/ft3] or 1.430 [Kgf/m3].
- Compressive strength: 4.7 [MPa].

Case 3

Manual compressed earth block (MCEB) stabilized with coconut fiber / Enokela and Alada (2012):
This research evaluated earth blocks samples stabilized with 0%, 1%, 2%, 3%, and 4% of coconut fibers. As the coconut content was increased, the compressive strength of the samples increased steadily to a peak of 8.62 KN/m2. After this peak the value started to drop.

- Composition: 10% Clay, 20% silt, 68% sand-gravel sandy soil, and 2% coconut fiber.
- Density: 121 [Kgf/m^3] or 1950 [Kgf/m^3].
- Compressive strength: 4.7 [MPa].

Case 4

Powered compressed earth block (PCEB) / Arumala and Gondal (2007):

This study performed physical tests using PCEB to evaluate local soil and estimate the affordablil-ity of low-income adobe dwellings in Eastern Shore of Maryland, US. Specimens were fabricated with and without cement content using powered block press. The standard characteristics of earth specimens without cement substances were:

- Specimen composition: 5% clay, 15% silt, 87% sand, and 3% gravel.
- Density:129.5 [lb/ft^3] or 2074 [Kgf/m^3].
- Compressive strength: 1.22 [MPa].

Case 5

PCEB stabilized with cement / Morris and Booysen (2000):

This study focused on comparing two common com-pressed earth blocks used in Africa. One block made with quaternary sand with 14% clay and 3% gravel

and the other block made of a decomposed granite soil with 4% clay and 40% gravel. Both were stabilized with 5% of cement using an hydraform block making machine. The results showed that the quaternary sand based specimen can achieved higher compressive strength than the granite soil typ

- Specimen composition: 14% Clay, 78% sandy soil, 3% gravel, 5% cement.
- Density: 112.5 [lb/ft^3] or 1810 [Kgf/m^3].
- Compressive strength: 5.5 [MPa].

Figure 1.8.3.1: Compressive strength comparison of preseted cases based on adobe block precentages.
Summary source: SM creation based on reviewed literature.

Table 1.8.3.2: Summary of compressive strength adobe block comparison.
Source: SM creation based on reviewed literature.

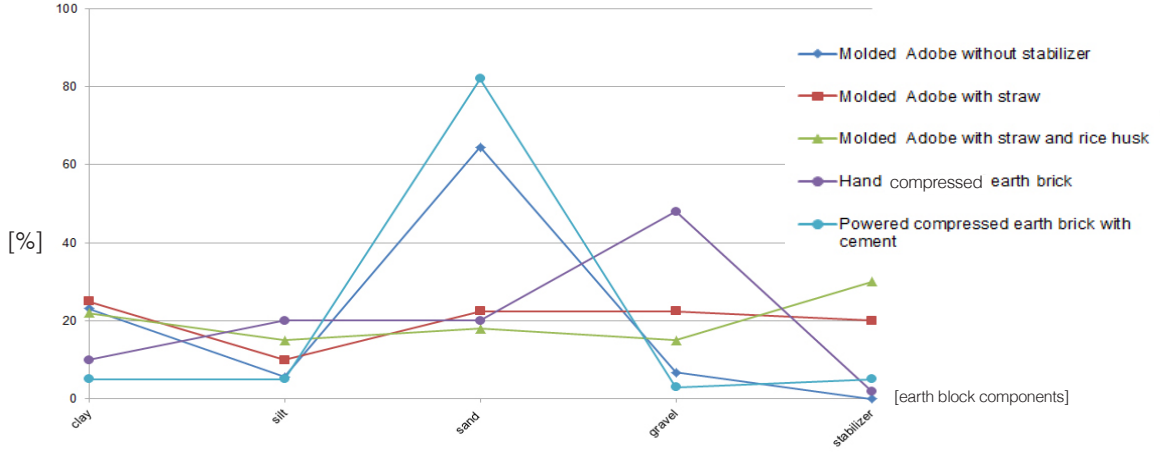

Earth brick type	Clay	silt	sand	gravel	stabilizer	compressive strength [MPa]
Molded Adobe without stabilizer	23.1	5.6	64.5	6.8	0.0	0.75
Molded Adobe with straw	25	10.0	22.5	22.5	20.0	3.3
Molded Adobe with straw and rice husk	22	15.0	18.0	15.0	30.0	4.7
Hand compressed earth block	10	20.0	20.0	48.0	2.0	1.2
Powered compressed earth brick with cement	5	5.0	82.0	3.0	5.0	5.5

1.8.4 Tensile strength

The reviewed literature shows that values for tensile strengths are significantly different between studies as that is not shown for the presented in section 1.7.3 comparing compressive strengths. However they all enphasizes that poor cohesion is the ultimate reason that casues the low tensile strength in adobe as represented in Figure 1.7.4.1. They also agree that there is no concensus about the effective enhancement of tensile strength by increasing the organic content. Figure 1.8.4.3 and Table 1.8.4.5 summarizes these cases showing compressive strength [MPa] by comparing percentages of material composition.

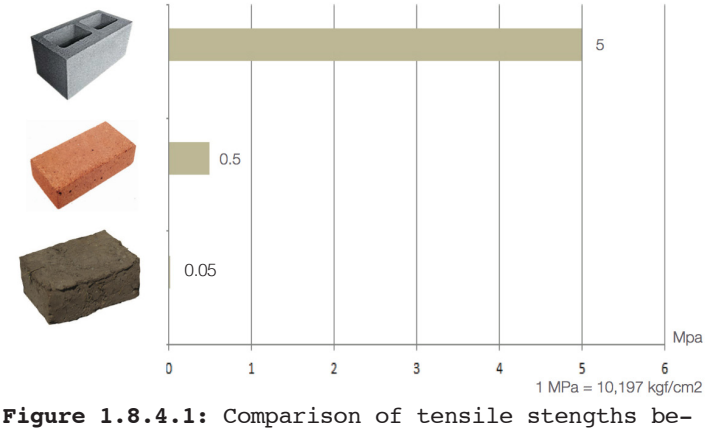

Figure 1.8.4.1: Comparison of tensile stengths between adobe, clay and concrete brick.
Summary Source: SM creation based on Milani and Paradisco (2010)

Case 1

MMEB stabilized with high sand content / Milani and Paradisco (2010).

This study was introduced in previous section about compressive

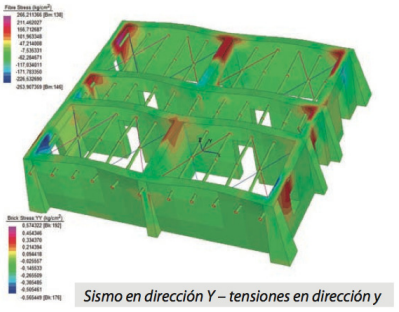

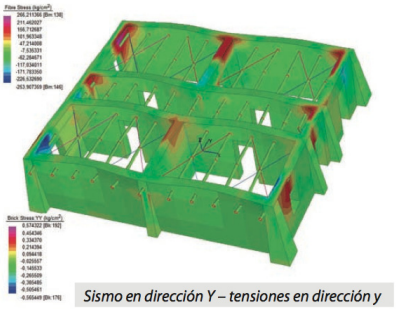

Figure 1.8.4.2: Stress diagrams for seismic analysis. **Sources:** Milani and Paradisco (2010)

strength.

- Specimen composition: 23% clay, 5.6% silt, 64.5% sand, and gravel 6.8%.
- Density: 1600 [Kgf/m^3] or 99.8 [Kgf/m^3].
- Tensile strength: 0.05 [MPa].

Case 2

Large adobe specimens and recycled content / Haesebrouck (2011).

This analysis reveals that tensile strengths in adobe Cuenca historic buildings increaseds by using large adobe blocks (50*15*12.5 cm). He states that the geometrical condition affects this wall aspect because the surface of mortar-adobe connections is reduced. Thus, the adobe wall can reach tensile strength above 1 MPa. The study also mentions that by using recycled adobe the block enhances its this capacity form 0.3 to 0.65 MPa. Studies were conducted in four historic buildings. The following details were obtained in the Museo Sombrero.

- Specimen composition: 26,8 % clay , 22,9% silt, 26,3% sand, and 24% gravel.
- Density:114 [lb/ft^3] or 1835 [Kgf/m^3].
- Tensile strength: 0.35 [MPa].

Case 3

MMAB in ancient constructions / Martins T and Varum H (no date).

In this analysis adobe based constructions located in Aveiro, Portugal, were tested to determine either conservation or rehabilitation strategies. The following detail was obtained from an adobe existing dwelling.

- Specimen composition: 23% clay, 18% silt, 24.5% sand, and 15% gravel.
- Density: 114 [lb/ft^3] or 1833 [Kgf/m^3].
- Tensile strength: 0.13 [MPa].

Case 4

MMEB in Rural adobe / Martins T and Varum H (no date).

This is a bulletin that evaluates the mechanical properties of hand made earth blocks and manual

powered machine stabilized block. The publication suggest that 1:12 ratio of the following specimen characteristics performance to obtain adequate tensile strengths.

- Specimen composition: 22% clay , 15% silt, 41% sand, gravel 12%, and 10% cement.
- Density: 119.8 [lb/ft^3] or 1922 [Kgf/m^3].
- Tensile strength: 0.84 [MPa].

Figure 1.8.4.3: Tensile strength comparison of preseted cases based on block content precentages.

Table 1.8.4.5: Summary of tensile strength adobe block comparison.
Source: SM creation based on reviewed literature.

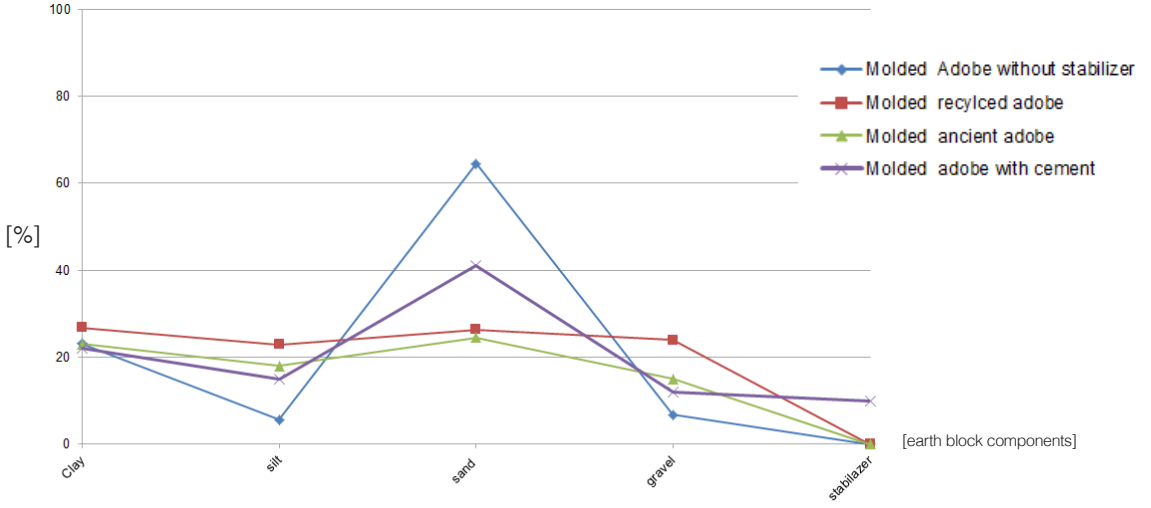

Earth brick type	clay	silt	sand	gravel	stabilizer	compressive strength [MPa]
Molded Adobe without stabilizer	23.1	5.6	64.5	6.8	0.0	0.05
Molded recylced adobe	26.8	22.9	26.3	24.0	0.0	0.35
Molded ancient adobe	23	18.0	24.5	15.0	0.0	0.4
Molded adobe with cement	22	15.0	41.0	12.0	10.0	0.9

Image: Typical Earthquake Damage - Cracking and Separation of Walls in the 1997 Jabalpur Earthquake
Source: http://www.world-housing.net

1.9 Seismic failures

Sharifu Islam and Iwashita, Terra (2008), mention that the seismic vulnerability of adobe constructions is mainly caused by the material poor tensile strength rather than low compressive strength. The authors add that the brittleness in adobe is also accompanied by deficient bonding between the mortar and earth blocks. Vargas (1986) agrees with this vision. In fact, during an earthquake the damages done to adobe walls caused by compressive strength (vertical or gravitational weight) is minimal. This type of failure is actually often caused by moisture infiltration, as was reviewed in section 1.3. Blondet et al. (2002) explain that the most common structural damages that occur in adobe build-

ings during seismic events are caused by horizontal forces, which have a direct relation to the tensile strength of adobe masonry. The same authors, Zegarra, Quiun, San Bartolomé, and Guisecke (1997), Flores et al. (2001), and Dowling (2004) mention that in horizontal forces the motions can be perpendicular or parallel to the plane of the wall as shown in Figure 1.9.1. The diagrams in this figure illustrate that perpendicular forces generate flexion, or the out-of plane behavior. The traction efforts that are apart of the flexion produce vertical cracks in corners or joints between perpendicular walls. The parallel forces, on the other hand, generate a cut

Figure 1.9.1: Seismic failures in adobe constructions
Images source: Eathquake resistance construction guide. Colombian Associaton of seismic engineering (no date).

Failures produced by pendicular forces to the wall

Fexure is generated and the traction effort that is part of the flection produces vertical cracks in corners or joins betweens perpendiculars walls

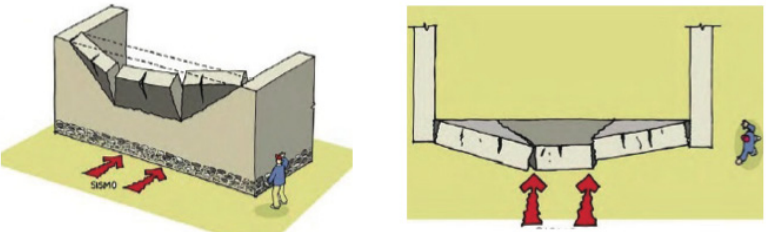

Failures produced by parallel forces to the wall

Cut (shear) effort is generated. This is expressed with diagonal cracks in corners or joins between vertical and horizontal planes in the same surface wall

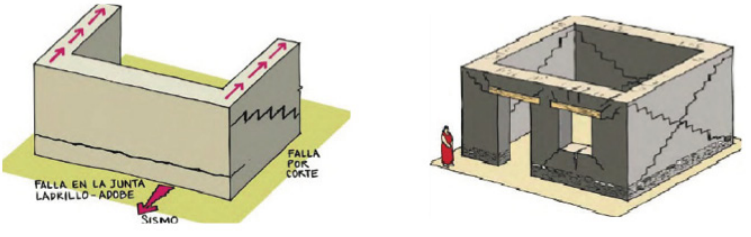




Images: Typical seismic failures poroduced in adobe structures simulated in in physical test.
Above images: Zegarra, L. et al.(1997).
Below images: Dowling, Samali, and Li (2005)

force in walls, or in-plane behavior. This makes diagonal corner cracks in joints between vertical and horizontal planes in the same surface wall. Blondet (1973) reveals that these damage patterns were first analyzed using shaking platforms in Peru in 1973. Since that period this nations has consistently researched the seismic design for adobe structures (Bariola et al. 1989; Zegarra et al. 1997; Quiun et al. 2005). This also has occurred in Mexico (Hernández et al. 1981; Flores et al. 2001), The United States (Tolles and Krawinkler 1990; Tolles et al. 2000), and Colombia (Yamin et al. 2004). Section 2.1 reviews the most common reinforcement systems that help to arficially increse adobe tensile strength. In general, physiscal tests employing scaled housing models or U-shaped ½ unreinforced or ½ reinforced adobe walls under moderate intensity forces on a uniaxial or biaxial shake platform. These tests confirm the consistence with common damages found in real adobe houses subjected to real earthquakes.

Chapter II
Seismic Mitigation and Affordable Housing in Chile

Image Source: http://www.flickr.com/photos/hawkey/3279361503/in/photostream/

2.1 Seismic mitigations using reinforcement systems

The technology to add stiffness or elastic-plastic capacities to adobe walls has rapidly evolved thanks to accurate theoretical and physical analysis based on mechanical properties. Blondet et al (2001) argues that a seismic reinforcement measure should attempt to keep the monolithic structure of the building. Ginells and Tolles (No date) agree with this condition, but they make the distinction that the retrofit system does not necessarily prevent the cracking effects. It should, however, restrain displacement between adjacent cracked walls. They also say that the severity of the seismic force determines the chosen

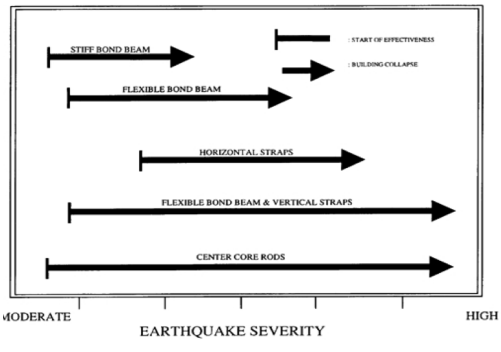

Figure 2.1.1: Reinforcement systems according to seismic force severity. **Image:** Ginells and Tolles.(No date)

base-retrofit system as is shown in Figure 2.1.1. The following content presents the most common retrofit techniques to mitigate horizontal forces (perpendicular or parallel to the wall plane) acting in the wall during seismic activity as reviewed in section 1.9. These mitigation measures are presented in order of effectiveness from high to severe seismic motion response.

Image: Crow beam
Image Source: http://www.flickr.com/photos/hawkey/3279361503/in/photostream/

A. Crown beams and superior wall joinst "L" or "T"

Effectiveness: Low and moderate protection. Zegarra et al. (1999) explain that this technique is the most basic and oldest type of seismic reinforcement used in adobe buildings. The beam is made of timber or concrete, acting as a belt upon external walls to keep them tied together as shown in Figure 2.1.2, and to transfer vertical loads from roofing structure. Minke (2006) mentions that the concrete or timber beam must be centered in the top of the wall and including corner locks that firmly attach the beam

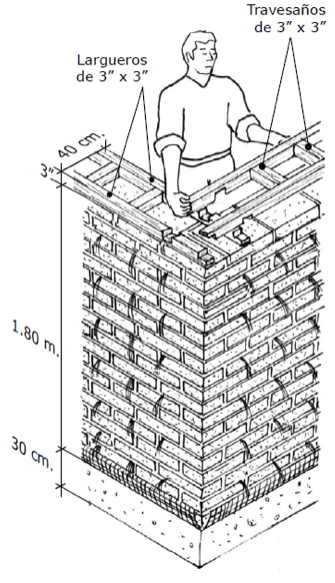

Figure 2.1.2: Crown beam
Source: Blondet et al (2002).

Figure 2.1.3: Internal and exterior vertical poles.
Image above: Blondet et al (2002).
Image below: Torrealva y Acero et al.(2005)

to the adobe wall, avoiding it from horizontally sliding on top of the adobe wall during seismic motions. Pumpelly (1908) refers to the Tabo monastery in Spiti valley, Himalayas, India, as the oldest adobe building still standing that uses reinforced timber ring beams.

B. Internal or external vertical poles

Effectiveness: Moderate to high protection.

Blonde, Villa, and Loaiza (2002) studied this system explaning, which creates a stable matrix by using interior or exterior vertical poles (canes) made of timber or bamboo reeds as shown in Figure 2.1.3. These aim to tie the adobe blocks with each other, increasing monolithic behavior, flexure and reducing basal displacement.

This system began to be used after the physical test conducted by Blondet in 1973. The exterior vertical cane case is often used with superior ring beam and horizontal fence wire reinforcement, whereas the interior vertical cane case includes

Image: Corner buttresses
Source: http://www.flickr.com/photos/hawkey/3279361503/in/photostream/

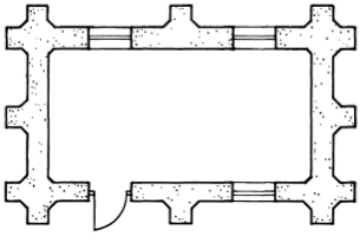

Figure 2.1.4: Housing floor plan using buttresses
Source: Minke (2001)

superior ring beam and horizontal chicken wire mesh reinforcement. Physical tests using internal cane pole, conducted by Blondet (1973), revealed that the compressive strength and the tensile strength can increase from two to six time the capacities shown in unreinforced adobe walls. However, Blondet et al. (2002) mention that this system is limited to the territory where the poles (canes) are produced. Also, Zerrate et al. (1997) discusses that employing internal vertical poles has more limitations than using exterior poles. This option tends to be more vulnerable to failures, requires more time in the installation process, skilled assistance, and also poles cannot be checked when they are encased in the structure.

C. Buttresses / pilasters

Effectiveness: Moderate to high protection.

Blondet et al. (2002) refer to this retrofit alternative preventing inward or outward overturning of the wall by incrementing wall area in walljoints

as shown in Figure 1.2.4. It is often used in South America, especially in Chile. Minke (2005) explains that if the wall is twelve time bigger than the thickness, it is necessary to reinforce the adobe wall with intermediate and corner buttresses.

D. Polymer or wire mesh

Effectiveness: Moderate to high protection.

Zerrate et al. (1997) researched this technique on which interior and exterior mesh is nailed against the adobe wall, turning the wall into a monolithic element as the istallation step serie shows in Figure 2.1.5. This study also discusses that the use of meshes started in 1994 led by Peruvian researchers to seismically protect 16 existing dwellings in different parts of South America. Two of them located in Moquegua were not affected by the 2001 earthquake, proving the effectiveness of this solution.

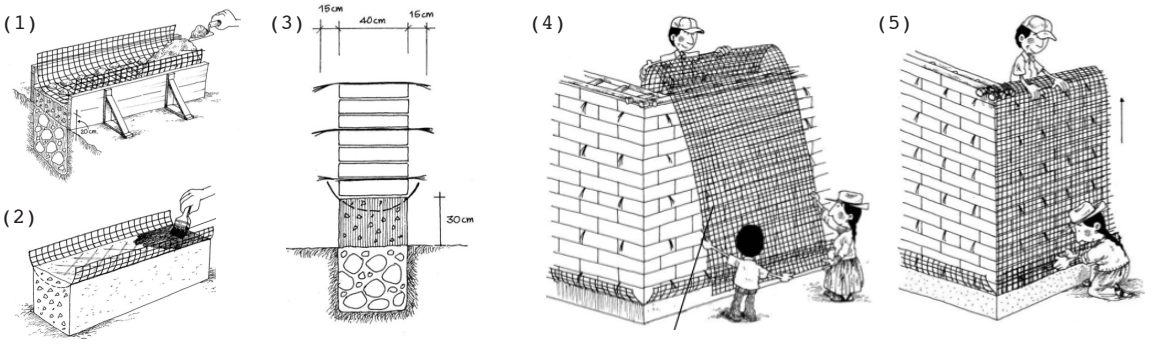

Figure 2.1.5: Polymer mesh installation.
Source: AIS Colombia (no date).

Image: Polymer mesh and tire strap reinforcement systems.
Source: Blondet et al (2011).

Regarding the economic aspect Blondet et al. (2002) mention that this solution has cost starting at US$ 200, which might be affordable to get for low income families to afford.

E. Car tire strap

Effectiveness: Moderate to high protection. Blondet, Villa, Brzev, and Rubiño (2011) explain that this system was created in academic researches in New Zealand, combining horizontal and vertical tire strap. These components wrap the adobe construction, providing monolithic response during the seismic event. Ginells and Tolles (No date) discusses that vertical straps and a flexible bond beam do not change the elastic behavior when damage is small. However, during severe earthquakes, they can greatly reduce the

Table 2.1.6: Reinforcement systems summary.
Source: Blondet et al (2005).

Wall reinforcement scheme	Type of building		Construction complexity			Cost			Seismic safety		
	New	Existing	Simple	Moderate	Complex	Low	Moderate	High	Low	Moderate	High
Internal cane reinforcement	X			X		X					X
External cane and rope mesh	X	X	X			X					X
External bamboo and internal wire mesh	X	X	X			X					X
Welded wire Mesh	X	X	X				X			X	
Polymer Mesh	X	X	X				X				X
Used car tire straps	X	X		X		X				X	
Polypropylene band	X	X		X		X					X
Integral masonry system	X				X			X			X

relative displacements of the cracked wall sections and prevent overturning.

Table 2.1.6 summarizes performance, cost, and installation complexity of described systems.

2.1.2 Case study: GTZ Work-Shop school for adobe reconstruction in Cobquecura, Bio Bio Region, Chile, 2010.

This project aimed to rehabilitate the adobe communitiy center "Casa Azul" affected by the M_w = 8.8 earthquake in Cobquecura on February 27th, 2010 (F2010). The Chilean regulation No 17,288, administered by the Educational Ministry of Chile throughout the Consejo de Monumentos Nacionales, in 2005 assigned to Cobquecura the category of Typical Zone. This was due to Cobquecura's rich heritage of traditional adobe constructions, mainly legated from the Spanish colonial period established until the first half of the XX century.

Images source: Cobquecura colonial housing unit.
Source: Technical team, GTZ Work-Shop school for adobe reconstruction in Cobquecura. www.cobquecura.wordpress.com

Analyzing the nature of the problem in Cobquecura the damage re-

Image: Theoretical and practical classes in reconstruction of Case Azul.
Source: Technical team, GTZ Work-Shop school for adobe reconstruction in Cobquecura. www.cobquecura.wordpress.com

port “Catastro de daños en viviendas de Cobquecura producto del terremoto de Febrero 2010” emitted by Cobquecura Council after the seismic hazard in F2010, highlights that out of 2,320 housing units 1,450 suffered damages. From this amount, 980 adobe housing units were affected, which represents 2/3 of the total town dwellings. As secondary consequences, this tragedy produced 70% unemployment and the loss of traditional adobe masonry housing along with its legacy.

Project objectives

• Utilize the reconstruction process as an opportunity for community development

• Conserve the heritage of traditional adobe houses.

• Create employment opportunities

Project implementation

•The plan approached the reconstruction relying on two resources: include the communities' capacities to form local builders and the participation with partnership relation between four stakeholders as Figure 2.1.7 shows: The Agency formed by Technical

Figure 2.1.7: Project implementation diagram.
Source: SM creation
Left images: Technical team, GTZ Work-Shop school for adobe reconstruction in Cobquecura. www.cobquecura.wordpress.com

assistants, the building company which required local builders, the local government which provided organization and funding, and the Community representatives formed by 220 householders.

Work-Shop school structure

• The builders' formation was based on theoretical and practical classes.

• *Theoretical matters*: Construction knowledge in renewable materials, seismic reinforcements for adobe housing, architectural drawings, climate & design, post-earthquake business opportunities, development and dartnership relations.

Image: Graduated students Work-Shop school GTZ
Source: technical team, www.cobquecura.wordpress.com

• *Practical matters:* Physical reconstruction of the "Casa Azul", on which students were taught in construction techniques of stone and adobe masonries, timber and mesh reinforcements, mud stucco plaster, and colonial clay tails.

Entrepreneurial aspects

• *Material:* Community center Casa Azul was rehabilitated by local using renewable sources.

• *Economic:* 45 graduate builders with technical knowledge in adobe masonry would be part of future reconstruction.

• *Social & cultural:* Firs housing committee was created and its website was established. http://cobquecura.wordpress.com/

Impact

• Local community members became active builders in the reconstruction process.

• Cultural heritage of traditional adobe building technique was rescued and conserved within the community.

• Created employment opportunities

• Built participation and partnership between stakeholders.

Lesson from practical implementation of reinforcement systems:

• Adobe masonry is brittle and weak.

• Seismic design code for adobe in Chile needs to be implemented. The seismic design code in Chile (SDC) NCh 433 of.96 does not have regulation for adobe architecture. In Cobquecura mitigation strategies to seismically protect adobe units lacked local and certified standard solutions.

• Communities have little information in adobe construction. They only keep in mind that adobe is weak, generating warning about reconstruction in adobe. The use of contemporary building techniques such as clay or cement brick and steel based systems has reduced the adobe construction. Because of these, the adobe legacy has been gradually abandoned.

• Polymer mesh was used to repair existing building Casa Azul. This solution showed to be effective but some limitations were presented. This requires

professional assistance to be installed and the polymer mesh limits future housing expansion. Also, openings in walls require cutting the mesh, which reduces its tensile resistance.

2.1.3 Challenges for seismic mitigations in adobe

Various research studies point out that new strategies for seismic mitigations in adobe construction needs to be explored.

1. Blondet et al. (2002) argue that there is a need to research more effective and affordable seismic protections using massive industrial materials that can easily be accepted by the inhabitants, accompanied by governmental support to develop, implement, and expand the use of the proposed technique.
2. Guerrero (2006) and De la LLera (interview Sept. 2011) are more specific about highlighting the sesimic isolation as an alternative solution:

"Earthen constructions are ideal candidates to be seismically protected with base isolation. This is an innovative strategy that has been adopted for monumental masonry buildings, since it does not involve great interventions on the upper structure. It decouples the horizontal movement of the building from the horizontal ground motion. This causes a decrease in the fundamental frequency of the structure, consequently

reducing the seismic force demand. The adaptation of this system for earthen construction will be of great value. However, the application of this technique for repair and seismic retrofit may be complex as the stability of the structure must be assured while the connection to the foundation is removed and substituted by base isolation bearings"

Guerrero (2006)

" THe use of seismic isolation in adobe seems to be of great value because adobe is weak and heavy. Although there are softwares to model effects of quakes in brittle materials like earth blocks, it is necessary to address physical silulations to test the solution effectiveness"

De la LLera (interview Sept 2011)
SRVE president (seismic difusers designers)
Director Engieneering School PUC-Chile
UC Berkekey Phd.

3. The use of polymer mesh rehabilitating the community center Casa Azul, as practical implementation of the GTZ Work-Shop school for adobe reconstruction in Cobquecura, The Bio Bio Region, Chile, 2010, showed two complications: This systems requires professional assistance, and once is installed, furture openings in the wall might affect the polymer mesh function. This is because the mesh needs to be cut in the opening area, losing tensile strength.

In order to address previous arguments, the following section reviews the physical principle of seismic interface bearings, also called seismic isolaton systems, putting special attention in describing base isolation. The characteristic comparison between these systems shown in Figure 2.2.7 attepmts to define the criteria that might be used in proposing affordable seismic base isolations to adobe buidings.

Image Source: seismic protection technologies (SIRVE) www.sirve.cl

2.2 Seismic mitigations using base isolation systems

Numerous publications mention that studies in bearing systems to mitigate seismic effects in building have rapidly grown thanks to the development of reliable software, shaking tables, and the estimation of site-specific earthquake motion. Naeim (2011) mentions that during a seismic event, the earthquake force transmitted to the building produces inter-story drifts, increases floor acceleration, and plastic deformation of the structure as shown in Figure 2.2.1. Seismic interface bearings, also called seismic isolation systems, aim to restrict the motion's amplitude of seismic events that affect conventional structures. Lee Li (no date) reveals that the method was introduced by the

Englishman Johannes Calantaries in 1909, exploring seismic diffuser layers in physical models. However, Naeim (1999) enphasizes that the first seismic isolation system was utilized in China after the M_W = 8 earthquake in Wuchang, April 13th, 1960. In that time, the inspections of an old rammed-soil building which did not collapse during the earthquake found a horizontal crack above the foundation wall. The inspection concluded that the horizontal crack originated as a natural "neck section" in the structure. During the initial period of the seismic event, the building remained sliding along this line, reducing the shaking force acting on the upper building. Hence, the neck section represented the first discovery of seismic base isolators (SBI). Özden (2006) declares that SBI do not artificially augment mechanical

Figure 2.2.1: Seismic deformation in isolated and un-isolated housing units.
Graph source: Mayes and Naeim (2002).
Sections' source: SM creation base on Mayes and Naeim (2002) diagrams.

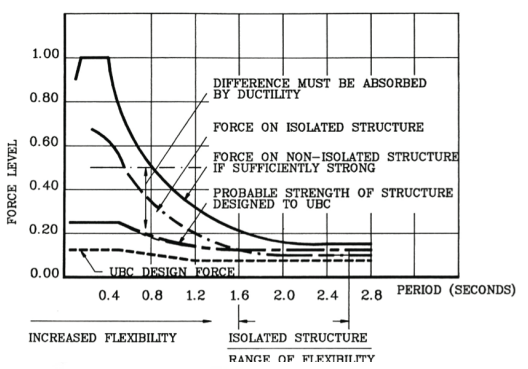

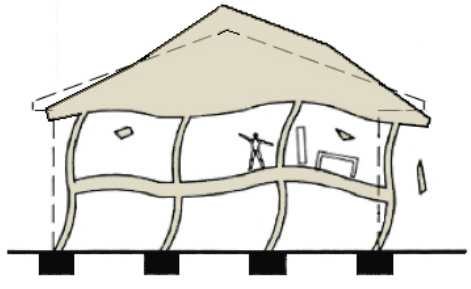

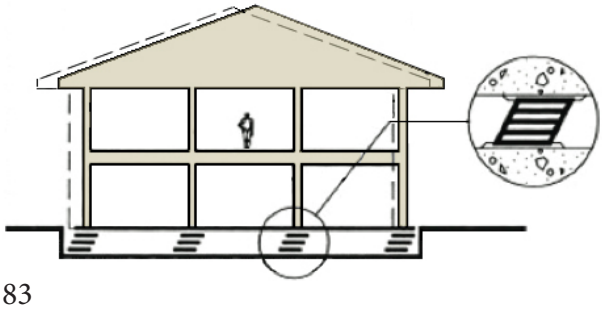

capacities of the building structure as understood by using seismic reinforcement systems. SBI instead changes the dynamic demand of the building structure on the ground level. Same author explains that SBI diffuses the earthquake force going up to the super structure. Therefore, these systems improve both the period of vibration and the capacity to dissipate energy.

Type of seismic base isolatiors

- **Friction bearing (FB)**

Vafia, Hamidi, and Ahmadi (2000) assert that in this system the sliding friction behavior is the mechanism that seismically isolates the superstructure, emphazising that the use of friction bearings as seismic isolation systems is an inexpensive alternative in comparison to other interface systems. The following content describes common FB.

- **Friction Dry-staked masonry bearing (FDSMB)**

Vasconcelos and Lourenço (2009) explain that this system is based on stone masonry with mortar free construction. The frictional coefficient varies

in the range of 0.03 to 0.25. The same authors add that in some cases, the use of asymmetrical-shaped stone favors to recenter the structure to original position after seismic event as shown in Figure 2.2.2. The Machupichu Inca ruins in South America possess examples of free mortar walls with asymmetrical-shaped stones. Cuadra, Karkee, Ogawa, and Rojas (2004) highlight that Incas were able to build walls that survived earthquakes. However, field seismic evaluations show that rigid roof were necessary to avoid glade collapse and produce the restraining effect in walls, allowing the wall to withstand earthquakes of moderate intensity. The symmetric masonry stone does not favor the recentering behavior of the superstructure. Vafia et al. (2000) add that variation on failure modes of the wall is produced by the hysteric behavior on which vertical loads generate diagonal step cracks on walls. They also mention that there are no patterns to estimate the cost of implementing this solution, nevertheless, this aspect must no be higher than 5% of the total construction expenses.

Figure 2.2.2: FDSMB

Image: Inca stone wall
Source: http://www.travel-pictures-gallery.com/easter-island/easter-island-0033.html

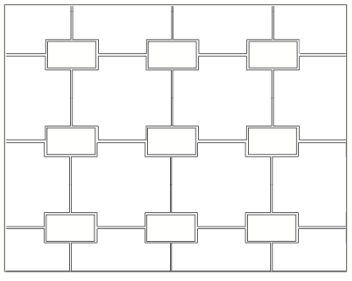

Diagram: unsymmetrical-shaped stone masonry.
Source: SM creation based on reviewed literature.

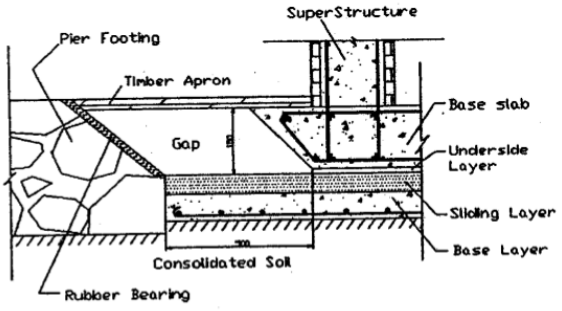

Material	Friction coefficient
Pebble (6–8 mm)	0.20
Polythene membrane	0.18
Polypropylene sheet (0.8 mm)	0.15
Polyvinyl chloride sheet (1.0 mm)	0.10

Figure 2.2.3: FRB propoused for heavy buildings made of weak materials.
Source: Xiao et al (2004).

• **Friction layer bearing (FLB)**

Xiao, Butterworth, and Larkin (2004) explore friction layers between the ground soil and the foundation pointing out that this solution might work for heavy buildings made of weak materials. His study proposed four seismic isolation materials with friction coefficient levels shown in Figure 2.2.3. Mojsilovic, Page, and Simundic (2010) also studied friction layers locating isolation materials between the first two masonry courses or between the concrete base and the wallette, using value of 0.35 as a design value for friction coefficient for embossed polythene membrane as shown in Figure 2.2.4. The low cost of these components, between 5% and 7% of the total construction cost, allows their use in low-income buildings.

Figure 2.2.4: FLB isolation materials between the first two masonry courses or between the concrete base and the wallette.
Source: Mojsilovic, Page, and Simundic (2010).

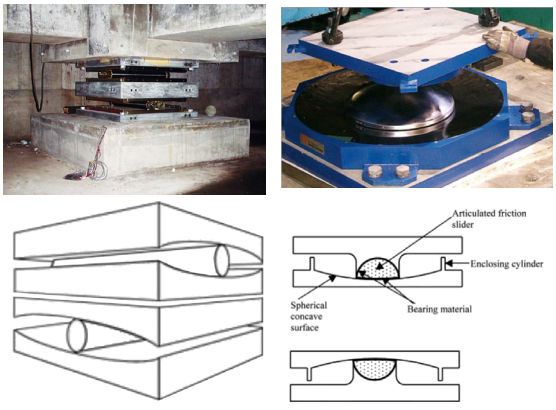

Figure 2.2.5: FRB and FPB
Left images: Roller bearing
Source: http://www.takenaka.co.jp/takenaka_e/rodin_e/seismic.html

Right images: Friction pendulum bearing
Source: EPS (2003)

- **Friction roller bearing (FRB) and Friction pendulum bearing (FPB).**

Almazán and De La Llera (2002) and EPS (2003) describe that in these systems superstructure slide on a friction re-centering devices such as the friction roller bearing (FRB) and the friction pendulum bearing (FPB). The FRB relays on a superstructure sliding on friction sloping steel rollers, whereas the FPB utilizes a spherical sliding interface. In both cases, the system dissipates energy and provides restorative stiffness due to concave bearing surface bearings coinciding with gravity center of supported structures as shown in Figure 2.2.5. The frictional coefficient varies in the range of 0.10 to 0.05, with a damping coefficient in a range of 10 to 40%. These bearings are not affected by aging or temperature and are capable of tolerating large displacement with relatively small system dimension. The high cost of these components, above 15% of the total construction cost, restrict their use

only to buildings provided with ring footing or suspended concrete floor.

- **Elastomeric bearing (EB)**

Kelly and Konstantinidis (2011) evaluate this bearing which relies on elastomer polymer layers that provide flexibility and hysteretic damping forces. They have high vertical stiffness, period shift, energy dissipaters, and generate low displacement. Bearings can transfer horizontal loads to structures by recess, dowels, or bolts. The following content describes common EB used for SBI as shown in Figure 2.2.6; (1) The natural rubber bearing (NRB), (2) high-damping rubber bearing (HDRB), and (3) the Lead-plug rubber bearing (LPRB).

Özden (2006) focuses his thesis on NRB made out

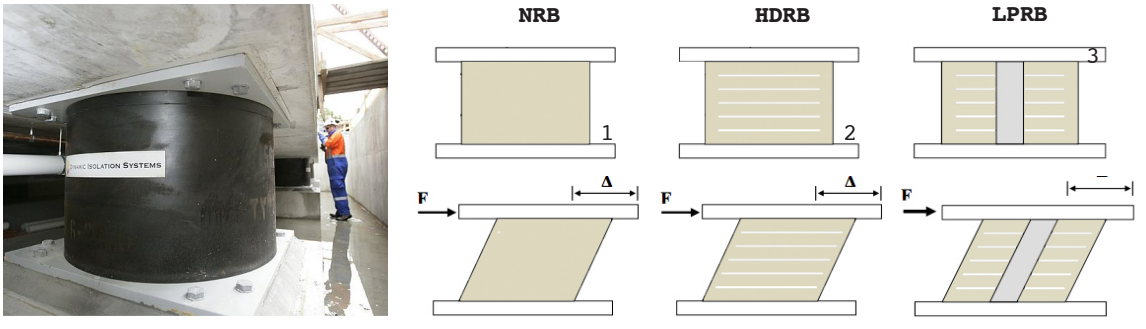

Figure 2.2.6: NRB, HDRB, and LPRB
Images source: www.dynamicisolationsystems.com
Diagram **source:** SM creation based on reviewed literature.

1.Connection plate
1.Rubber layer
3.Stiffner plate

Image: Andalucia community. First low-rise building in Chile seimically isolated by using NRB. **Source:** Chapeo (2011)

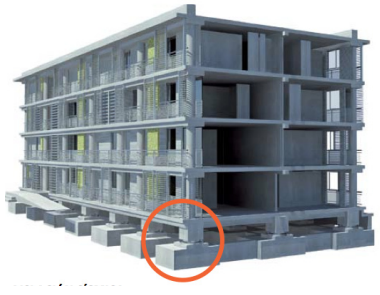

Image: Proyect "Zero damages" using NRB for low-rise housing units in Santa Cruz. Chile.
Source: Chapeo (2011)

of car scrap rubber layers, reaching 20% of damping coefficient and estimating costs in a range of 5% to 10% from un-isolated options. Naeim (2011) illustrates that the HDRB is composed by rubber layer and steel shims, can withstand larger shear deformations than standard NRB, with damping coefficient in a range of 10% to 16%. In terms of economy, this interface can increase the building cost in about 5% to 15% from building with no seismic isolation. The same author describes that LRB is a variation of HDRB, including one or more circular central holes. The center lead plug provides a vertical stiffness for static loads, period shift, and energy dissipation higher than NRB and HDRB. The damping coefficient varies in a range of 8% to 25%. In terms of economy, SIRVE Chile provides affordable elastomeric bearings, accounting with the first low-income residential buinding in Chile equiped with this system in 1994 (Andalucia community).They have evaluated that elastomeric bearings can increase the building cost about 5% to

20% from non-isolated options.

• **Self-centering strut bearing (SCSB)**

Christocpouls, Filiatrault, and Folz (2002) explain that this system employs a flag-shaped hysteretic loop, which limits residual displacements after seismic event. The system utilizes the weight of pre-cast concrete panels to recenter forces, including tendons that connect concrete panels to its foundation in case the weight of concrete panels cannot re-center them. SIRVE Chile has developed this system for one story building units with suspended concrete floor, increasing the total construction cost in about 10% to 15%.

• **Steel damper bearing (SDB)**

SIRVE describes that elasto-plasticity property of steel components is the principle that governs this system. The energy

Image: Housing unit seismically isolated by using SCS
Source: www.sirve.cl

dissipation is generated by the hysteretic loop. This system shows two types of steel dampers, one is round in section of the rods and the other is square in section, incrementing the total construction cost in about 10% to 15%.

- **Fluid viscous damper bearing (FVDB)**

Hussain, Lee, and Retamal (On line) show that this system operates using fluid viscous components, following the principle that viscous fluid flows through orifices.

The fluid is oil. The difference of pressure between interior chambers creates the flow of the oil. This energy is converted into heat, which is later dissipated.

Image: SD
Source: http://www.elemka.gr/

Image: FDH
Source: http://www.elemka.gr/

It possesses a damping coefficient of 37 %, reducing dynamic displacements by 50%. The inclusion of this system can improve the overall performance, reducing cost and size of other isolations utilized for seismic protection, but the combination of systems can increase the total cost between 15% to 20%.

Figure 2.2.7: Summary of SBI and selection of affordable alternatives
Source: SM creation

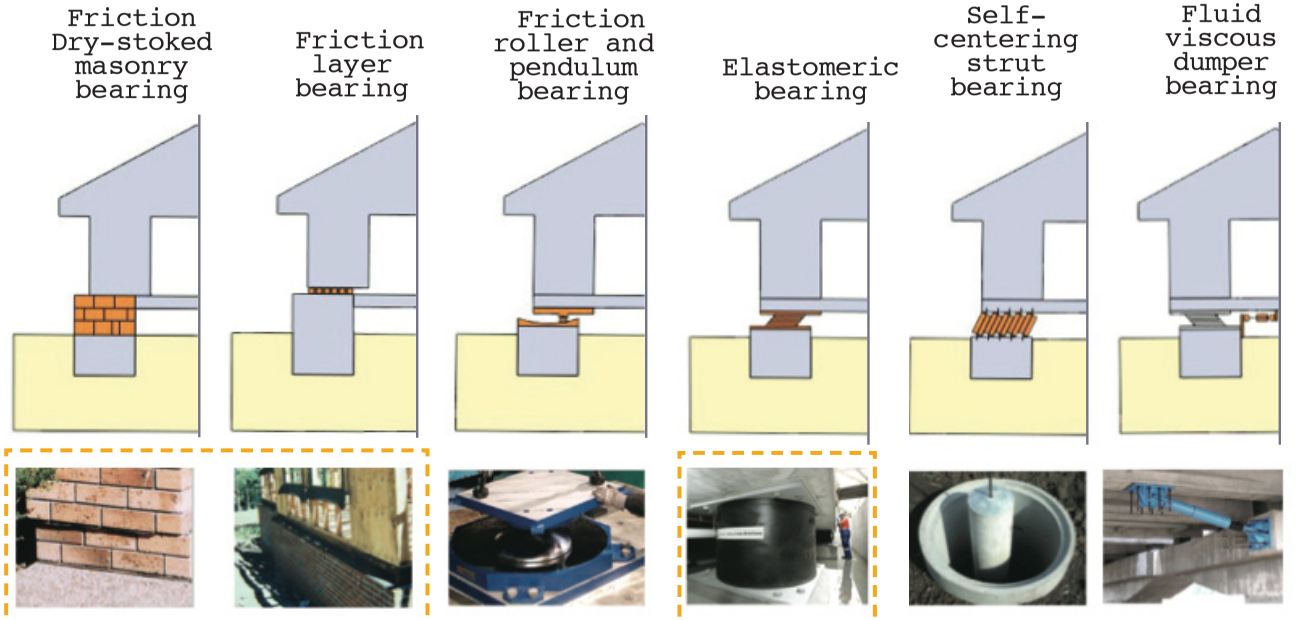

components	free mortar join	pebbles,or polythene, or polyvinyl	steel pen-dulum in-terface	rubber pad	pre-cast concrete and steel tendoms	oil and silicone and steel
re-centering system	no	no	yes	yes	yes	yes
cost (% of the total cost)	5% <	5% to 7%	15% to 20%	5% to 20%	10% to 15%	15% to 20%
energy used in fabrication	low	low	moderate to high	moderate	moderate to high	moderate to high
recycled content	yes	yes	yes	yes	yes	yes

• Observation from studied cases

Economy is a primary aspect in the adobe housing constructions as was reviewed in section 1.5. Therefore, this aspect should also determine the choice of SBI to seismically protect these buildings. According to reviewed literature this research considers that the SBI could be composed by combining physics properties of three studeid cases highlighted in Table 2.2.7: (1) The friction Dry-staked masonry bearings and (2) the friction layer bearings would be employed for defining the seismic diffuser component, whereas (2) the rubber bearing can suit the need of re-locate the superstructure to the center of gravity after structure displacement caused by seismic motion.

Image Source: www.serviuatacama.cl

2.3 Chilean context for affordable adobe housings

2.3.1 Affordable housing programs

According to the CASEN survey (2009), Chile possesses a total of 4,685,490 residential units. From this number, 968,092 housing units are identified as the deficit, which represents 18% housing properties. This is composed by 12% of irretrievable units, 44% of home shearing units, and 44% of overcrowded units. The same document reveals that the housing deficit is reduced by about 200,000 units every 4 years, trending to estimate the completion of the total deficit within this decade.

In this line, Elemental Chile, group which has steadily designed multifamily low-income projects

subsidized by the Housing Ministry (MINVU), arques that Chile is close to overcome the housing emergency, thereby, the new challenge is enhancing the building quality and increasing its capital value over time. The following content presents current subsidy FSV and SHR given by the MVUC for low income housing units.

A. Fondo solidario de la Vivienda (FSV)

This program aims to provide housing solutions to the 1st and 2nd poorest citizen groups in Chile. FSV funds dwelling units with a cost up to US$ 43625 (900 UF). Families interested in this subsidy are required to apply with US$ 1450 (30 UF).

FSV funds housing projects with following characteristics:

• New plot construction: New property in new plot including urbanization.

• Collective construction in rural area: Group of properties in new plots including urbanization.

• Lot densification: New property within a lot with existing property.

• Owned plot construction: New property within an existing lot.

• Acquisition and reparation of existing property: Modification to existing building.

The Housing Ministry also encourages territorial locality, providing a subsidy program that complements the FSV with additional funds up to 200 UF to appliers if the project contains less than 150 housing units and 60% of the total appliers are local residents.

B. Subsidio Habitacional Rural (SHR)

This program aims to provide a more permanent solution to the 2nd poorest citizen groups and middle class population in rural areas of Chile. The program funds up to US$ 22,400 (420 UF) to appliers who own a lot and possess saving of $US 48 (10 UF). This fund can increase in US$ 339 (70 UF) if urbanization is required, and US$ 96 (20 UF) if a family member has physical disability.

Regardless of which program is used, both alternatives require the following building standard es-

tablished in MINVU Chile (2009) adjusted in Article 49 MINVU Chile (2012):

1. Dwelling should have a minimum of two bedrooms and all the rooms have to commit to the minimum square area per room shown in the D.S. No 174.

2. The given property should have a minimum total floor area of 450 ft^2 (48 m^2) allowing incremeting total floor area to a minimum of 600 ft^2 (55 m^2).

3. The building cost should not be higher than US$ 4,3625 (900 UF).

Image: SHR in Atacama
Source: www.minvu.cl

4. The extension of the total square area should be previously approved by local council.

5. Building specifications should meet Chil-

Image: FSV in Viña del Mar
Source: www.minvu.cl

Image: FSV in Punta Arenas
Source: www.minvu.cl

2.3.2 The incremental housing concept with participative design.

In Chile architectural firms are addressing proposal type FSV and SHR by employing the incremental dwelling concept with participative design. Elemental Chile group has led this proposals. Aravena and Iacobelli (2012) enphasize that an alternative to provide low-income housing units with value over

Image: before and after affordable multifamily building in Monterrey, Mexico.
Source: www.elemental.cl

Image: before and after affordable multifamily building in Iquique, Chile.
Source: www.elemental.cl

time is by locating them in consolidated urban or rural areas. However, they add, elevated land cost and limited FSV's budgest do not allow to complete 500 ft^2 to 600 ft^2 in these urban areas. They conclude, thereby, that the solution is to use the FSV budget to acquire the land in these locations and build dwelling portion that owners would not afford to build in the sooner future. The occupiers receive an unfinished building, but it possesses the main building structure that let them to easily finish the 600 sf total building without major costs. In addition, this strategy considers participative design with the owners, letting them plan how to

complete the total floor area regarding their particular needs. This strengthens not only the sense of property between owner and building, but also the social integration with the inhabited territory.

2.3.3 Chilean thermal design code applied to adobe walls.

The TDC in OGUC Artículo 4.1.10 defined in 2000 "R" value for roof partition. Later, in 2007 the ventilated floor, wall, and window partitions were included in the code set. According to daily hottest temperatures estimation during a full year, TDC divides the national territory in sevent climate zones as shown in Figure 2.3.3.1.

As was reviewed in section 1.4, the VIII Bio-Bio Region has been historically the South geographic limit for adobe architecture because humidity affects this material. The VIII Bio-Bio Region beyonds the Climate zone 4, which establishes R value of 0.59 m^2K/W or U value of 1.7 W/m^2K.

Table shown in table 2.3.3.2 was developed in this

Figure 2.3.3.1: Climate zones in Chile
Source: TDC 4.1.10, MINVU Chile Chile.

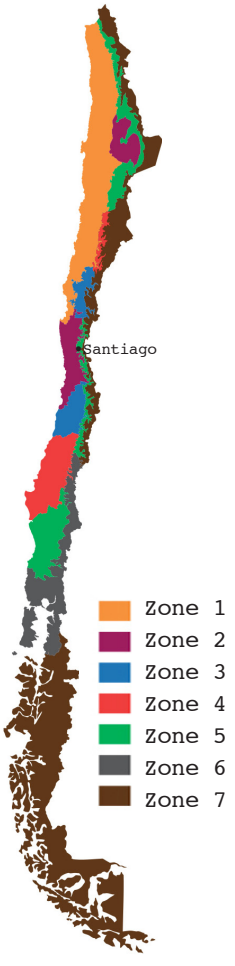

research to determine the adobe wall thickness meeting U values required for wall partitions in each climate zone. The calculation of these values uses thermal conductivity for adobe of 0.71 W/m-K or 4.923 (Btu*in/h*ft^2°F), employed by Choksiri-wanna and Lertwattanaruk (2011), which represents an adobe block with reduced organic content as was reviewed studied case in section 1.7.2 of this re-search.

2.3.4 Seismic design code in Chile applied to adobe walls.

The SDC NCh 433 of.96 does not have regulation for adobe architecture. The "Anteproyecto de Norma" NTM 002 2010 (NTM 2010) is the first document in de-

Table 2.3.3.2: Adobe wall thickness for adobe wall from thermal zone 1 to 4 using thermal conductivity of 0.71 W/m-k (adobe block with reduced vegetable content)
Source: SM creation based on TR OGUC Artículo 4.1.10 and Heathcote (2010).

Thermal Code OGUC Artículo 4.1.10							Windows			Wall thickness for Adobe without vegetable content	
	Roof		Walls		ventilated Floor		Monlitic	Hermetic Double			
Thermal Zone	U W/m2k	R m2k/W	U W/m2k	R m2k/W	U W/m2k	R m2k/W		3,6 W/m2K >=U> 2,4 W/m2K	U<2,4 W/m2K	inches	cm
1	0,84	1,19	4,0	0,25	3,60	0,28	50%	60%	80%	7.1	18
2	0,60	1,67	3,0	0,33	0,87	1,15	40%	60%	80%	9.4	24
3	0,47	2,13	1,9	0,53	0,70	1,43	25%	60%	80%	15.3	39
4	0,38	2,63	1,7	0,59	0,60	1,67	21%	60%	75%	16.5	42
5	0,33	3,03	1,6	0,63	0,50	2,00	18%	51%	70%	____	____
6	0,28	3,57	1,1	0,91	0,39	2,56	14%	37%	55%	____	____
7	0,25	4,00	0,6	1,67	0,32	3,13	12%	26%	37%	____	____

Figure 2.3.4.1: Seismic zonation map of the country
Source: NCh 433. Of.96.

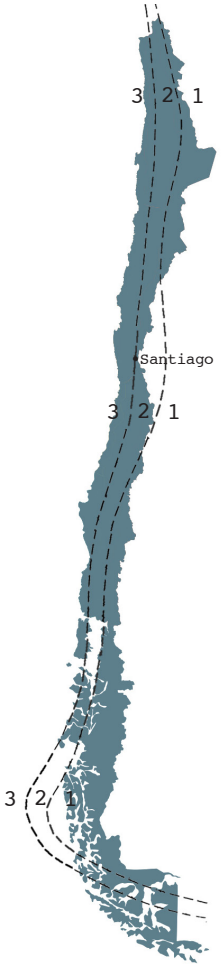

velopment to regulate this natural material. Current seismic design code in Chile (SDC) NCh 433 was elaborated by the Chilean Government in 1996, and has not been updated since then. After the last earthquake in F2010, researches are aiming to update the NCh 433 of.96.

SDC divides the national territory in three seismic zones, specifying the peak ground acceleration "A_o" as shown in Figure 2.3.4.1 and Table 2.3.4.2. This code also classifies the soil type "*T'*" in four groups as shown in Table 2.3.4.3 and the importance class of the building "*I*", also in four categories as shown in Table 2.3.4.4.

Two methods are specified for seismic design procedures, the Static analysis method (SAM), which uses the static equivalent of the lateral forces in the Romanic Code and the Spectral modal analysis method (SMAM).

Static analysis method (SAM):

The NCh 433 of.96 specifies that SAM applies to

Table 2.3.4.2: Ground zone according to seismic zone
Source: NCh 433.Of96 Chilean Code.

Seismic zone	A_0
1 (at the border with Argentina)	0.20 g
2	0.30 g
3 (shores)	0.40 g

Table 2.3.4.3: Foundation soil types
Source: NCh 433.Of96 Chilean Code.

Foundation soil	S	T_0 [s]	T' [s]	n	p
I	0.90	0.15	0.20	1.00	2.0
II	1.00	0.30	0.35	1.33	1.5
III	1.20	0.75	0.85	1.80	1.0
IV	1.30	1.20	1.35	1.80	1.0

Table 2.3.4.4: Importance class of building
Source: NCh 433.Of96 Chilean Code.

The importance class of the building	I
A (high importance)	1.2
B	1.2
C	1.0
D (low importance)	0.6

structures which meet the following conditions:

• Are built on soil type C (unsaturated sands and gravels, cohesive soils with the undrained shear, S_u, between 0.025 and 0.10 MPa) or D (cohesive soils with S_u ≥ 0.025 MPa) and are located in the seismic zone I (with the PGA = = 0.20g – table 2.3.4.2).

• Do not exceed 5 stories or 20 m height.

• In structures which have 6 to 15 stories, the application of the method is permitted provided that: (1) the ratio between the total building height and the modal vibration periods with the highest translational equivalent mass in “x” and “y” directions are at least equal to 40 m / s and (2) the distribution of the horizontal seismic forces of SAM is such that shears and overturning moments at each

level must not differ with more than 10 % with respect to those obtained through a spectral modal analysis with the same base shear force.

The following formulas allow to determine the shear force Q_o and the seismic coefficient C:

C: Seismic coefficient.

I: Importance class of the building.

P: total weight of the superstructure n.

T': Parameters depending on the foundation soil

$$Q_0 = CIP$$

$$C = \frac{2.75 \cdot A_0}{g \cdot R} \cdot \left(\frac{T'}{T^*} \right)^n$$

shown in Figure 2.3.4.2.

A_o: peak ground acceleration

R: seismic response reduction factor

*T**: Mode vibration period with the highest translational equivalent mass in the direction of analysis.

With regard to the seismic coefficient, the value A_0 /6g and values in table 2.3.4.5 are the minimum and maximum numbers accepted by the SDC.

The distribution of the seismic forces over the

Table 2.3.4.5: Seismic coefficient parameters. **Source:** NCh 433. Of.96.

R	C_{max}
2.0	0.90 $S \cdot A_0$ / g
3.0	0.60 $S \cdot A_0$ / g
4.0	0.55 $S \cdot A_0$ / g
5.5	0.40 $S \cdot A_0$ / g
6.0	0.35 $S \cdot A_0$ / g
7.0	0.35 $S \cdot A_0$ / g

height of the structure is proportional with the mass and the height of each floor with respect to the base of the building, as shown in following formulas:

$$F_k = \frac{A_k \cdot P_k}{\sum_{j=1}^{N} A_j \cdot P_j} \cdot Q_0$$

Where:

$$A_k = \sqrt{1 - \frac{Z_{k-1}}{H}} - \sqrt{1 - \frac{Z_k}{H}}$$

Z_k: distance from floor k to the base of the building.

H: height of the structure.

Structures with two or more levels are required to be always calculated as if there was such a rigid diaphragm. However, if it is desired to design a non diaphragm floor, the element which resist seismic forces should be designed to resists horizontal force of $1.20F_N g/P_N$ times the corresponding mass.

SAM results in seismic forces applying in two direction (X and Y). These forces must be combined with those resulted from the accidental eccentricity or torsion analysis, forming the torsion moment.

± 0.10 $b_{by}Z_k/H$ for the seismic action in Y direction.

± 0.10 $b_{bx}Z_k/H$ or the seismic action in X direction.

Where

b_{kx} and b_{ky}: Largest dimension of the structure.

k: Story level.

Spectral modal method (SMAM)

This method is applied to structures with regular modes of regular vibration and 5% approximately damping ratios. The spectrum S is determined using the following formula:

In this formula I and A_o used values given in figure 2.3.4.1., 2.3.4.3. Figure 2.3.4.6 represents the amplification factor "α", which results for each vibration mode, n, with the following formula.

$$S_a = \frac{I \cdot A_0 \cdot \alpha}{R^*}$$

T_n: vibration period for the n-th vibration mode.

T_o, p: parameters depending on the type of foundation soil.

$$\alpha = \frac{1 + 4.5\left(\frac{T_n}{T_0}\right)^p}{1 + \left(\frac{T_n}{T_0}\right)^3}$$

The reduction factor R* is calculated as shown the following formula and is represented by the figure 2.3.4.7:

$$R^* = 1 + \frac{T^*}{0.1 \cdot T_0 + \frac{T^*}{R_0}}$$

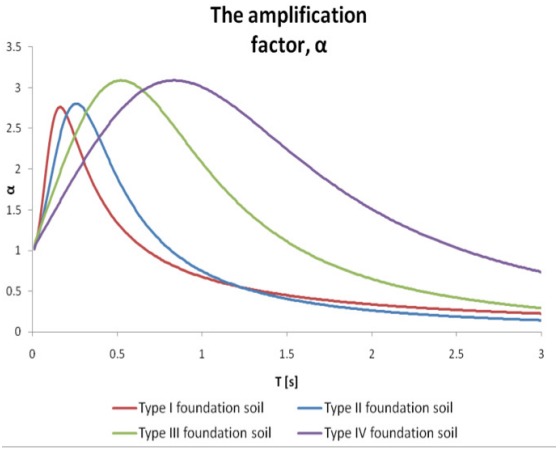

Figure 2.3.4.6: Amplification factor **α**
Source: NCh 433.Of96 Chilean Code.

T^*: mode vibration period with the highest translational equivalent mass in the direction of analysis.

R_o: the global reduction factor of the structure, given in tables by the Chilean code.

R_o can take the value of 4 or 9

depending on the amount of contribution of walls or frames to the lateral force resisting system.

Figure 2.3.4.7: The reduction factor R*, for foundation soil type I and IV and different types of structural systems.
Source: NCh 433.Of96 Chilean Code.

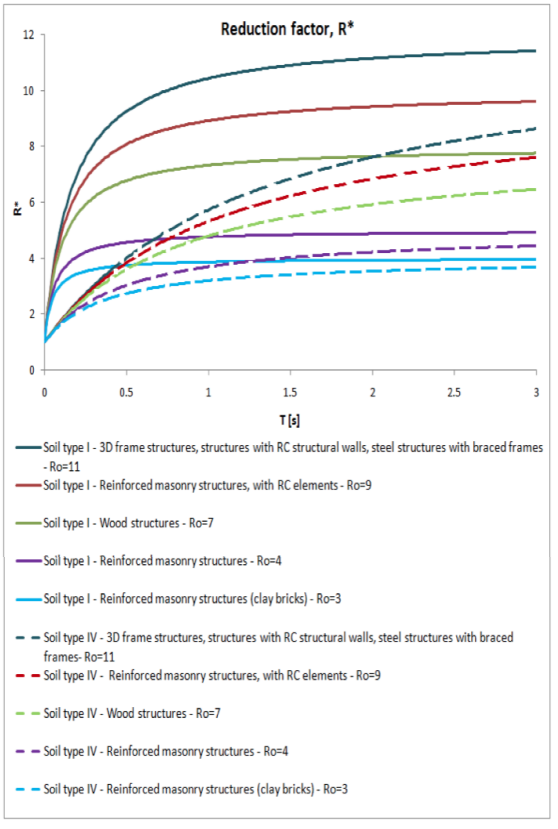

2.4 Problem statements

1. PRTM (2010) report evidences that adobe properties were the most affected by the M_w = 8.8 earthquake in Chile in F2010 as was reviewed in section 1.1. Its poor seismic resistance, leaded by the low tensile strength, generates not only substantial loss in lives and costs in reconstruction, but it also affected the traditional architecture based on dried sun earth block.

2. The warning of employing adobe has increased and the use of it has been reduced due to three main aspects: (1) communities lack of information in adobe construction, (2) the rapid introduction of contemporary industrialized & fast construction techniques such as clay or cement bricks or steel based systems.

3. The seismic design code in Chile (SDC) NCh 433 of.96 does not have regulation for adobe architecture, thereby mitigation strategies to seismically protect adobe lack of local and certified standard solutions.

4. As was reviewed in section 2.1 the polymer mesh is currently one of the most effective seismic retrofit systems to avoids adobe building collapse, achieving moderate to high protection by increasing the tensile capacity of adobe structures. However, its intallation requires porfessional assistance ,and also, in high intensity seismic events the adobe block remains with servers damaged, which might address further thermal limitations, moisture infiltration, and seimic damages.

5. As was reviewed in section 2.3, the Chilean housing Ministry can only afford to locate low-income housing types FSV or FHR in non consolidated neighborhoods. This results in inhabitants lacking healthy, growing with vulnerability, and housing properties that can not increase their capital value.

2.5 Research objectives

1. Explore an affordable alternative to reduce earthquake damage in new housing units and traditional housing built out of adobe in Chile.

2. Conserve the adobe tradition in Chile, which constitutes one of its cultural components and defines the national identity.

3. Complement with knowledge in adobe construction in Chile to provide communities with confidence of employing this natural material to build their homes.

4. Contribute to develop the seismic design code for adobe architecture “Anteporyecto de Norma NTM 002” (2010).

5. Propose adobe for designing affordable housing type FSV and FHR in consolidated neighborhood using expanded building concept with participative design. This would increase the housing unit capital value and greater social integration with the territory.

2.6 Summary approach

Chapter I and II: These chapters have presented the main context of adobe architecture in Chile, focusing on understanding both aspects, conditions that affect its poor seismic resistance and strategies that are currently employed to mitigate damages.

This content presents the SBI, based on studies done in steel and concrete structures, with the aim of knowing alternatives of seismic protection in adobe structures beside reinforcement systems.

2.7 Organization report

With the aim of reducing earthquake damages in adobe housings in Chile, this research will explore the effects of using a SBI. The following Chapter presents the analysis of both proposals: The Adobe dwelling prototype and the SBI designed for the adobe dwellling prototype.

Chapter III Proposal: The Adobe dwelling prototype organization: The location is chosen according to the current TDC and the SDC, climate conditions are analyzed, the prototype layout is presented and alternatives of expantion are shown with architectural drawings. After this, the layout is adjusted with daylight design, passive ventilation design, and energy usage design employing the prototype fully finished unit of 645 ft^2.

Chapter IV Proposal: Seismic base isolator for the adobe dwelling prototype.

The first part of this chapter presents theoretical concepts involved in the analysis, condition for the seismic analysis, seismic building codes required for the analysis, mechanical properties of materials, and analysys methodology. The second part of this section focuses on presenting the analytical parameters defined by SAM and SMAM.

The third part is the seismic analysis: The software package SAP 2000 is used to model the proposed methodology, comparing four adobe structures using SAM and SMAM.

A. Adobe structure (AS) model with basal restriction to lateral displacement and rotation, with and without polymer mesh using SAM.

B. AS model with basal restriction to lateral displacement and rotation, with and without polymer mesh using SMAM according to NCh 433 of.96 and R_o = 1.

C. AS model with basal restriction to rotation and vertical displacement, with springs to restrict

horizontal displacement, with and without polymer mesh, using SAM.

D. AS model with basal restriction to rotation and vertical displacement, with springs to restrict horizontal displacement, with and without polymer mesh, using SMAM according to NCh 433 of.96.

The last part of this chapter attemps to estimate cost analysis, local & broad implications, and installation process to evaluate the affordability of the proposed SBI.

***

Chapter III
Proposal: The Adobe Dwelling Prototype

Image: Adobe prototype designed to evaluate the proposed SBI.
Source: SM creation.

This section presents the adobe dwelling prototype used to evaluate the proposed seismic base isolator. The adobe prototype is located in the Concepcion, VIII Bio-Bio Region. This unit is designed considering both the structural conditions necessary to evaluate the seismic isolator analyzed in Chapter IV, and additionally, suggests improvements to standard affordable housing in Chile with subsides type FSV and SHR. The implementation of this system holds the potential for far reaching social integration and environmental impacts. Following this line of thinking, the dwelling layout approaches the development goals by addressing two fundamental concepts reviewed in section 2.3.2:

1) The modular building concept.

2) The incremental housing concept with

participative design.

Construction settings of the adobe dwelling prototype meet the thermal design code MINVU (2006) OGUC 4.1.10, the Seismic design code in NCh 433 Of 1996 Mod 2009/ D.S.61, and the minimum conditions required by FSV and SHR MINVU Chile (2009). SketUp architect modeling was created folloiwng recommendations in PUC (2009) "Design Guide for Energy Efficient Affordable Housing" and Edmister (2009) "The energy free homes for a small planet" to adjust the layout. Finally, to determine energy usage, daylight, natural ventilation, and the incremental floor area alternatives respectively, the designed layout is assessed in modeling performance software Integrated Enviromental Solutions (IES VE) by using tool packages Flucs DL, Radiance fc, Macro Flow, and Apache simulator.

Image: Bio-Bio river mouth in Concepcion.
Source: http://dmat.cfm.cl/images/ConcepcionDesembocadura2-big.jpg

Adobe prototype details:

- Location: Concepcion, VIII Bio-Bio Region.
- Climate zone: Zone 4
- Seismic zone: 3
- Total gross area : 645 ft^2 (60 m^2)
- HVAC System: Split system + nat. ventilation.
- EUI: 41 kBtu /ft^2

3.1 Geographical location

Figure 3.1.1: Combined map of climate zones and seismic zones in Chile.
Souce: SM creation based on reviewed literature.

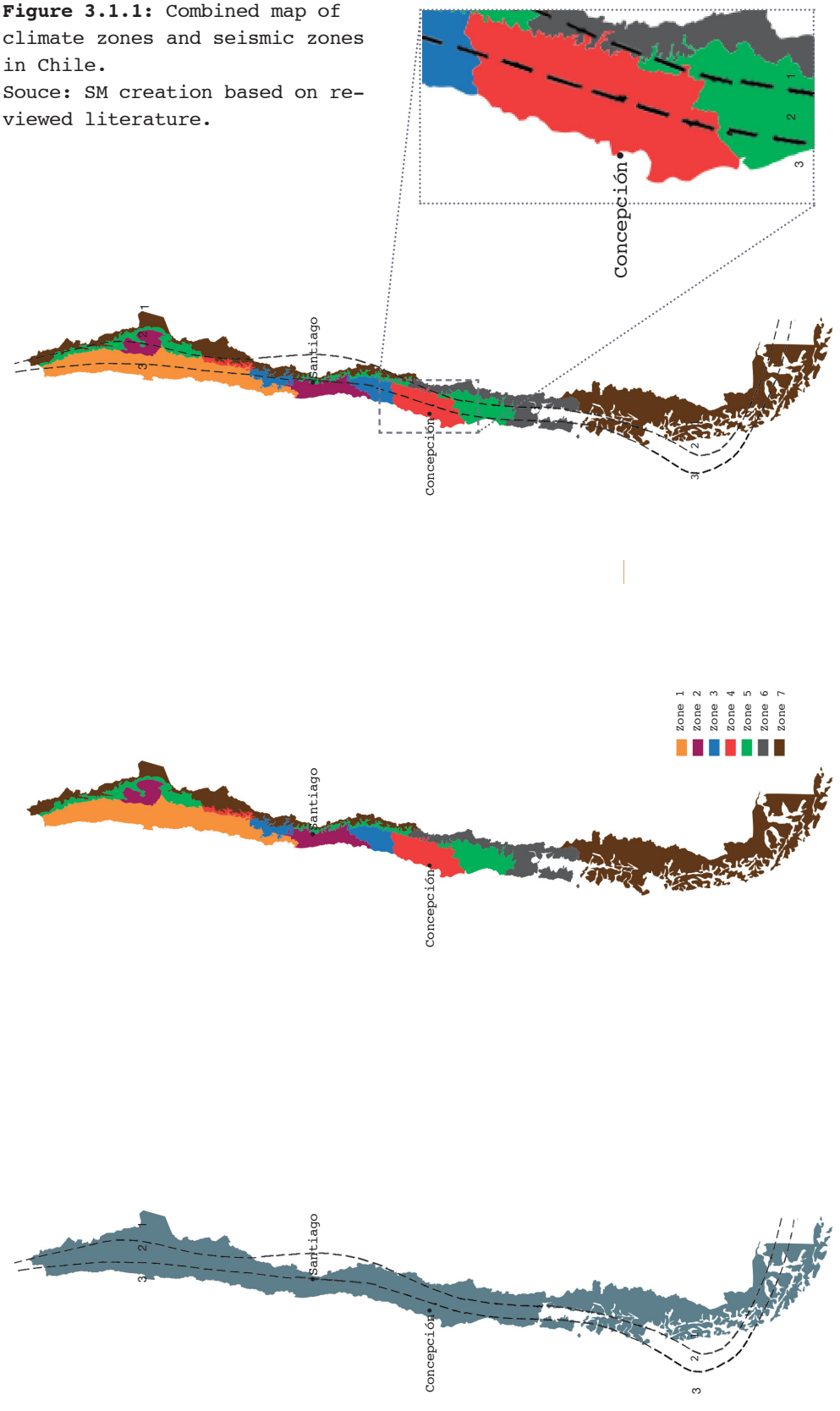

Figure 3.1.1 C: Combined map Seismic zones and Climate zones
Source: SM creation based on NCh 433-1996 and NCh 433.Of96 Chilean Code.

Figure 3.1.1 B: Climate zones
Source: MINVU (2006) OGUC 4.1.10

Figure 3.1.1 A: Seismic zones map
Source: Sesimic Building Code NCh 433-1996

The most basic design of the structures in Concepcion are a direct reflection of the weather conditions within the region, and therefore serves as the framework for designing the adobe dwellings that have been chosen for analysis using systems of seismic base isolation. This city is located within the Climate Zone 4 according to the TDC MINVU (2006) OGUC 4.1.10, and Zone 3 according to the SDC in NCh 433 Of 1996 Mod 2009/ D.S.6 (reviewed in section 1.4 and 1.7). Climate Zone 4 is the southeast territory where adobe constructions are used and the seismic Zone 3 is the most vulnerable soil type territory for seismic design in Chile.

3.2 Climate conditions

Figure 3.2.1: Annual temperatures and precipitations
Source: www.theweatherchanel.com

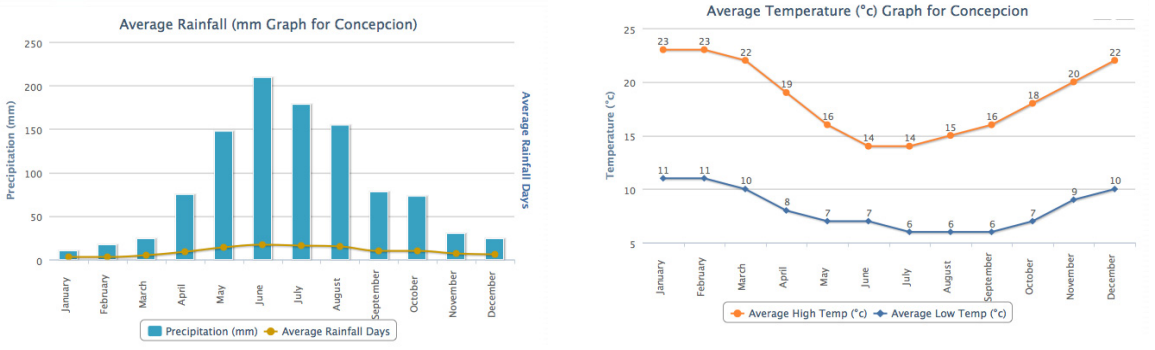

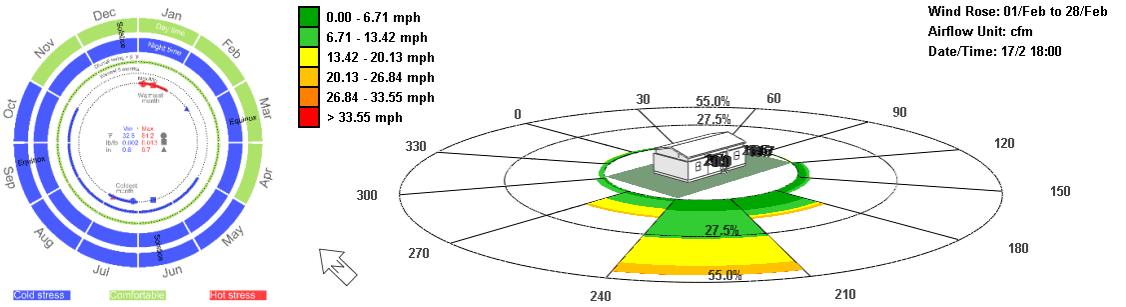

Figure 3.2.2: Weather summary and wind direction in summer (February 17th)
Source: Weather report IES VE.

Weather profile simulation data used in IES VE:

CHL_Conception. 856820_IWEC.epw

Location: Conception

Latitude: 36.77 S

Longitude: 73.07 W

Temperatures:

Highest T°:

The warmest period of time is between January and April with the highest annual temperature registering at 84.2° F during January.

Lowest T°:

The coldest period of time is between July and October with the lowest annual temperature registering at 32.5° F during July.

Precipitation:

The annual rainfall is 43.705". Generally the dri-

est month of the year is February with an average of 0.575" of rainfall. The wettest month is July with 8.744" of rainfall. The wettest four months are from July to October.

Solar energy:

The annual hourly mean global radiation is 187.5 Btu/ft^2 and the main daily global radiation is 1430.4 Btu/ft^2.

Winds:

The annual mean wind speed is 12.6 ft/s. The annual mean direction of wind is East of North -121.1°

Climate advantages in Concepcion area for passive technologies:

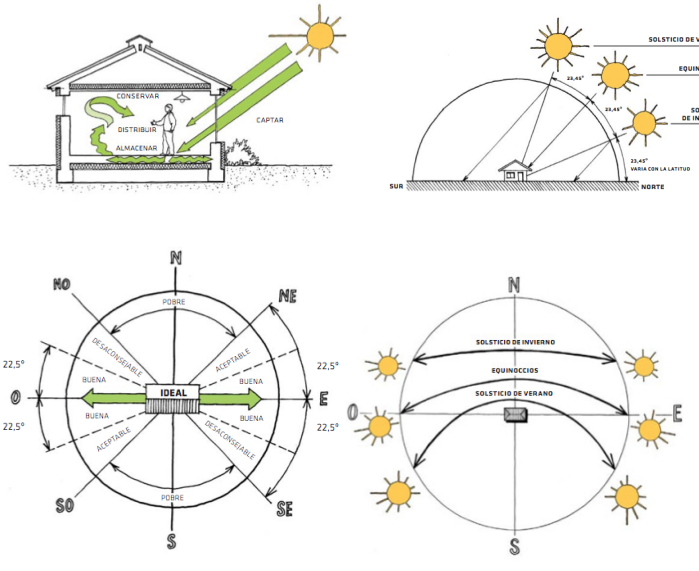

- Solar exposure: Elongate buildings E/W.
- Solar gain: Summer night cooling in con-

Figure 3.2.3: Diagrams of passive desgin strategies in Chile.
Source: "Design guide for energy efficient affordable housing" described in PUC (2009)

junction with thermal mass. Convective indirect solar/mass storage sol-air systems (Baer, Barra etc) and trombe type indirect solar gain collectors. Sun buffer spaces or winter gardens (opaque roof, unheated, > 1 storey better). Winter direct passive solar heating with diurnal swing in temps.

• Ventilation: The double skin transparent facade with cavity shades provides a solar bufferspace in winter. Effective cross ventilation (windward and leeward openings), including suction zone forms - roof wind troughs, and north lights (top floors).

• Light: Shelves inside and outside the extension improves daylight uniformity and provides solar shading.

Image: Adobe prototype placed in rural area of the VIII Bio-Bio Region.
Source: SM creation

3.3 Prototype layout

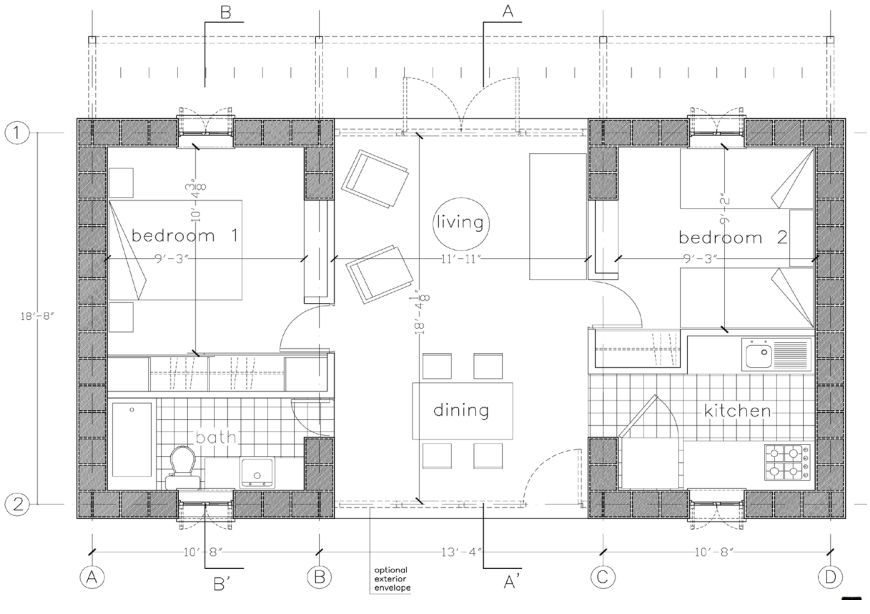

Figure 3.3.1: Dwelling floor plan. **Source:** SM creation.

As shown in Figure 3.3.1 the proposed dwelling is a one story E/W which elongates the building to gain maximum solar exposure according to PUC (2009) "Design guide for energy efficient affordable housing" and passive design criteria in Edminster (2009) "the Energy Free Homes for a small Planet."

The prototype unit is composed by two "C" adobe walls as shown in the floor plan in Figure 3.3.2. The building layout combines two design criteria:

1) Modular Building:

The proposed dwelling allows a flexible configuration which can be used in the different geographical territories of Chile as shown in figure 3.3.3. The layout design enables settlement like detached units, strip proposals, or multifamily structures around a coreyard. See you. un abrazo !

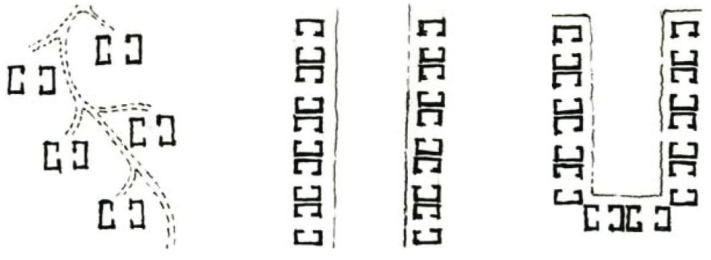

Sprawl Strip multifamily

Figure 3.3.2: Modular building configurations.
Source: SM creation.

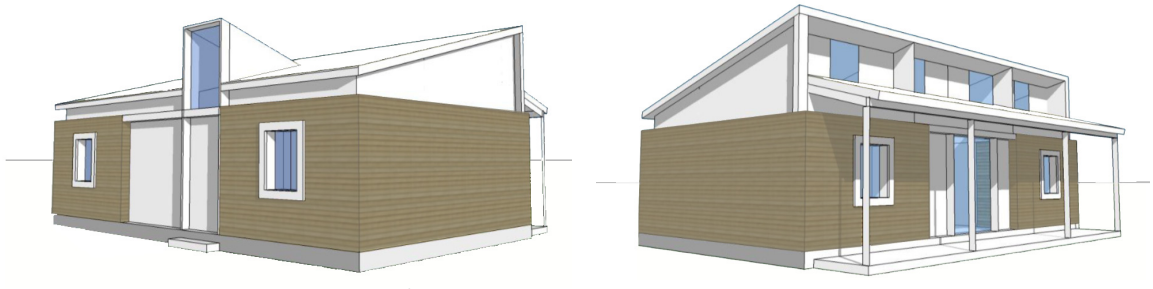

Images: Front and back elevations
Source: SM creation using SketchUp and Photoshop.

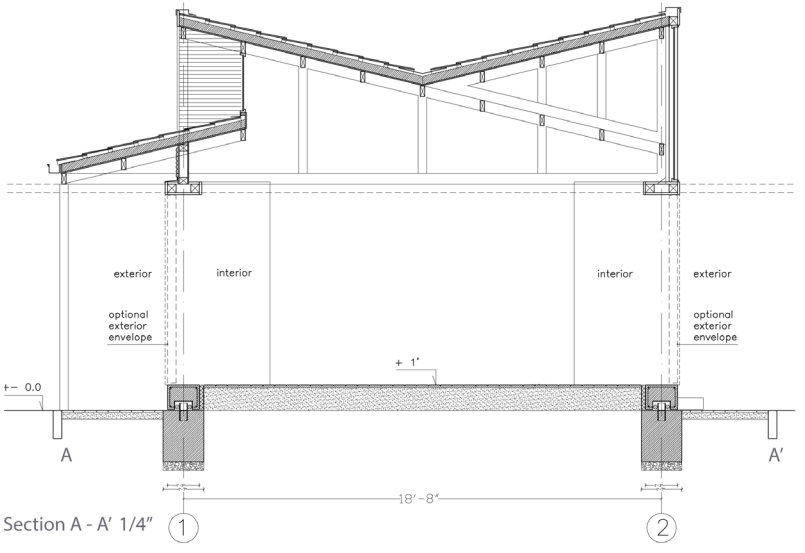

Section A - A' 1/4"

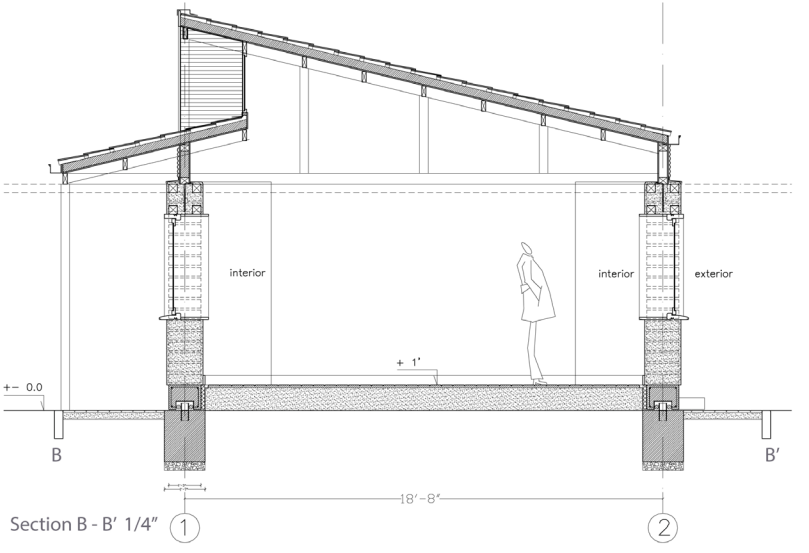

Section B - B' 1/4"

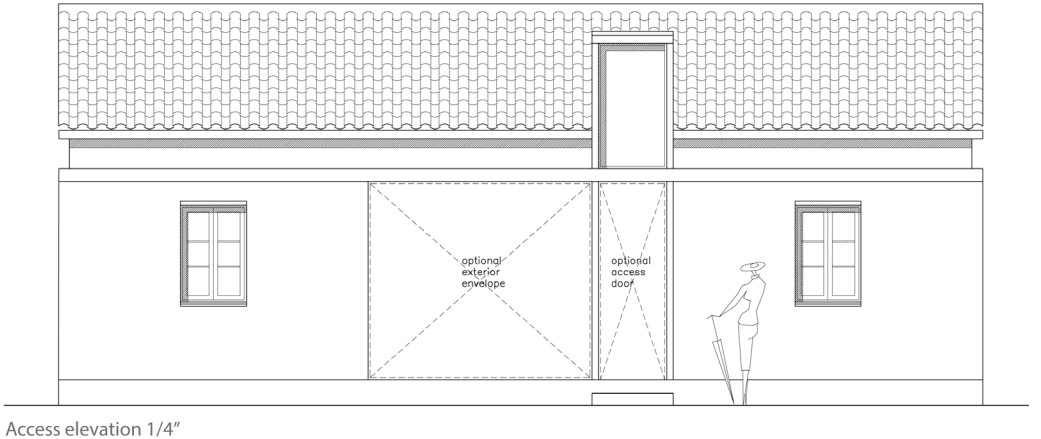

Access elevation 1/4"

Figure 3.3.3: Architecture of the dwelling. Ssection and optional acces elevations in following page.
Source: SM creation.

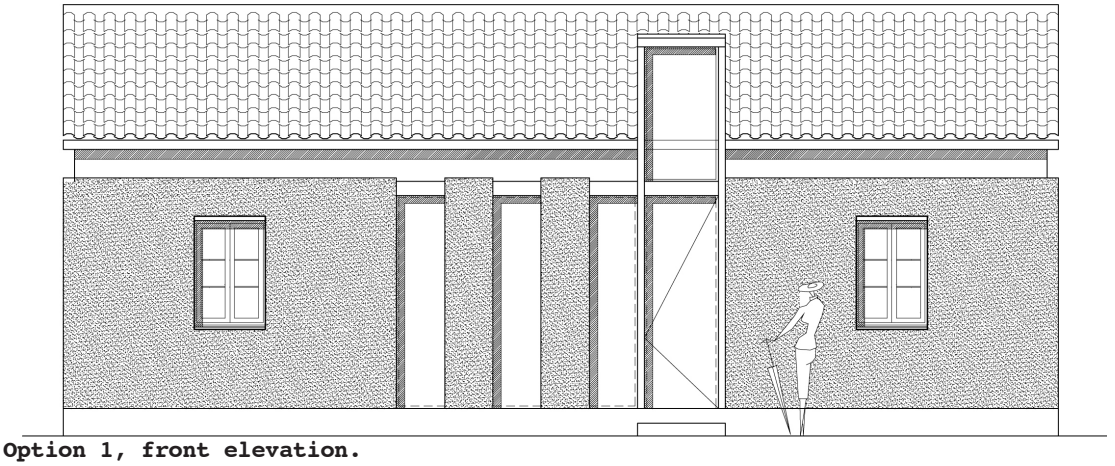

Option 1, front elevation.
Finishing: Adobe + glazed panels.

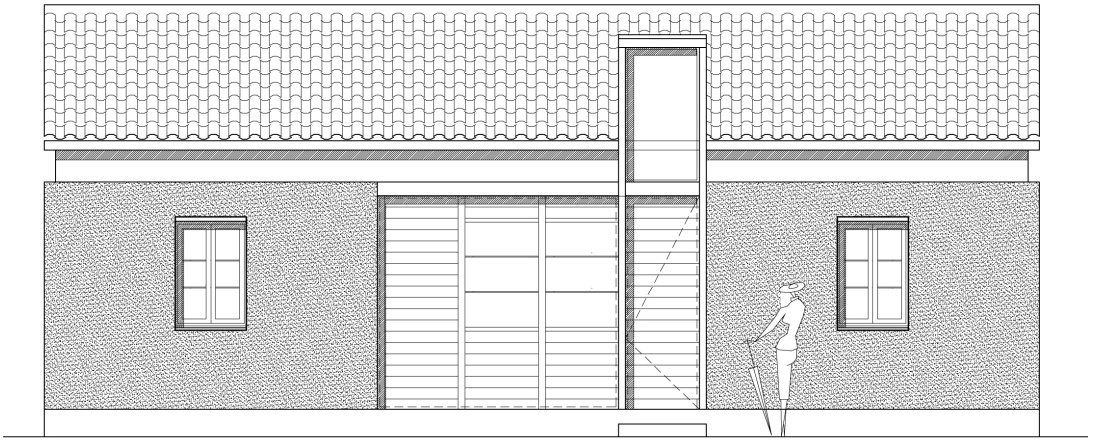

Option 2, front elevation.
Finishing: Timber stud + sliding windows.

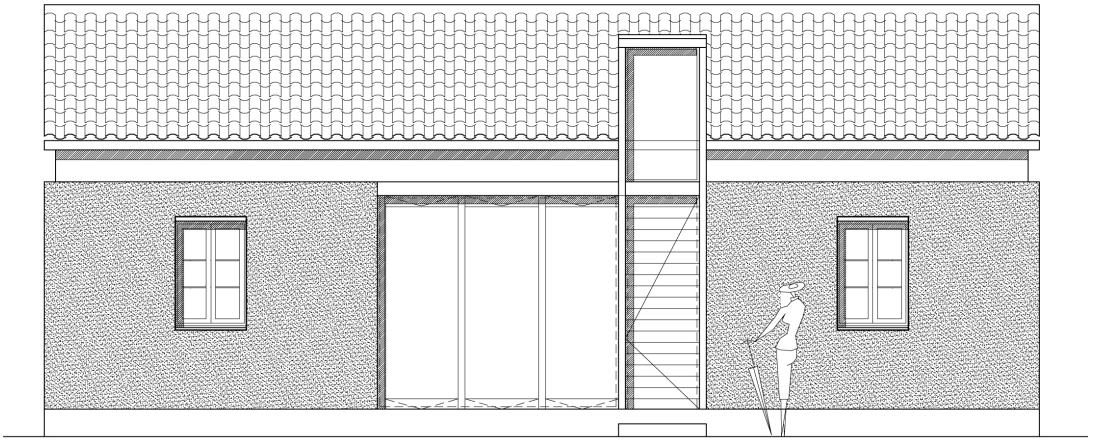

Option 3, front elevation.
Finishing: glazed panels.

2) The incremental housing concept with participative design.

This establishes a design framework with the aim of both allowing customization as well as the strengthening of the social integration within the local territory. The proposed adobe prototype does not include an exterior envelope in the center area of the building (between the two "C" adobe walls). Thus, by employing this design strategy the total floor area can incremet from 452 ft^2 (42 m^2) to 645 ft^2 (60 m^2). The additional floor area created by the expansion can be completed with adobe structure, lighter structures, or translucent envelope solutions as illustrated in Figure 3.3.3 with acces elevation options.

3.4 Construction settings (IES VE)

Table 3.4.1: thermal design code in Chile.
Source: SM creation based on TDC OGUC Artículo 4.1.10 and Heathcote (2010).

Thermal Code OGUC Artículo 4.1.10							Windows			Wall thickness for Adobe without vegetable content	
	Roof		Walls		ventilated Floor		Monlitic	Hermetic Double			
Thermal Zone	U W/m2k	R m2k/W	U W/m2k	R m2k/W	U W/m2k	R m2k/W		3,6 W/m2K >=U> 2,4 W/m2K	U<2,4 W/m2K	inches	cm
1	0,84	1,19	4,0	0,25	3,60	0,28	50%	60%	80%	7.1	18
2	0,60	1,67	3,0	0,33	0,87	1,15	40%	60%	80%	9.4	24
3	0,47	2,13	1,9	0,53	0,70	1,43	25%	60%	80%	15.3	39
4	0,38	2,63	1,7	0,59	0,60	1,67	21%	60%	75%	16.5	42
5	0,33	3,03	1,6	0,63	0,50	2,00	18%	51%	70%	____	____
6	0,28	3,57	1,1	0,91	0,39	2,56	14%	37%	55%	____	____
7	0,25	4,00	0,6	1,67	0,32	3,13	12%	26%	37%	____	____

Table 3.4.2: Prototype baseline construction settings.
Source: SM creation based on IES U value computing.

Construction setting	Type	(R) value Z4 Ch.OGUC 4.1.10	(U) value Z4 Ch.OGUC 4.1.10	(U) value assigned
1 Exterior walls	2 In mud stucco with 16 In Adobe block	0.59	1.7 to 1.1	0.216
2 Exterior walls above adobe wall	Framed wall with 2 In Insulation above adobe wall	0.59	1.7 to 1.1	0.104
3 Interior walls	Light -weight plasterboard partition	----	----	0.2807
4 Ground floor slab	Un insulated solid-ground floor	1.67	0.6 to 0.36	0.124
5 Roofs	Sloping Roof (insulated to 1995 UK Reg)	2.3	0.38 to 0.28	0.041
6 Exterior windows	Low-e double-glazing 6mm +6mm (2002 reg)	----	----	0.370
7 Interior windows	Single-glazed domestic windows	----	----	0.8505
8 Roof light	low e double -glazed roof lights	----	----	0.2807

IES Apache was used to determine baseline construction settings according to Zone 4 TDC MINVU (2006) OGUC 4.1.10. Adobe wall was created using Choksiriwanna and Lertwattanaruk (2011) organic content adobe brick with thermal conductivity k of 0.71 W/m-K or 4.923 (Btu*in/h*ft^2°F) as was reviewed in section 1.7.2 of this research. For climate zone 4 U value of 1.7 W/m^{2}K is required. This research purpouse for the baseline model 16" structural adobe wall with 1" exterior and interior mud plaster, computing a total thickness of 18" with U value of 0.216 W/m^{2}K.

The other construction components assigned to the baseline model also meet minimum U value required for Thermal zone 4 as shown in Table 3.4.2.

3.5 Daylight design (IES VE)

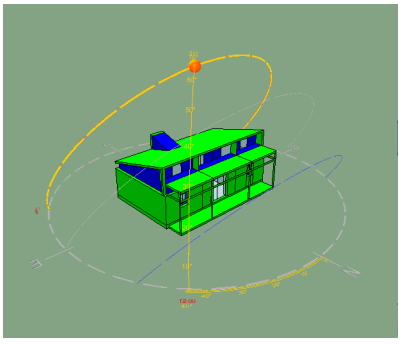

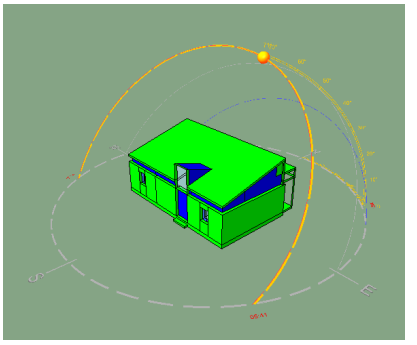

Images: E/W Adobe prototype wit E/W orientation for maximum solar exposure.
Source: SM creation using Model viewer II, IES VE.

IES Flucs DL program was employed to determine the preliminary window design for the prototype dwelling. Three cases are analyzed using different window wall area ratios (WWAR) to identify optimal daylight factors (dl) and foot candle (fc) as shown Figure 3.5.1.

Case 1: 13% WWAR

Case 2: 15% WWAR

Case 3: 16% WWAR + skylights.

The LEED Credit 8.1 is used as a goal for optimal daylighting design, requiring 50% to 70% total gross area over the threshold 25 foot candle. The results show that 16% WWAR + skylights provides the optimum daylight levels for this adobe dwelling prototype. In case 3, 55.3% of the total floor area

is over the threshold LEED Credit 8.1 request.

Case 1: 13% WWAR

Case 1 is assumed as the base line for daylight deign. The model contains layout design with an ordinary double sloped roof. In regards to the glazing components, four regular 2′ x 4′ windows are included in bedrooms, bathroom, and kitchen; 4 regular 2′ x 4′ interior windows are placed between rooms, and two 3′ x 8′ glazing doors are located in the center of the dining area facing North.

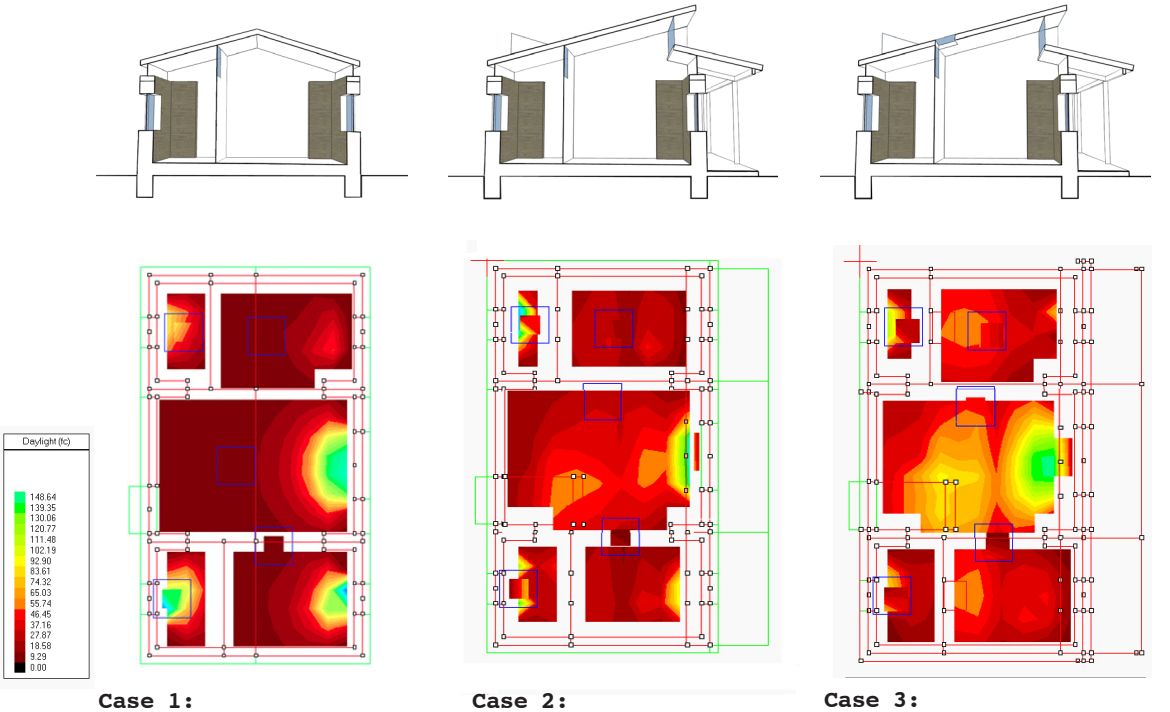

Case 1:
Doble slope roof
13% WWAR

Case 2:
Single slope roof
15% WWAR

Case 3:
Single slope
16% WWAR + skylight

Figure 3.5.1: Daylight analysis in studied cases using IES Flucs DL.
Source: SM creation using Sketchup and IES Radiance.

This strategy results in a glazing area of 161 ft^2, which represents 13% WWAR. However, the IES daylight report shows that the dinning/living room only meets the floor area over 25 fc threshold LEED Credit 8.1 request. The interior transparencies between rooms do not contribute with any significant improvement in terms of DL factor and FC levels.

Case 2: 15% WWAR

This case analyzes improvements to Case 1 to increase DL factors and FC levels. The 4 regular 2'x 4' windows located in bedrooms, bathroom, and kitchen remain with same dimensions so that the monolithic wall attributes are not affected, while simultaneously reducing seismic failures by using bigger windows as reviewed in section 1.6.3. The strategies used in this case are: New glazing areas of 118 ft^2 that are located South and North above the adobe wall, the double sloped roof is replaced by a single 23° sloped roof to allow light to enter into the rooms and living space in the winter and and a 5' awning on the north-facing windows to provide shade in the summer. Light admitted during

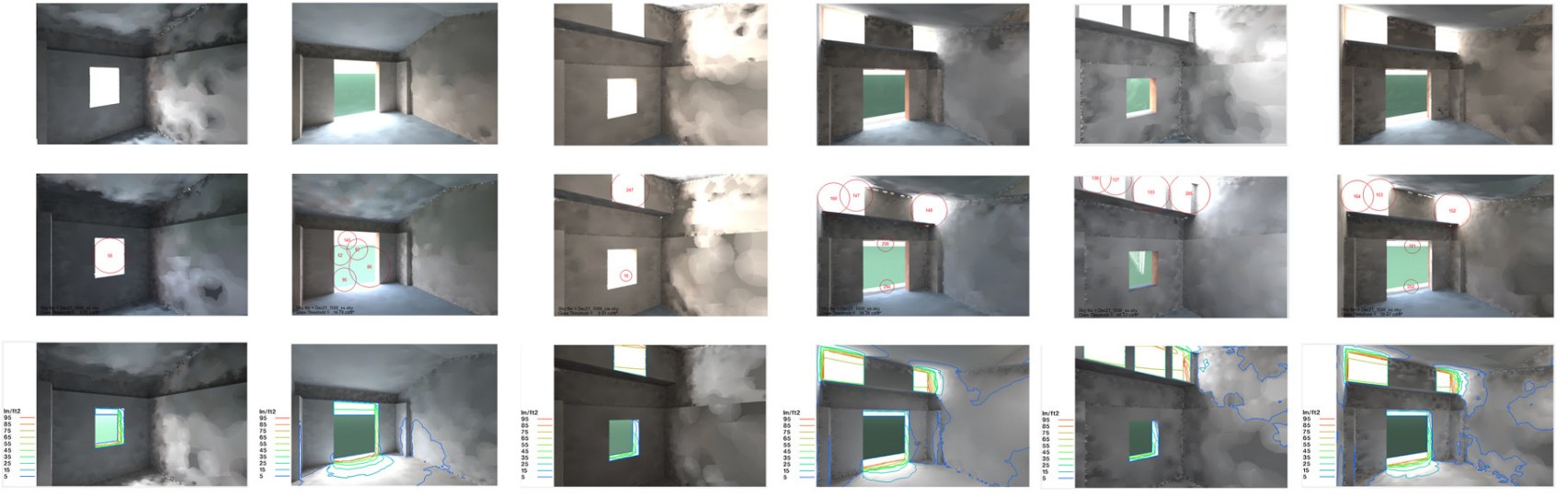

Rooms	areas	wall ares	Baseline glazed area	Added glazed area	Total glazed ares
Dinning / living	265.89	768.23	44.38	48.54	92.92
kitchen	67.03	313.56	9.11	8.09	17.2
Bathroom	55.414	285.67	9.11	8.09	17.2
Bedroom 1	134.25	533.03	9.11	8.09	17.2
Bedroom 2	122.63	511.06	9.11	8.09	17.2
Total ft2	645.214	2411.55	80.82	80.9	161.72

Rooms	% area over (25fc)	Average daylight (fc)	Average daylight factor %
LEED Credit 8.1 apply	50 to 70	25	2.0
Dinning / living	58.3	35	3.1
kitchen	13.3	17.4	1.5
Bathroom	22.2	26.4	2.3
Bedroom 1	6.9	12.4	1.1
Bedroom 2	7.2	13.4	1.2
Ext window area % of ext walls	13%		
Average DL factor	2.00%		
Area over 25 fc threshold	30.50%		FAIL !!!

Rooms	areas	wall ares	Baseline glazed area	Added glazed area	Total glazed ares
Dinning / living	265.89	768.23	44.38	48.54	92.92
kitchen	67.03	296.82	9.11	24.8	33.91
Bathroom	55.414	268.93	9.11	24.8	33.91
Bedroom 1	134.25	499.58	9.11	50.22	59.33
Bedroom 2	122.63	477.58	9.11	50.22	59.33
Total ft2	645.214	2311.14	80.82	198.58	279.4

Rooms	% area over (25fc)	Average daylight (fc)	Average daylight factor %
LEED Credit 8.1 apply	50 to 70	25	2.0
Dinning / living	58.3	35	3.1
kitchen	13.3	17.4	1.5
Bathroom	22.2	27	2.4
Bedroom 1	10.3	15.6	1.4
Bedroom 2	20.0	17.5	1.5
Ext window area % of ext walls	15%		
Average DL factor	2.10%		
Area over 25 fc threshold	31.80%		FAIL !!

Rooms	areas	wall ares	Baseline glazed area	Added glazed area	Total glazed ares
Dinning / living	265.89	768.23	44.38	48.54	92.92
kitchen	67.03	296.82	9.11	24.8	33.91
Bathroom	55.414	268.93	9.11	24.8	33.91
Bedroom 1	134.25	499.58	9.11	58.22	67.33
Bedroom 2	122.63	477.58	9.11	58.22	67.33
Total ft2	645.214	2311.14	80.82	214.58	295.4

Rooms	% area over (25fc)	Average daylight (fc)	Average daylight factor %
LEED Credit 8.1 apply	50 to 70	25	2.0
Dinning / living	58.3	35	3.1
kitchen	13.3	22.6	2.0
Bathroom	22.2	27	2.4
Bedroom 1	53	27	2.5
Bedroom 2	56	32	2.7
Ext window area % of ext walls	16%		
Average DL factor	2.80%		
Area over 25 fc threshold	55.30%		PASS !!

Figure 3.5.2: Radiance comparison images between three studied cases
Source: SM creation using IES Radiance.
Table 3.5.3: Summary of strategies employed in each estudied case.
Source: SM creation using IES Radiance.

the winter will passively heat the living space and rooms, reducing energy loads on the active heating systems. This strategy generates a total window area of 279 ft^2, which represents 15% WWAR. Although this particular configuration and scaling increased the DL factor and FC level in almost all the rooms, only 32% of the total area passed the 25 threshold LEED Credit 8.1 request.

Case 3: 16% WWAR + skylight

This case explores enhancements of DL factors and FC levels for case 2. The strategy focuses on increasing daylight levels in the bedrooms, bathroom, and kitchen area. Thus, 16 ft^2 of new glazed area are included above the adobe wall and on top the roof. This strategy generates a total window area of 295 ft^2, which represents 16% WWAR + skylights. This particular set of design variations results in 53.3% of the total area meeting the 25 threshold LEED Credit 8.1 request. Additionally, Radiance Fc analysis illustrates that the interior windows contributes by increasing the DL factor and FC levels of the section of roof that they are attached to.

3.6 Natural ventilation (IES VE)

The interior temperatures of the Living/dinnig room without natural ventilation in case 3 as illustrated in Figure 3.6.2 shows that in summer February 2nd the interior air temperature exceeds the rate of comfort (between 65 to 80 ˚F), increasing occupants' disatisfaction during the evening. On the other hand, in winter July 6th the interior temperature, while the exterior temperature is lower than 55˚F, the interior is kept within the range of comfort. In consequence, passive strategies of natural ventilation are required to be employed to reduce

Figure 3.6.1: Case 1 Macro Flow without natural ventilation.
Source: IES Macro Flow.

Figure 3.6.2: Case 1 temperatures in winter and summer without nat.ventilation.
Source: IES Macro Flow.

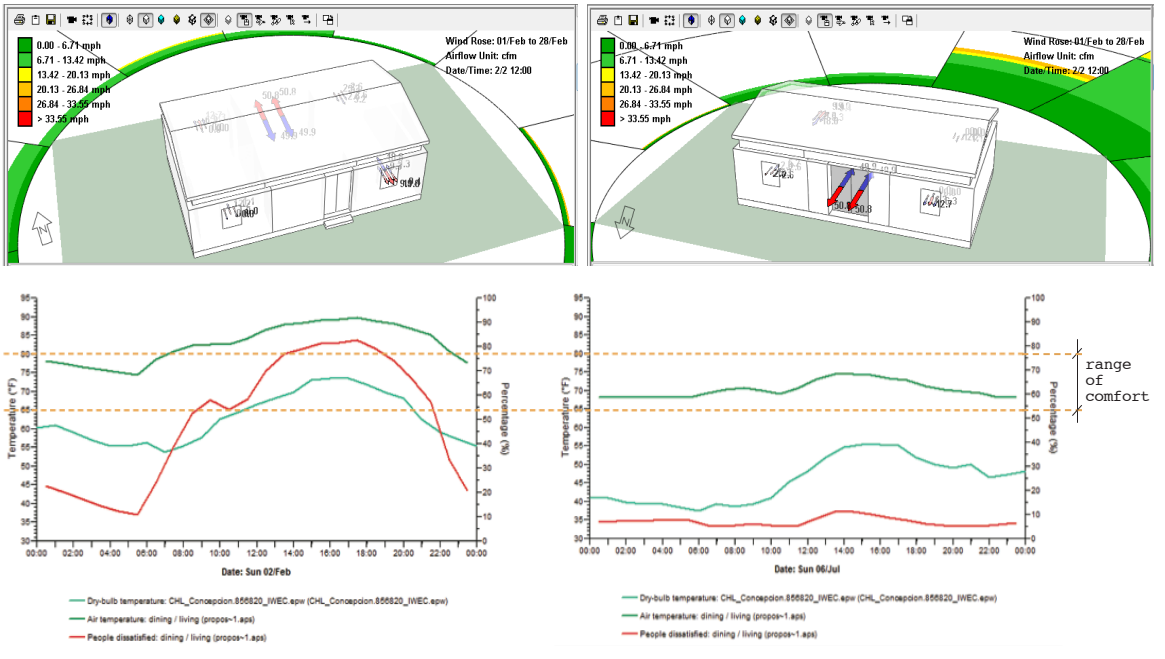

Case 4 is created based on case 3. This new model analyzes temperature improvements and energy reduction by including natural ventilation. Macroflow application and the Macroflo Data base Manager are used in this analysis. The openable windows are selected for the consideration of appropriate window types and the location in the wall. Thus, all exterior windows are adjusted to the Macroflo opening type Exterior window opening 20%.

Selected Profile:

- Exposure Type: semi-exposure wall.
- Opening: Custom/sharp edge orifice.

Figure 3.6.3: Case 4 Macro Flow without natural ventilation.
Source: IES Macro Flow.

Figure 3.6.4: Case 4 Temperature in winter and summer without naturla ventilation.
Source: IES Macro Flow.

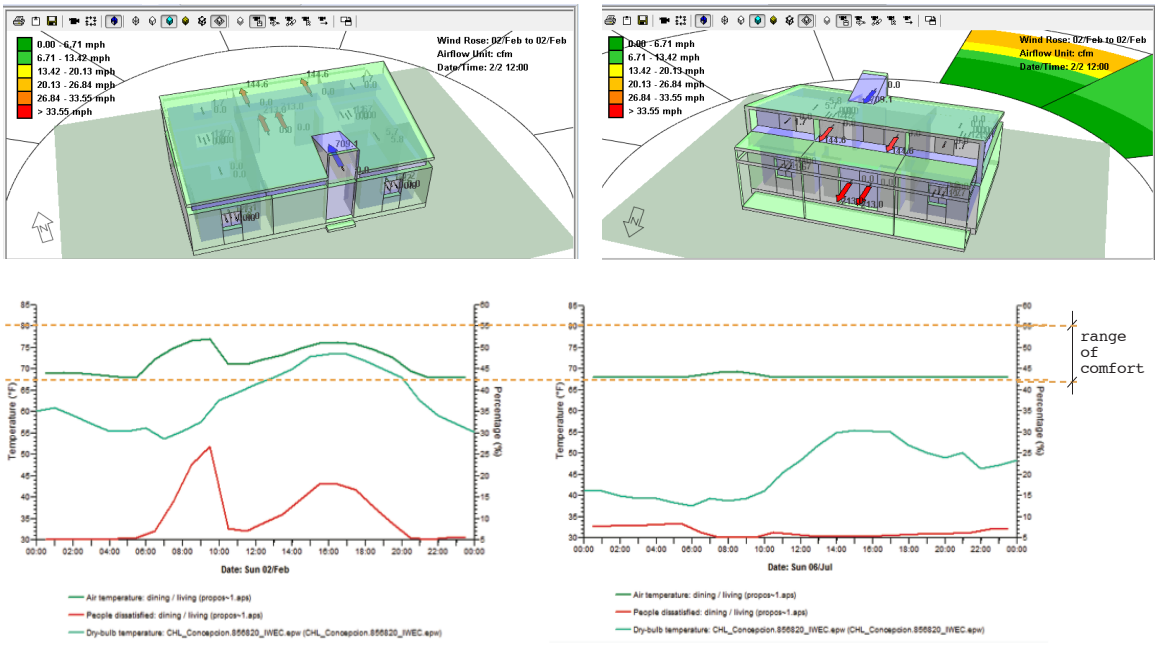

- Openable Area: 20%.
- Crack Flow Coefficinet: 12 cfm (ft˚in Hg^0.6).
- Crack lenght: 100% of opening perimeter.
- Opening threshold: 45.00 ˚F Including ef fects of wind turbulence.

The effects of employing this passive strategy is evaluated in February 2nd and July 6th as tested case 1. Results of this simulation reveal that from case 1 (without natural ventilation) to case 4 (with natural ventilation) interior air temperature and people dissatisfaction parameter are adjusted within the rate of comfort both in summer and win- ter as shown in Figure 3.6.4.

3.7 Energy design (IES VE)

Loads	EUI KBtu/sf
Heating	15
Cooling	0
Fans/aux	9
Lights	15
Equipments	2
Total	41

Table 3.7.1: EUI summary.
Source: SM creation

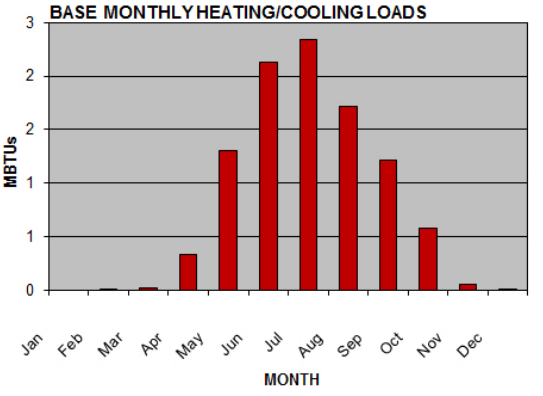

Figure 3.7.2: Base monthy heating/cooling loads

IES Apache is used to determine the total energy use consummed by four cases during a full year: the three studied cases used in the daylight analysis and case 4, which includes natural ventilation. For all the cases, the energy analysis considers HVAC setup Split system. As a result of this analysis the EUI shows a reduction from 51 kBtu/ft^2 to 41 kBtu/ft^2, as shown in Table 3.7.1 and 3.7.3, which is 3 kBtu/ft^2 lower than the average energy used of residential units in the Concepcion area according to IES energy report. Also, housing units that attemps to meet 2030 Challenge net zero carbon emission are requested to start with energy used of 18 kBtu/sf.

Tables 3.7.3: Energy reduction summary from Case 1 to 4 (IES Apache)

Case 1

Roof: single slope
WWAR: 13%
EUI: 51 kBtu/ft²
Without nat. ventilation

	Boilers energy (MBtu)	Chillers energy (MBtu)	Ap Sys aux + DHW/solar pumps energy (MBtu)	Ap Sys heat rej fans/pumps energy (MBtu)	Total lights energy (MBtu)	Total equip energy (MBtu)	Total energy (MBtu)
	propos~1.aps	propos~1.aps	propos~1.aps	propos~1.aps	propos~1.aps	propos~1.aps	propos~1.aps
Date							
Jan 01-31	0.000	0.000	0.491	0.000	1.367	0.112	1.970
Feb 01-28	0.001	0.000	0.444	0.000	1.234	0.101	1.781
Mar 01-31	0.021	0.000	0.491	0.000	1.367	0.112	1.991
Apr 01-30	0.339	0.000	0.476	0.000	1.323	0.109	2.245
May 01-31	1.308	0.000	0.491	0.000	1.367	0.112	3.278
Jun 01-30	2.123	0.000	0.476	0.000	1.323	0.109	4.030
Jul 01-31	2.338	0.000	0.491	0.000	1.367	0.112	4.308
Aug 01-31	1.712	0.000	0.491	0.000	1.367	0.112	3.682
Sep 01-30	1.212	0.000	0.476	0.000	1.323	0.109	3.118
Oct 01-31	0.575	0.000	0.491	0.000	1.367	0.112	2.546
Nov 01-30	0.051	0.000	0.476	0.000	1.323	0.109	1.958
Dec 01-31	0.005	0.000	0.491	0.000	1.367	0.112	1.975
Summed total	9.683	0.000	5.786	0.000	16.092	1.321	32.882

Case 2

Roof: double slope
WWAR: 15%
EUI: 44 kBtu/ft²
Without nat. ventilation

	Boilers energy (MBtu)	Chillers energy (MBtu)	Ap Sys aux + DHW/solar pumps energy (MBtu)	Ap Sys heat rej fans/pumps energy (MBtu)	Total lights energy (MBtu)	Total equip energy (MBtu)	Total energy (MBtu)
	propos~1.aps	propos~1.aps	propos~1.aps	propos~1.aps	propos~1.aps	propos~1.aps	propos~1.aps
Date							
Jan 01-31	0.000	0.000	0.491	0.000	1.367	0.112	1.970
Feb 01-28	0.001	0.000	0.444	0.000	1.234	0.101	1.781
Mar 01-31	0.021	0.000	0.491	0.000	1.367	0.112	1.991
Apr 01-30	0.347	0.000	0.476	0.000	1.323	0.109	2.254
May 01-31	1.329	0.000	0.491	0.000	1.367	0.112	3.299
Jun 01-30	2.145	0.000	0.476	0.000	1.323	0.109	4.051
Jul 01-31	2.359	0.000	0.491	0.000	1.367	0.112	4.329
Aug 01-31	1.727	0.000	0.491	0.000	1.367	0.112	3.697
Sep 01-30	1.219	0.000	0.476	0.000	1.323	0.109	3.125
Oct 01-31	0.579	0.000	0.491	0.000	1.367	0.112	2.549
Nov 01-30	0.052	0.000	0.476	0.000	1.323	0.109	1.959
Dec 01-31	0.005	0.000	0.491	0.000	1.367	0.112	1.975
Summed total	9.782	0.000	5.786	0.000	16.092	1.321	32.981

Case 3

Roof: double slope
WWAR: 16% + skylight
EUI: 43 kBtu/ft²
Without nat. ventilation

	Boilers energy (MBtu)	Chillers energy (MBtu)	Ap Sys aux + DHW/solar pumps energy (MBtu)	Ap Sys heat rej fans/pumps energy (MBtu)	Total lights energy (MBtu)	Total equip energy (MBtu)	Total energy (MBtu)
	propos~1.aps	propos~1.aps	propos~1.aps	propos~1.aps	propos~1.aps	propos~1.aps	propos~1.aps
Date							
Jan 01-31	0.001	0.000	0.491	0.000	1.367	0.112	1.971
Feb 01-28	0.004	0.000	0.444	0.000	1.234	0.101	1.784
Mar 01-31	0.040	0.000	0.491	0.000	1.367	0.112	2.011
Apr 01-30	0.383	0.000	0.476	0.000	1.323	0.109	2.289
May 01-31	1.294	0.000	0.491	0.000	1.367	0.112	3.264
Jun 01-30	2.040	0.000	0.476	0.000	1.323	0.109	3.947
Jul 01-31	2.239	0.000	0.491	0.000	1.367	0.112	4.209
Aug 01-31	1.656	0.000	0.491	0.000	1.367	0.112	3.627
Sep 01-30	1.182	0.000	0.476	0.000	1.323	0.109	3.088
Oct 01-31	0.601	0.000	0.491	0.000	1.367	0.112	2.571
Nov 01-30	0.105	0.000	0.476	0.000	1.323	0.109	2.012
Dec 01-31	0.017	0.000	0.491	0.000	1.367	0.112	1.987
Summed total	9.561	0.000	5.786	0.000	16.092	1.321	32.760

Case 4

Roof: double slope
WWAR: 16% + skylight
EUI: 41 kBtu/ft²
With natural ventilation

	Boilers energy (MBtu)	Chillers energy (MBtu)	Ap Sys aux + DHW/solar pumps energy (MBtu)	Ap Sys heat rej fans/pumps energy (MBtu)	Total lights energy (MBtu)	Total equip energy (MBtu)	Total energy (MBtu)
	propos~1.aps	propos~1.aps	propos~1.aps	propos~1.aps	propos~1.aps	propos~1.aps	propos~1.aps
Date							
Jan 01-31	0.000	0.000	0.491	0.000	1.367	0.112	1.971
Feb 01-28	0.003	0.000	0.444	0.000	1.234	0.101	1.782
Mar 01-31	0.034	0.000	0.491	0.000	1.367	0.112	2.004
Apr 01-30	0.364	0.000	0.476	0.000	1.323	0.109	2.271
May 01-31	1.261	0.000	0.491	0.000	1.367	0.112	3.231
Jun 01-30	2.001	0.000	0.476	0.000	1.323	0.109	3.908
Jul 01-31	2.199	0.000	0.491	0.000	1.367	0.112	4.170
Aug 01-31	1.625	0.000	0.491	0.000	1.367	0.112	3.595
Sep 01-30	1.161	0.000	0.476	0.000	1.323	0.109	3.067
Oct 01-31	0.587	0.000	0.491	0.000	1.367	0.112	2.558
Nov 01-30	0.097	0.000	0.476	0.000	1.323	0.109	2.003
Dec 01-31	0.014	0.000	0.491	0.000	1.367	0.112	1.985
Summed total	9.346	0.000	5.786	0.000	16.092	1.321	32.545

Chapter IV
Proposal: Seismic Base Isolator (SBI) for the Adobe Dwelling Prototype

This section summarizes the criteria, development, results, and conclusions of the effects of using a SBI in the designed adobe dwelling.

As was described in section 3.1, the analysis uses a one story 645 ft^2 adobe dwelling with a 16″ structural wall (40 cm), finished with 2″ (5cm) of earth stucco, without a rigid diaphragm, and with a wooden roof subjected to seismic forces.

Effects of using a BSI are analyzed in the adobe dwelling with and without polymer mesh. The BSI is formed by two components, acting together during the seismic event, located between the footing and the foundation wall: (1) the frictional interface layer component, which diffuses horizontal forces,

and (2) the re-centering components, which limits lateral displacements of the adobe structure subjected to dynamic forces.

Four cases of adobe dwellings are modeled as shown in table and diagram below:

Case 1:

Adobe structure without polymer mesh and with rigid ring foundation wall.

Case 2:

Adobe structure with polymer mesh and rigid ring foundation wall.

Case 3:

Adobe structure without polymer mesh, with seismic base isolator.

Case 4:

Adobe structure with polymer mesh, with seismic base isolator.

The seismic analysis of each case employs both the Static Method and the Spectral Modal Method, considering a soil type E in the costal seismic zone 3 according to the Chilean seismic Code (2009) in

Table: Study cases summary.
Source: SM creation.

	Case 1	Case 2	Case 3	Case 4
Adobe structure	X	X	X	X
Polymer mesh		X		X
Rigid ring foundation wall	X	X		
Seismic base isolator (SBI)			X	X

Figure: Study cases.
Source: SM creation.

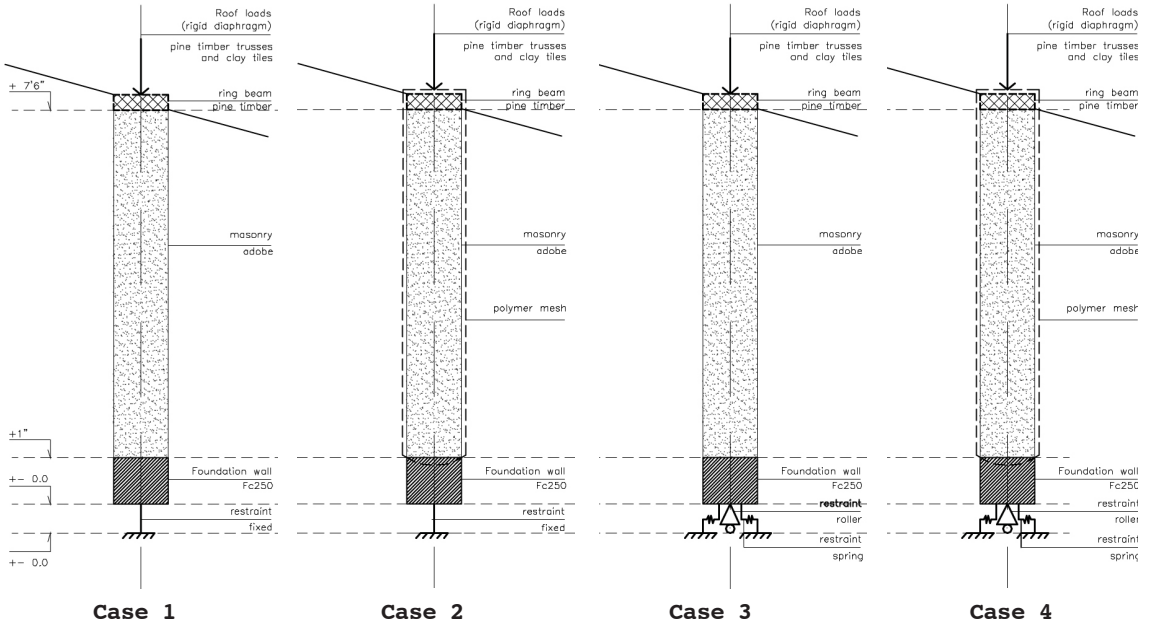

NCh 433 Of 1996 Mod 2009/ D.S.61 reviewed in section 3.1, which offers the most vulnerable soil type territory for seismic design in Chile or the highes peak ground acceleration A_o .

These methods are sesimically simulated in the package SAP 2000 with porcess steps described in Appendix # 1. Results show that the SBI reduces seismic forces in about 17.5%. Also, the differences between the maximum seismic stresses and the admis-

sible wall stresses is 5 [lb/in2] shorter than by using polymer mesh, diminishing damaged areas generated in the wall in about 11.4%, which is 2% less of affected area if the adobe dwellings is protected with polymer mesh. This system also augments the total cost in 2%, which is almost half of constrcution badgets stimated by emplying polymer mesh.

4.1 Physics concepts used in the analysis

Source: Koshkin and Shirkévich (1975)

The friction force (Ff). This force is equal to the friction coefficient " μ " times the normal or reaction force of the object "N" as shown in Figure 4.1.1

Figure 4.1.1: Friction force diagrams
Source: SM creation based on reviewed literature

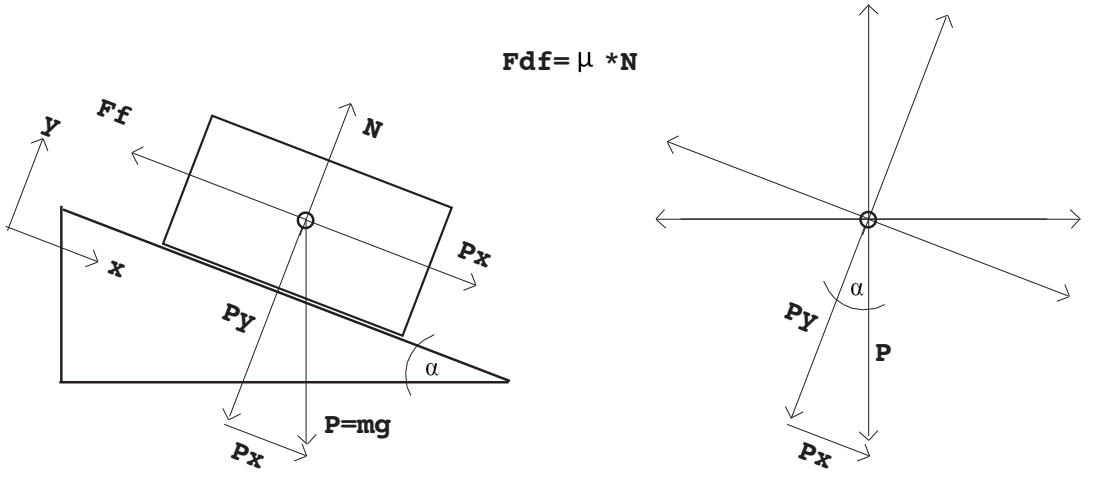

$a = 0 \iff \sum \overrightarrow{extF} = 0$

$\sum Fy = 0 = N + (-Py) = 0 \Longrightarrow N = Py\ Po\ \cos(\alpha)$

$\sum Fx = 0 = Px + (-fF) = 0 \Longrightarrow fF = Px$

$fF = P * sen(\alpha) \Big/ \frac{P*\cos(\alpha)}{P*\cos(\alpha)}$

$fF = \not{P} * sen(\alpha) * \frac{N}{\not{P}*\cos(\alpha)}$

$fF = \frac{sen(\alpha)}{\cos(\alpha)}$

$Ff = (\alpha) = tg\ (\alpha) * N$

$\mathbf{Ff = \mu N}$

$\cos(\alpha) = \frac{Py}{P}$

$sen(\alpha) = \frac{Px}{P}$

$\cos(\alpha) = tg\ (\alpha)$

F: Force
g: gravitational acceleration
m: Mass
N: Normal force
P: Object weight
μ: Friction coefficient
vF: Vertical force
hF: Horizontal force

Activation of Friction force.

The friction force (Ff): This force occurs between two surfaces in contact. As shown in Figure 4.1.2 the friction static force (Fsf) happens between two surfaces in contact opposed to the initial displacement. On the other hand, the friction dynamic force (Fdf) happens between two surfaces in contact opposed to the displacement between both surfaces.

Figure 4.1.2: Activation of the friction force.
Source: SM creation based on reviewed literature.

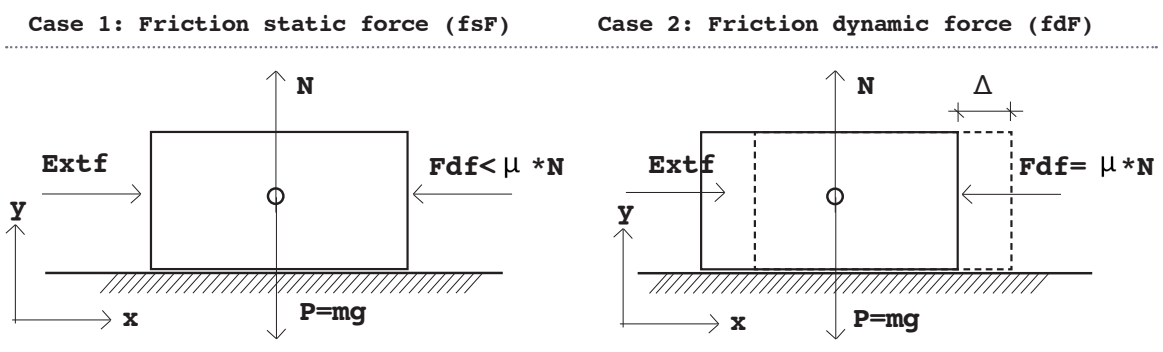

1st Newtom law F = m * a

$\sum vF = N - mg = m * a = m * 0 = 0$

$\Longrightarrow$ There is not desplasement

$\Longrightarrow$ N = m * g (object weight)

$\sum hf = extF - fF = m * a$

$\Longrightarrow$ There is not desplasement

$\Longrightarrow$ a = 0 m * a = 0

$\Longrightarrow$ extF = fF

$\sum vF = 0$

$\sum hF = fdF - extF = m * a$

$\Longrightarrow$ There is horizontal desplazament

$a \neq 0 \Longrightarrow m * a \neq 0$

$\sum Hf = extF - fdF = m * a$

$\Longrightarrow$ $extF - fdF = \Delta F$

$\Longrightarrow$ $\Delta F = m * a$

$\Longrightarrow$ extF > fdF

Hooke law in rubber components and Young Modulus or Modulus of elasticity.

Source: Koshkin and Shirkévich (1975)

The unitarionan streching " ε" is the distribution of the streching value times the original object lenght as shown figure 4.1.3.

The Hooke law: The unitarion streching of a material is in direct proportion to the applyed force "F" as shown in Figure 4.1.4. Figure 4.1.5 illustrates the fsF and the fdF.

Figure 4.1.3: The Hooke law

$$\varepsilon = \text{Unitarian streching} = \frac{\text{Unitarian streching}}{\text{Original object length}} = \frac{\delta}{L}$$

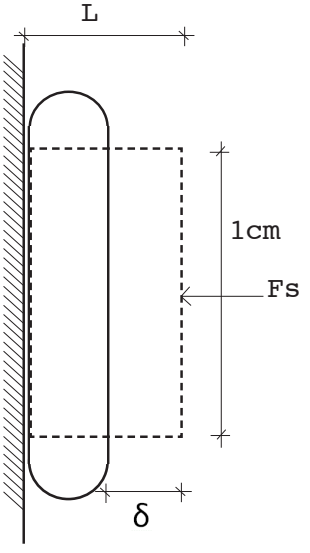

Figure 4.1.4: Elastic force diagrams

$$\varepsilon = \frac{\delta}{L} = \frac{F}{AL}$$

$$\sigma = \frac{F}{AL} = E\,\varepsilon$$

L: Rubber thickness
E: Modulus of elasticity
δ : Delta of deformation
ε : Epsilon for unitarian streching
σ : Object stress

Figure 4.1.5: Fsf and Fdf
Source: SM creation based on reviewed literature

a: Elastic period
b: Plastic period
c: Rupture point

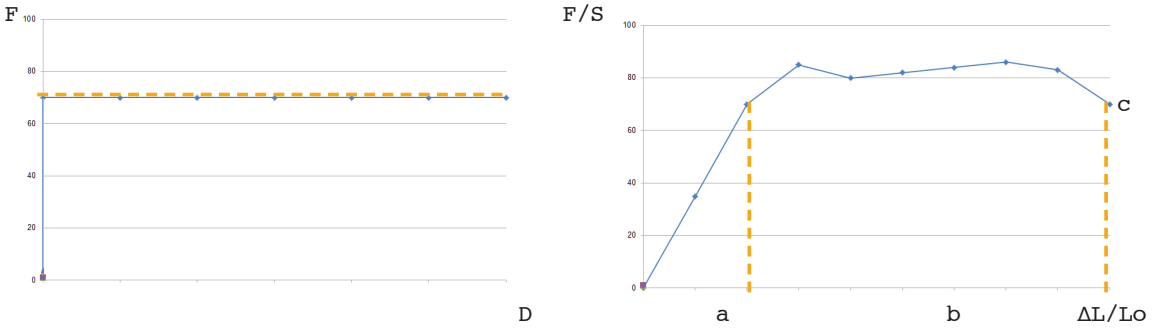

4.2 Proposed SBI: Concept and function Mery_Plan_A_

The proposed base seismic isolator aims to diffuse the ground motion that goes up to the adobe structure, instead of artificially increasing the wall strength as reinforcement systems do. In this case, The proposed base seismic isolator is formed by two components as shown in Figure 4.2.1, acting together during a seismic event as shown in diagram B

Figure 4.2.1: Components of the proposed sesimic base isolator.
Source: SM creation

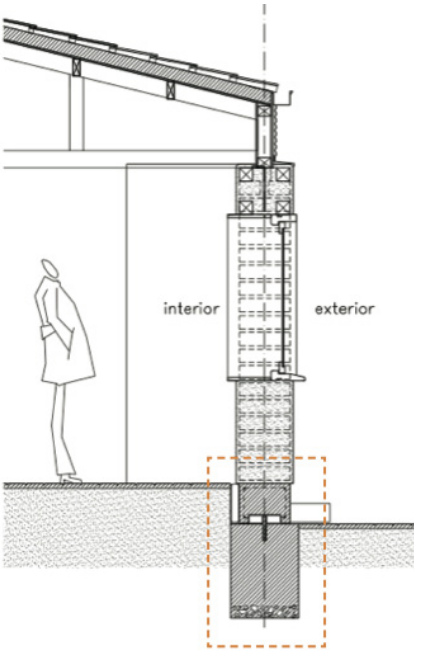

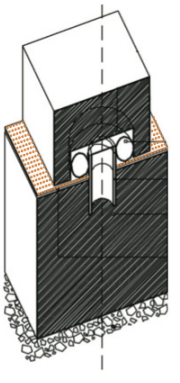

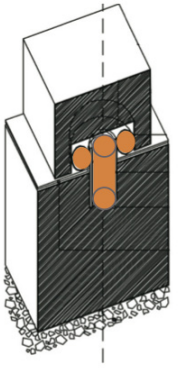

	component 1	component 2
Physical principle:	friction	material streching
Function:	difusses sesimic force	limits lateral displacement
Pieces:	6 to 8mm gravels	steel pipe lock with a scrap car tire donnut

Figure 4.2.2: Concept diagram of the SBI acting in a seismic force.
Source: SM creation

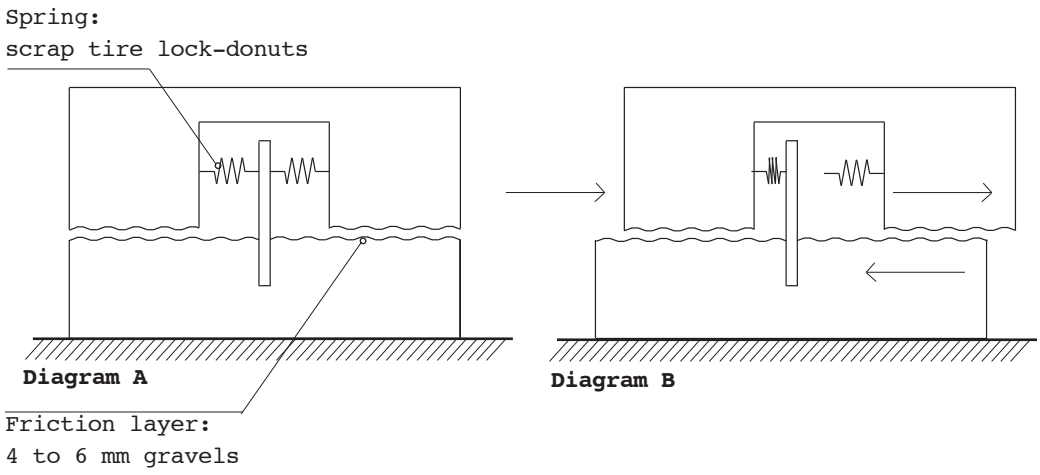

of figure 4.2.2. They are located between the footing and the foundation wall. These components are (1) the frictional interface layer component, which diffuses horizontal forces and (2) the re-centering component, which limits lateral displacements of the adobe structure subjected to dynamic forces.

The frictional interface component is formed by a 6 mm to 8 mm pebble layer, whereas the re-centering component is constituted by an spring actuator, located every 5 feet along the foundation wall as shown in architectural plans in Figure 4.2.3 and 4.2.4, which is stretched when the isolator is affected by lateral motions, allowing the superstructure to be relocated in the center of gravity as shown wall sections in Figure 4.2.5.

Figure 4.2.3: Foundation plan with distribution of re-centering components
Source: SM creation

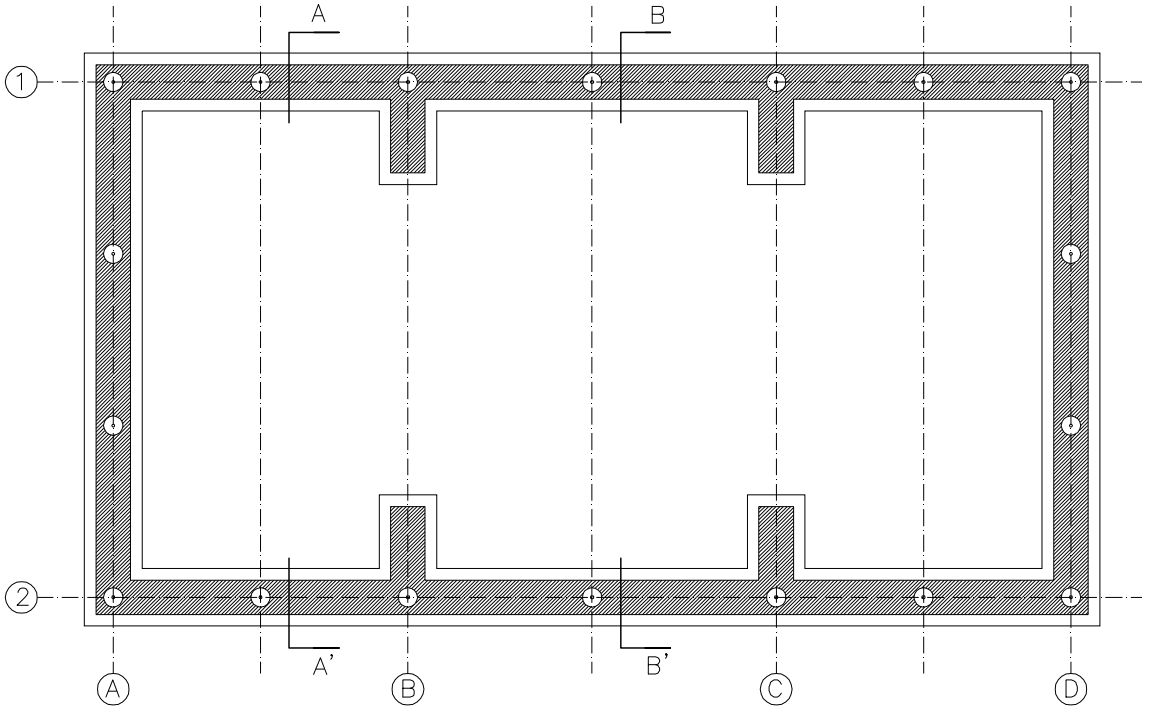

Figure 4.2.4: Section A–A' and B–B'
Source: SM creation

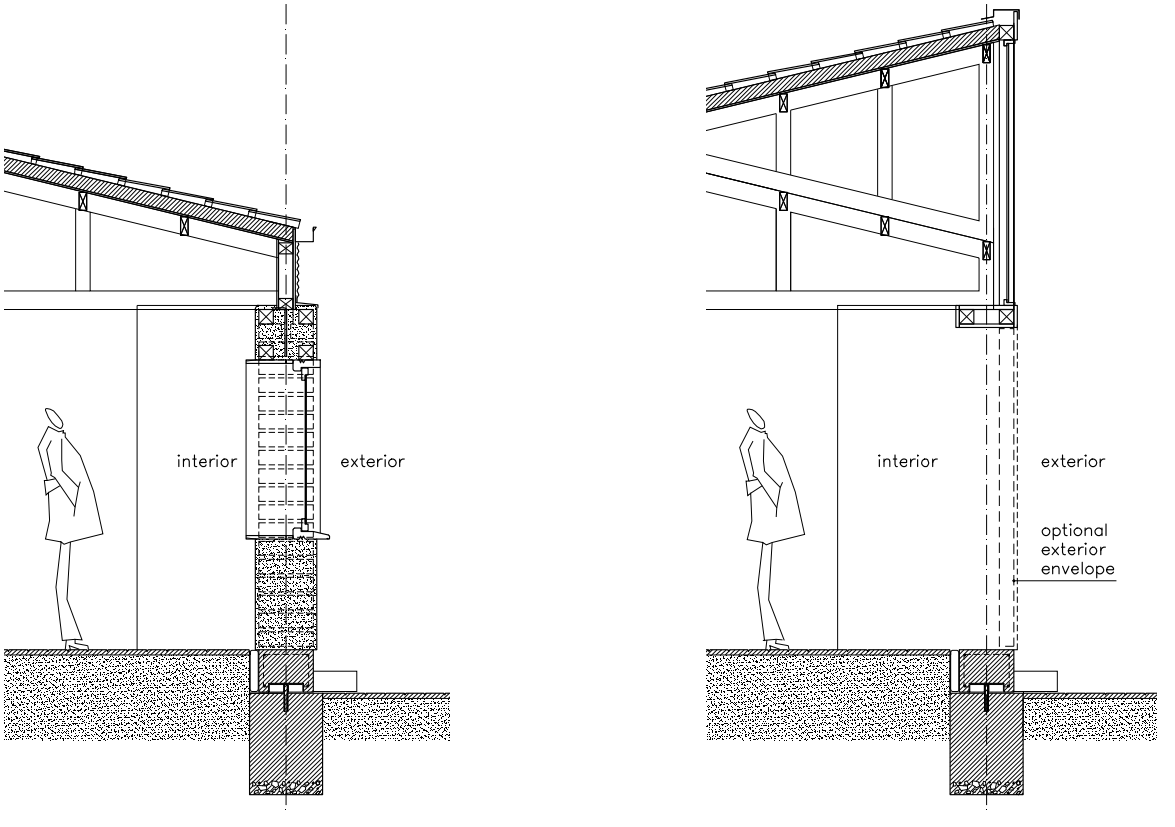

Figure 4.2.5: Section detail showing the SBI componets acting in seismic activity.
Source: SM creation

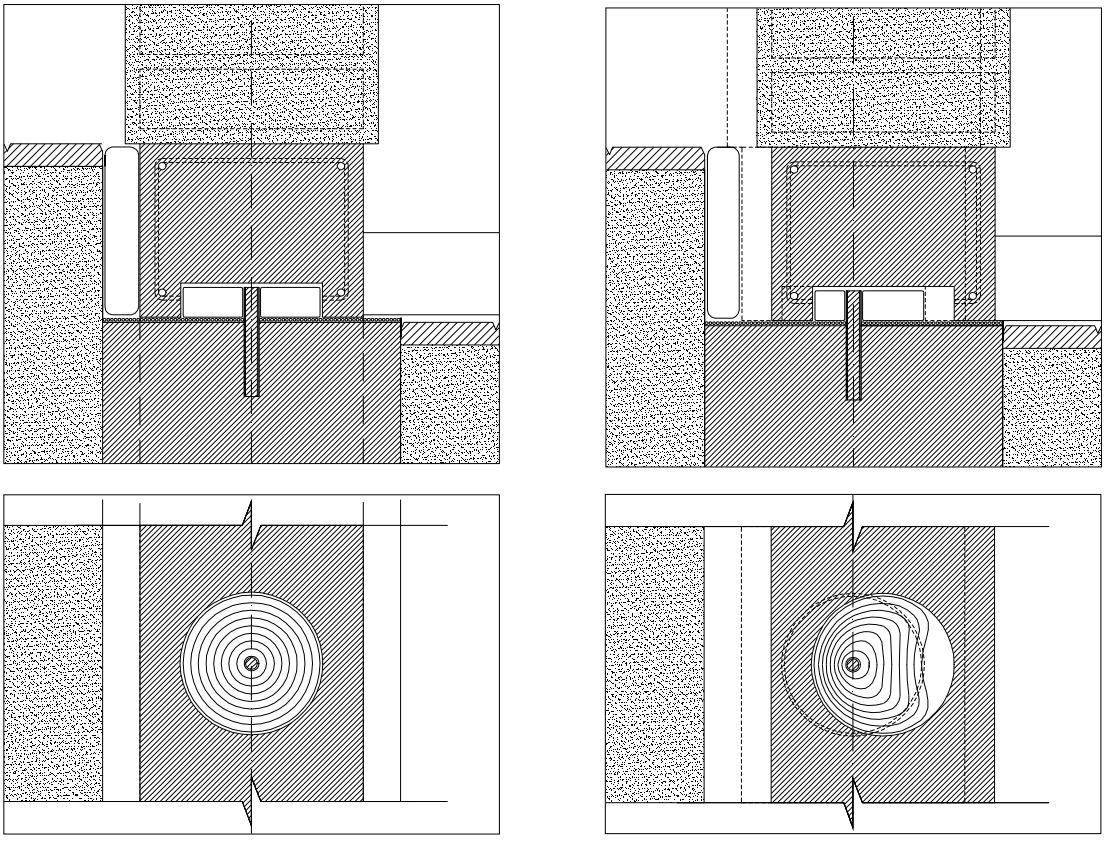

4.3 Condition for the seismic analysis.

4.3.1. Seismic building Codes

This analysis employs the national building code stabilized by the Instituto Nacional de Normalizacion, focusing especially on the Seismic Code NCh 433 of.96.

- Seismic Code NCh1537 of.2009 Cargas permanentes y sobrecargas.

- Seismic Code NCh432 of. 71 Cálculo de la acción del viento.

- Seismic Code NCh1198-2006 - Madera - Construc-

ciones en madera – Calculo.

- Seismic Code NCh429.of.57 Hormigón Armado – I Parte.

- Seismic Code NCh430.of.61 Hormigón Armado – II Parte.

- Seismic Code Técnica de Perú, E.080 "Adobe" y su Anexo N°1 "Refuerzo de Geomalla en Edificaciones de Adobe".

4.3.2. Mechanical properties of materials.

Materials used in this analysis were collected from researches related to seismic design, material list provided in the Chilean Building Code, and the building material suppliers available in Chilean as table 3.2.5.1 shows.

Left image: Materials used for modeling foundation wall, the SBI, and the footing.
Right image: Materials used for modeling adobe bricks.
Source: SM.

Table 4.3.2.1: Material list used for the seismic analysis.
Source: SM creation based on reviewed literature

Material list	Weight		Density		Tensile stress		Compressive stress	Shear stress	Elastic Modulus	Compressive Modulus	Yiel limite	Friction coheficient
	W		γ		σs		σc		E	Ec	F'y	μ
	[Kgf/m^2]	[lb/ft^2]	[Kgf/m3]	[lbf/ft3]	[Kgf/cm2]	MPa	MPa	MPa	MPa	MPa	MPa	
Adobe 16" Milani and Paradisco (2010)			1600	99.8			0.75	0.025	200			
Adobe stucco 2.5" Milani and Paradisco (2010)			1600	99.8			0.75	0.025	200			
Concrete H-25 NCh 1537. Of 2009			2540	158.5					25300			
Pebble 6mm to 8mm Xiao (2004)												0.202
Pine NCh 1537. Of 2009			750	46.8					8000		9.6	
Polymer mesh NP, E.080 "Adobe" Anexo N°1					350	34.32		0.007				
Steel pipe A37-24ES NCh 1537. Of 2009											240	
Rebar steel A 630-420H NCh 1537. Of 2009											240	
Rubber D. Özden, B. (2006)							8.5 (in 2")			30		
Colonial Tile www.rattarotejas.com.ar	64	13.1										

4.3.3. Dead loads (DL) and live loads (LL)

DL and LL used for the seismic analysis are listed below:

- Structural weight.
- Tile weigh: 13.1 [lbf/ft^2] or 64 [Kgf/m^2].
- Roofing liveload: 39 [Kgf/m^2] or 7.9 [Kgf/m^2][1].This value includes the reduction coefficient established by the NCh1537of.(2009).
- Wind effect on the adobe structure[2].
- Seismic effects on the structure.

---

1 NCh 1537 proposes OL=100 [Kgf/m^2] exponential zed with both the 0.93 reduction coefficient per tributary area and the 042 sloping roof. These exponentials 0.39 to be used in OL. (see table 3 NCh 1537 of.2009)

2 La Normativa nacional propone usar una carga de 70 [Kgf/m2] (NCh432 Tabla 1) para estructuras de 4 [m] de altura ubicadas en campo abierto ponderado por el factor por pendiente de techo (NCh432 - Anexo A – Fig. 10): 1,2sen(ang del techo) – 0,4.

4.3.4. Modeling of wall section.

A basic 1/2 full size wall section with the SBI was modeled to prove both proposed installation process step and function performance of SBI components. The modeling represents a section of the wall showing SBI components. It uses proposed materials and respects same steps employed by the traditional adobe construction to build the foooting and the foundation wall as is described in section 4.8.

The practical experience of modeling the wall section shows that the traditional construction process is not altered by introducing the SBI. In regard to the function of the SBI, the frictional layer formed by 3mm gravels layers allows the superstructure to slide on top of the footing wall.

Model in process step 1:
Construction of the foundation wall and the footing.
Source: SM

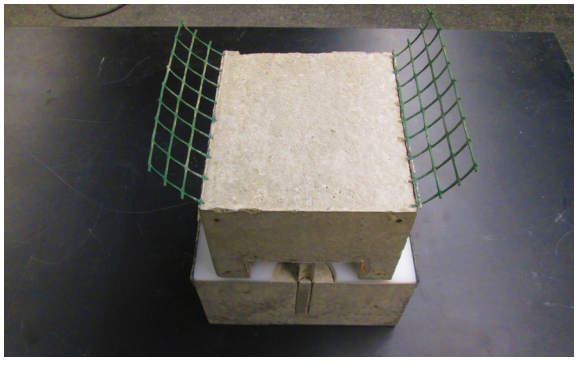

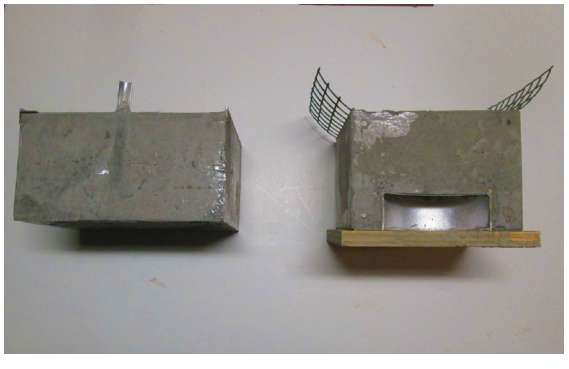

Also, the scrap tire lock-donuts represented by dense foam is streched once the footing is subject-ed to lateral displacements.

Model in process step 2:
Construction of the adobe blocks.




Modelin process step 3:
Assembling the components for the section wall and testing SBI displacement



Modelin process step 4:
Assembling the components

Modelin process step 5:
Testing SBI displacement

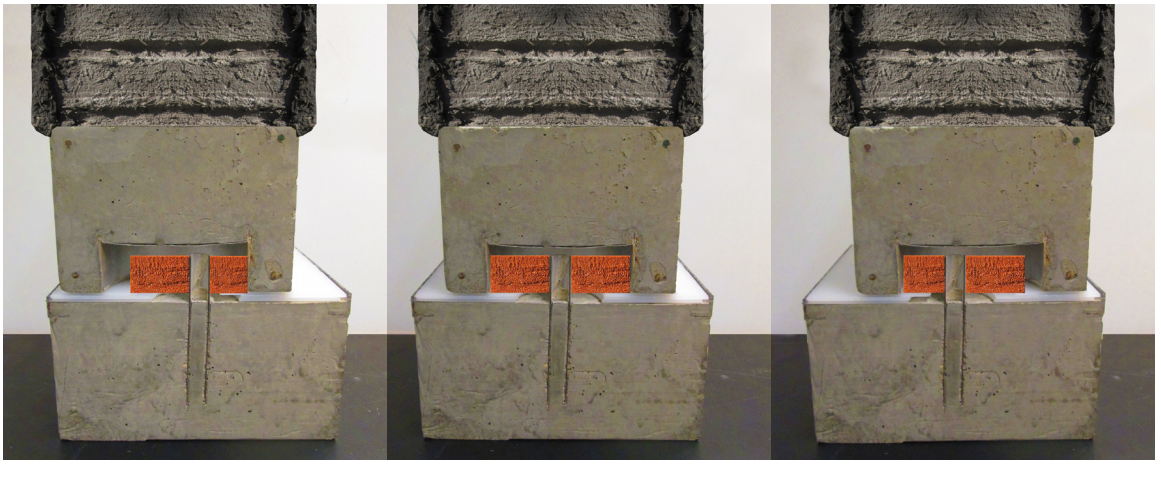

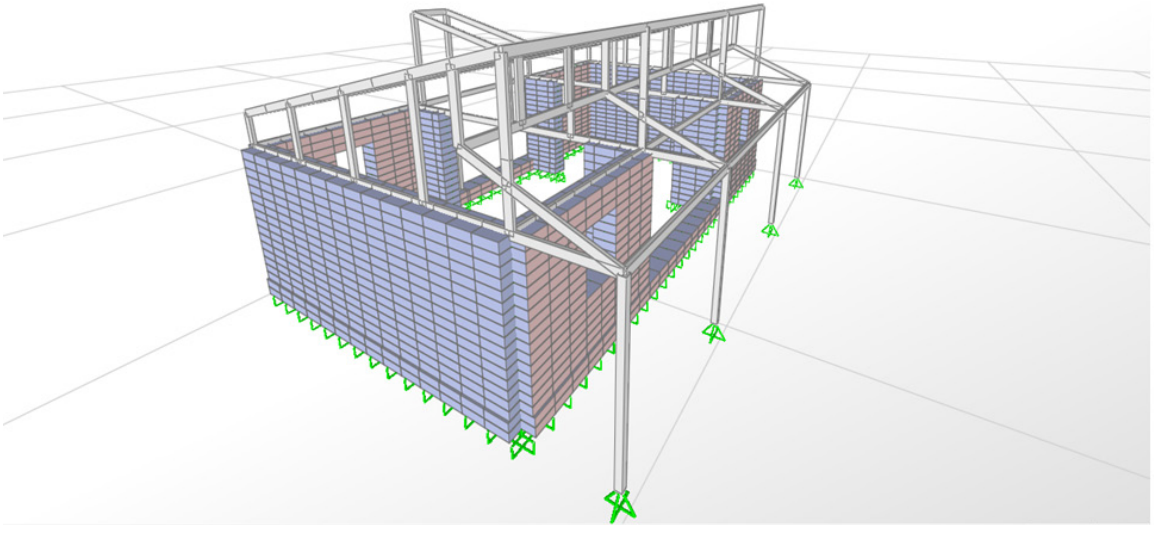

Image: Prototype Model SAP2000
Source: Appendix 2

4.4 Methodology

With the aim to determine seismic effects of the base isolator, this analysis uses the software with finite elements SAP 2000. By considering conditions presented previously four models were analyzed using the same architectural layout, but changing functioning behavior in the structural components.

NCh 433.Of 1996 Mod (2009) and attached D.S.61 is used in this seismic analysis. This document establishes two methods to simulate seismic effort of the structure. Also, the same code indicates that adobe structures are required to be evaluated using the Static Method, whereas the Spectral Mode Method conditions the use of the Ro value, which is not

given for adobe structures.

The seismic **Static Analysis Method** simulates the seismic behavior if the structure using “static” horizontal forces. The horizontal forces are formed by X and Y forces, which represent a percentage of the structure. The same document mentions that the seismic assessment by the **Spectral Modal Analysis Method** simulates the seismic structure behavior by using the acceleration spectrum on the structural base. As a proposal case for this research the Spectral Modal Method also employs formulas shown in figure 4.4.1 according to the NCH 433. Of 1996 Mod (2009) by using the R_o value = 1. This value gives the lowest reduction factor highest basal acceleration.

Figure 4.4.1: Spectrum design, augmenting factor, and reduction factor.
Source: NCh 433.Of 1996 Mod (2009)

$$S_a = \frac{IA_0\alpha}{R^*} \qquad \alpha = \frac{1+4{,}5\left(\frac{T_n}{T_o}\right)^p}{1+\left(\frac{T_n}{T_o}\right)^3} \qquad R^* = 1+\frac{T^*}{0{,}10\,T_o+\frac{T^*}{R_o}}$$

Sa: Acceleration Spectrum

α **:**Augmenting factor for the effective máximum acceleration

R*: Reduction spectral aceleration factor

In this research, the reason for choosing R^0 value =1 is because this number involves the least favorable situation, or the most conservative case, which is the searched situation, resulting in highest spectrum of acceleration A_o.

The studied cases considered in this research are four shown in Table 4.4.2 and Figure 4.4.3 These are:

Table 4.4.2: Study cases.
Source: SM creation.

	Case 1	Case 2	Case 3	Case 4
Adobe structure	X	X	X	X
Polymer mesh		X		X
Rigid ring foundation wall	X	X		
Seismic base isolator			X	X

Figure 4.4.3: Study cases.
Source: SM creation.

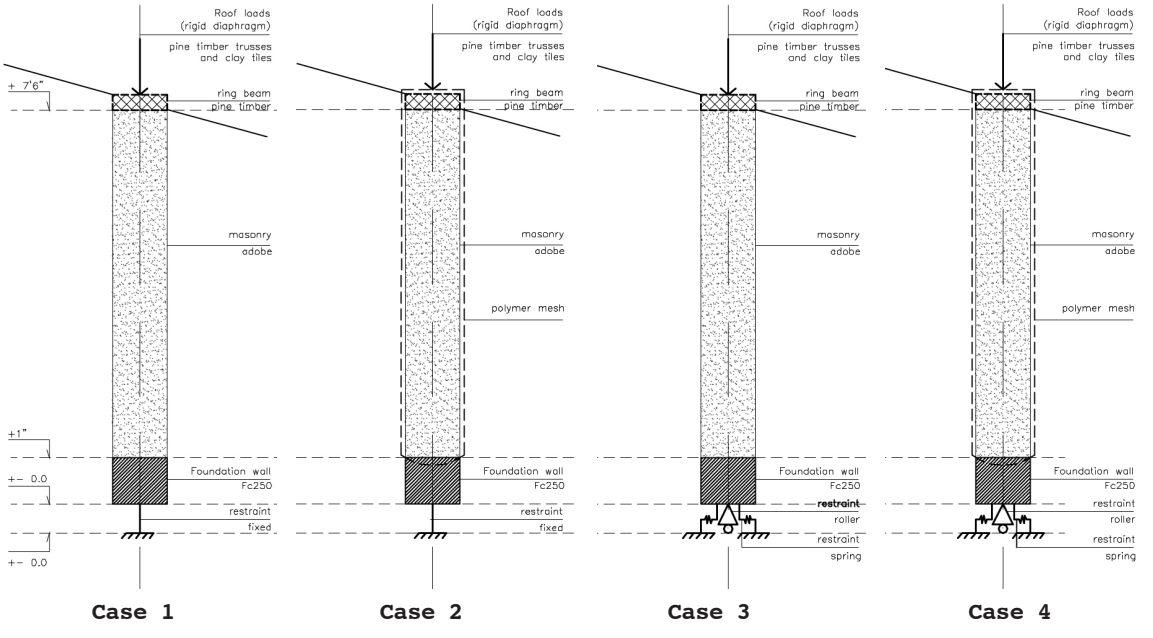

A) Adobe structure model with basal restriction to lateral displacement and rotation, using the seismic analysis Static Method according to NCh433. This model will be used to obtain the stresses of the adobe structure and these values will be verified to the structural wall strength with and without polymer mesh (Case A1 and A2).

B) Adobe structure model with basal restriction to lateral displacement and rotation, using the spectral modal analysis method according to NCh433 and the proposed criteria Ro = 1. This model will be used to obtain the stresses of the adobe structure and these values will be verified to the structural wall strength with and without polymer mesh (Case B1 and B2).

C) Adobe structure model with basal restriction to vertical displacement and rotation, by using a diffuser system. Thus, the frictional component or layer will be represented by employing horizontal forces in the opposite direction to the seismic

forces, whereas the horizontal displacement limitation will be represented by employing springs. The seismic analysis Static Method will be used according to NCh433. This model will be used to obtain the stresses of the adobe structure and these values will be verified to the structural wall strength with and without polymer mesh (Case C1 and and C2).

D) Adobe structure model with basal restriction to vertical displacement and rotation, by using a diffuser system. Thus, the frictional component or layer will be represented by employing horizontal forces in the opposite direction to the seismic forces, whereas the horizontal displacement limitation will be represented by employing springs. The seismic analysis Spectral Modal Method will be used according to NCh433 and the proposed criteria Ro =1. Reductions in seismic forces by frictional layer are estimated according to the static method described in Model C. This reduction will be applied to the basal acceleration, which might result in diminishing the structural effects from seismic forces. This model will be used to obtain

the stresses strengths of the adobe structure and these values will be verified to the structural wall strength with and without polymer mesh (Case D1 and D2).

4.5 Seismic analysis

Analytical parameters defined by the Static analysis method (SAM) and the spectral modal analysis method (SMAM).

The Static analysis method and Spectral modal method is defined by equations provided in NCh 433. Of 1996 Mod (2009). The following content develops these formulas for both methods.

Seismic weight estimation (P)

P= DL + (0,25 * LL)

DL = Dead load (Carga muerta CM)

LL = Live load (Sobre carga SC)

- **Static analysis Method**

Fx = Fy = Qo = C*I*P = (basal stresses)

C: Seismic coefficient [without unit].

I: Importance class of the building.[without unit].

P: Total weight of the superstructure [kgf].

C_{max} is given by Seismic Code and this will be used for the seismic coefficient “C”.

R = 2 will be value used in adobe according to Table 2.3.4.2, 2.3.4.3, 2.3.4.4, and 2.3.4.5 (Table 5.1 on NCh 433 and Table 6.4 on Nch 433):

C_{max} = 0,9 *S*Ao/g

S= ground type parameter [without unit].

g: Gravitational acceleration= 9,8 [m/s2].

Ground type “E” is chosen in this analysis considering its low resistance ground. Also Zone 3 is selected (Costal Chilean Zone) because of its higher basal acceleration.

S = 1,3

A_o = 0,4g (effective acceleration)

C_{max} = 0,47

I = 1,0 (not public properties, Table 6.1 NCh 433)

- **The spectral modal analysis method (SMAM)**

NCh 433.Of 1996 Mod (2009) and attached D.S.61 states that the spectral modal analysis method for the seismic analysis simulates the seismic request forces in the structure throughout the application of the acceleration spectrum (Sa) in the basal structure. Thus, spectrum values generated in a table are located in SAP 2000 (Define > Function > Response Spectrum) according to the period time: Section 2.3.4 of this research show the development of the Design Spectrum formed by the acceleration spectrum (Sa), Augmenting factor for the effective

Figure 4.5.1: Spectrum Design.
Source: NCh 433.Of 1996 Mod (2009)

$$S_a = \frac{IA_0\alpha}{R^*} \qquad \alpha = \frac{1+4{,}5\left(\frac{T_n}{T_o}\right)^p}{1+\left(\frac{T_n}{T_o}\right)^3} \qquad R^* = 1+\frac{T^*}{0{,}10\,T_o+\frac{T^*}{R_o}}$$

Sa: Acceleration Spectrum

α :Augmenting factor for the effective máximum acceleration

R*: Reduction spectral aceleration factor

maximum acceleration (α), and Reduction spectral acceleration factor (R*) as shown in following formulas.

From this mode the following periods of highest translational weigh are obtained:

T*X = 0,144326 [s].

T*Y = 0,001211 [s].

Additional parameters to obtain Sa are shown in Table 4.5.2 according to NCh433 and D.S.61.

This allows one to obtain Sa in the building for axis X and Y represented in axis X and Y, which are

Table 4.5.2: Ground factor, Zone factor, and Structure type factor.
Source: NCh 433.Of 1996 Mod (2009).

Ground factor			Zone factor			Type of structure factor	
Type	E		Zone	3		**Category**	A
S	1.3		**Ao**	0.4		**R**	2
To	1.2		Constant factor			**Ro**	1
T'	1.35	[s]	**g**	9.8	[m/s]	**I**	1
n	1.8	[s]					

Figure 4.5.3: S_a in X and Y axis
Source: Apendix 2

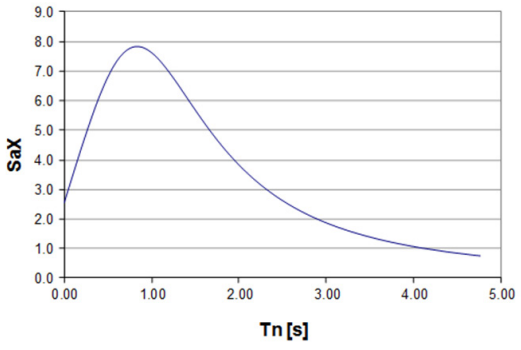

Sa in X axis using SMAM

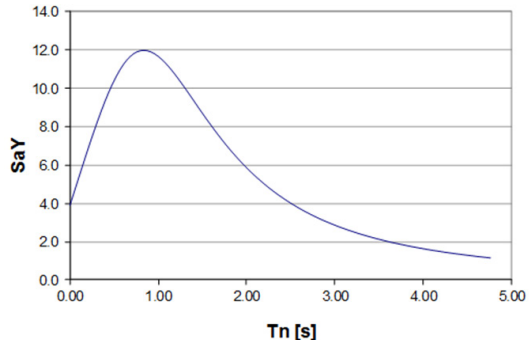

Sa in Y axis using SMAM

represented in figure 4.5.3.

The model in SAP 2000 is adjusted with Sa in axis X and Y represented in these graphs. The model takes these values with N degree of dynamic freedom and transforms them in N structure degree of dynamic freedom, which are the modes structural vibration. Each vibrational mode possesses unique period. SAP 2000 considers to each mode the assigned weigh and applies the corresponding graph acceleration to each vibrational period. After this, SAP 2000 integrates all the vibrational modes and combines them into a unique response for each seismic direction. View Appendix 1 to review SAP 2000 modeling steps.

4.6 Seismic analysis: SAP 2000 models' development

4.6.1 Analysis A: Adobe structure model with basal

restriction to lateral displacement and rotation, using SAM according to NCh 433 of.96.(View SAP 2000 steps described in Appendix 2)

Roof Dead loads (DL) and Liveloads (LL):

Tile DL: 64 [Kgf/m^2]

Roof structure DL: 16 [Kgf/m^2]

Total roof DL: 80 [Kgf/m^2]

LL by Seismic Code: 100[Kgf/m^2]

Reduction per area by Seismic code: 0.93

Sloping roof reduction by seismic code: 0.42

Total Reduction: 0.391

Total roof LL: 39.06 [Kgf/m^2]

Adobe wall

Adobe DL: 1600 [Kgf/m]

h : Wall height: 2.7 [m]

w : Wall thickness: 0.45 [m]

OL = 0

C= 0,047 (seismic coefficient)

Sf (seismic force) = Sp * C

Table 4.6.1.1 summarizes the computing of live loads and deads loads using SAM, whereas figure 4.6.1.2 illustrates the loads distribution in the prototype model.

Table 4.6.1.1: Summary of loads that act in the model using Static analysis method according to NCh 433.Of 1996 Mod (2009)
Source: SM creation.

	Studied componen	Code equation or rule	Adobe wall	Axis A and D	Axis B and C	Exterior roof	Unit
TD	Tributary distance	Meddle distance between analyzed truss and closer truss		1.625 or 5.33	3.658 or 12	0.495 or 1.62	[m] or [lbf/ft]
DL	Dead laods	Total DL * TD		80 * 1.625	80 * 3.658	80 * 0.495	[Kgf/m]
				130 or 940	**292.6 or 2112**	**39.6 or 286**	[Kgf/m] or [lbf/ft]
LL	Live laods	Total LL * TD		39.06 * 1.625	39.06 * 3.658	39.06 * 0.495	[Kgf/m]
				63.42 or 458.7	**142.9 or 1033**	**19.33 or 139**	[Kgf/m] or [lbf/ft]
P	Seismic weight	[DL * (h / 2) * w] + (0.25 * LL)	[1600 * (2.7 / 2) * 0.45] + (0.25 * 0)				"
		DL + (0,25 * LL)		130 + (0.25 * 63.42)	292.6 + (0.25 * 142.9)	39.6 + (0.25 * 19.33)	"
			972 or 7030	**145.9 or 1048**	**328.3 or 2374**	**44.43 or 321**	[Kgf/m] or [lbf/ft]
F	Seismic force	P * C	972 * 0.47	145.9 * 0.47	328.3 * 0.47	44.43 * 0.47	"
			456.8 or 3304	**68.56 or 495**	**154.3 or 1116**	**20.88 or 151**	[Kgf/m] or [lbf/ft]

Figure 4.6.1.2: Tributary distribution of loads of the prototype model.
Source: Appendix 2

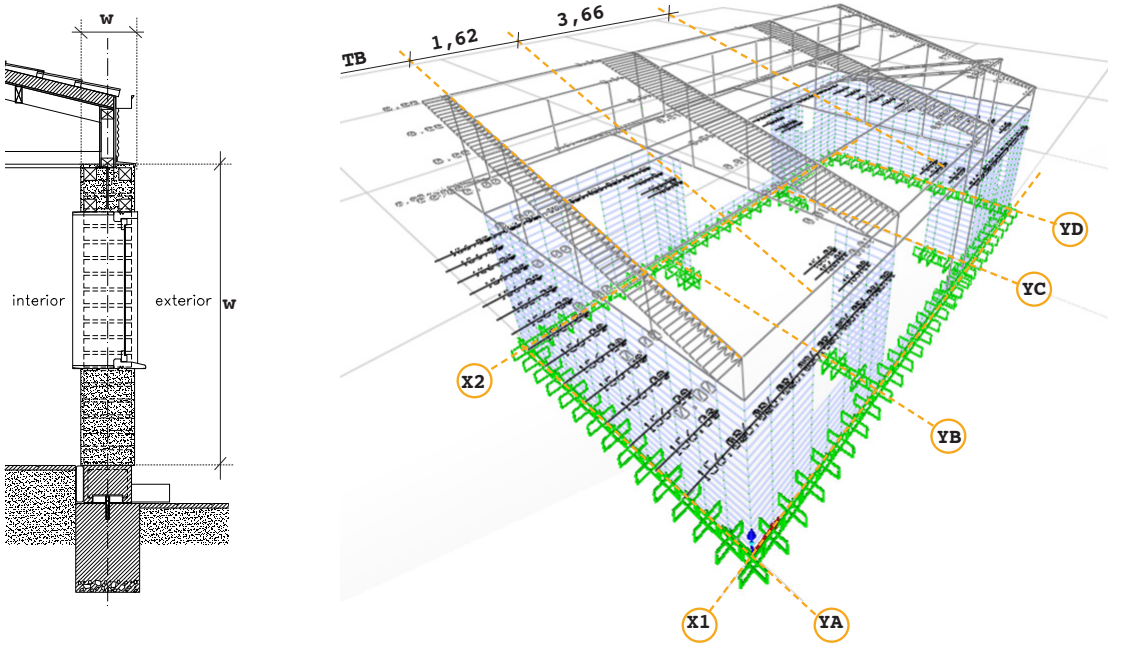

"h" is divided by two because the seismic weight is only considered using the superior half portion of the wall weight, whereas the inferior half portion of the wall weight is direct transfered to the ground.

Maximum displacement in superior wall border 0,9 [cm]

A.1 AS model with basal restriction to lateral displacement and rotation, using SAM.

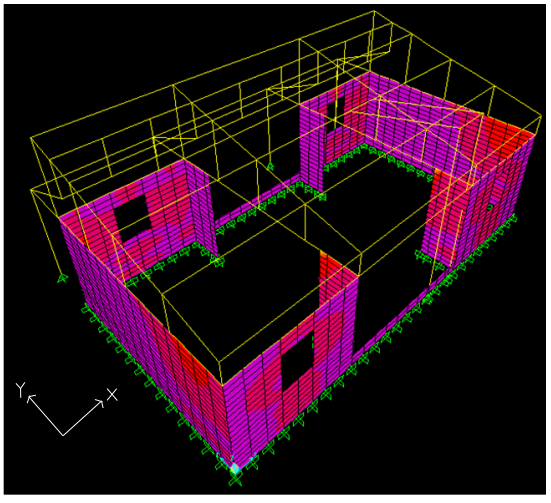

Stress strenght model in X axis

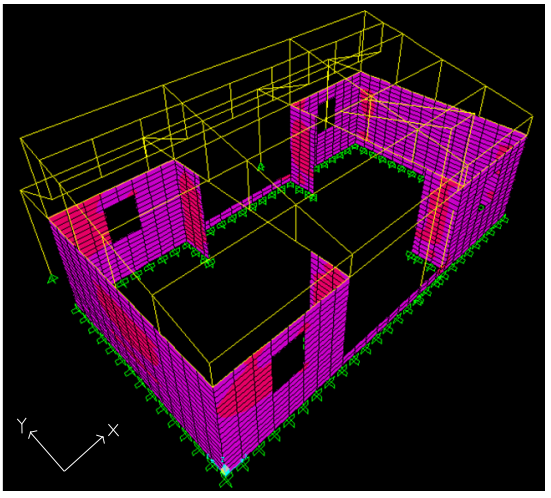

Stress strenght model in Y axis

Figure 4.6.1.3: SAP 2000 models case A1, showing X and Y axis forces. In red the wall stresses above admisible.

Table 4.6.1.4: Case A1 comparison between maximum seismic stresses and admissible.

Wall axis	Maximum seismic stresses		Admissible wall stresses		Result
	[Kgf/cm²]	[lbf/in²]	[Kgf/cm²]	[lbf/in²]	
X1	0.78	11	0.255	3.62	Fail !
X2	0.81	11.5	0.255	3.62	Fail !
YA	1.02	17	0.255	3.62	Fail !
YB	2.2	31.2	0.255	3.62	Fail !
YC	2.22	31.2	0.255	3.62	Fail !
YD	0.96	13.65	0.255	3.62	Fail !

Observations: Figure 4.6.1.3 the red areas represent the fail areas or the areas where the seisimic stresses is over the admissibles wall stresses.

Case A1 shows the model “without” polymer mesh subjected to seismic forces in X and Y axis has all the walls with failed areas. However, it also shows that less damages occurs in Y axis walls than in X axis walls. As Table 4.6.1.4 shows, in case A1 the differences between the maximun seismic stresses and the admissible wall stresses go from 7.38 [lb/in²] in X1 to 27.58 [lb/in²].

A.2 AS with polymer mesh and foundation wall using SAM.

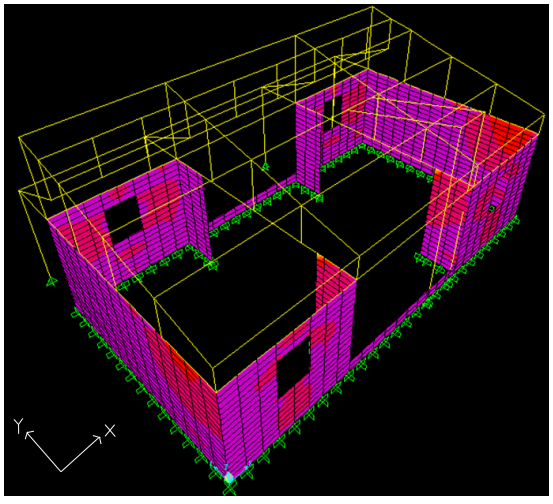

Stress strenght model in X axis

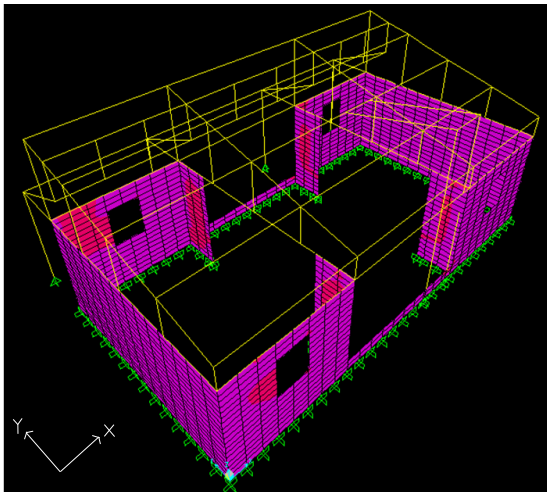

Stress strenght model in Y axis

Figure 4.6.1.5: SAP 2000 models case A2, showing X and Y axis forces. In red the wall stresses above admissible.

Table 4.6.1.6: Case A2 comparison between maximum seismic stresses and admissible.

Source: Appendix 2.

Wall axis	Maximum seismic stresses		Admissible wall stresses		Result
	[Kgf/cm²]	[lbf/in²]	[Kgf/cm²]	[lbf/in²]	
X1	0.78	11	0.32	4.55	Fail !
X2	0.81	11.5	0.32	4.55	Fail !
YA	1.02	17	0.32	4.55	Fail !
YB	2.2	31.2	0.32	4.55	Fail !
YC	2.22	31.2	0.32	4.55	Fail !

Observations: As figure 4.6.1.5 illustrates case A2 poses less areas than A1, on which the maximum seismic stresses is above the admissible stresses, because the use of the polymer mesh. This increases the addmissible wall stress by 0.93 [lb/in²] from 3.62 [lb/in²] in case A1 to 4.55 [lb/in²] in A2. Thus, the differences between the maximun seismic stresses and the admissibles wall stresses in A1 go from 7.38 [lb/in²] in X1 to 27.58 [lb/in²], whereas in A2 this goes from 6.45 [lb/in²] to 26.65 [lb/in²] , which is 1 lb/in² lower than range in A1.

4.6.2 Analysis B: Adobe structure model with basal restriction to lateral displacement and rotation, using SMAM according to NCh 433 of.96 and Ro=1.

B.1 AS without polymer mesh and foundation wall using SMAM.

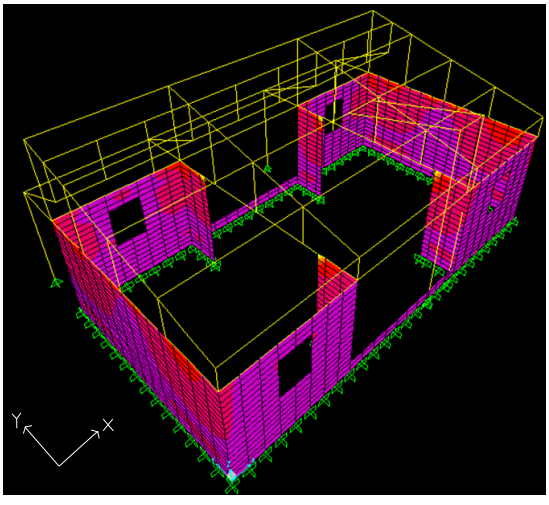

Stress strenght model in X axis

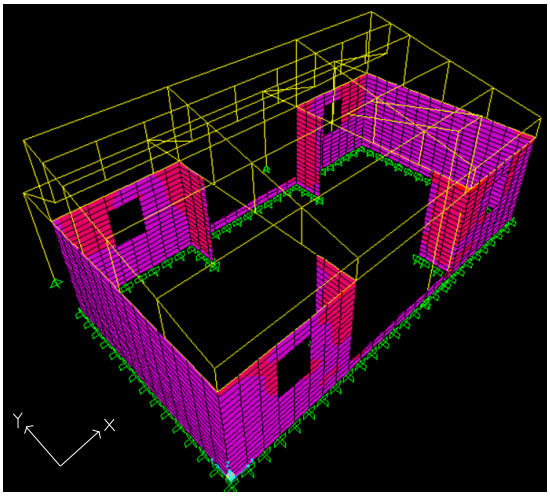

Stress strenght model in Y axis

Figure 4.6.1.7: SAP 2000 models case B1, showing X and Y axis forces. In red the wall stresses above admissible.

Table 4.6.1.8: Case B1 comparison between maximum sesimic stresses and admissible.

Source: Appendix 2

Wall axis	Maximum seismic stresses		Admissible wall stresses		Result
	[Kgf/cm²]	[lbf/in²]	[Kgf/cm²]	[lbf/in²]	
X1	1.46	20.7	0.255	3.62	Fail !
X2	1.01	14.36	0.255	3.62	Fail !
YA	1.41	20.05	0.255	3.62	Fail !
YB	3.37	47.9	0.255	3.62	Fail !
YC	3.23	45.94	0.255	3.62	Fail !
YD	1.5	21.3	0.255	3.62	Fail !

Observations: Figure 4.6.1.7 shows that in the model B1 "without" polymer mesh using SMAM with Ro=1, all walls do have areas that fail and it also shows that less damage occure in Y axis walls than in X axis walls. In this case, the maximum seismic stresses increase because SMAM utilizes a more conservative analysis using R_0=1, which represent

the least favorable value used for mayor seismic forces. Thus, table 4.6.1.7 shows that in red areas the differences between the maximun seismic stresses and the admissibles wall stresses go from 10.74 lb/in^2 in X2 to 44.28 lb/in^2 in YB.

B.2 AS with polymer mesh and foundation wall using SMAM.

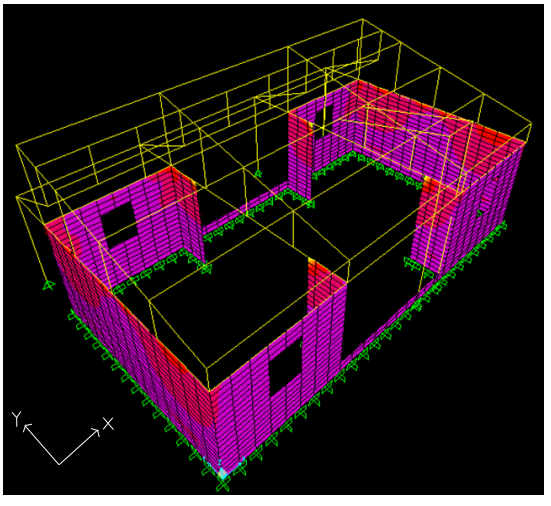

Stress strenght model in X axis

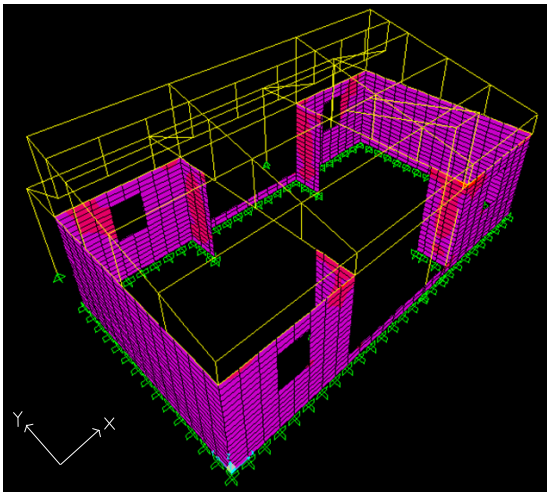

Stress strenght model in Y axis

Figure 4.6.1.9: SAP 2000 models case B2, showing X and Y axis forces. In red the wall stresses above admissible.

Table 4.6.1.10: Case B2 comparison between maximum seismic stresses and admissible.

Source: Appendix 2

Wall axis	Maximum seismic stresses		Admissible wall stresses		Result
	[Kgf/cm^2]	[lbf/in^2]	[Kgf/cm^2]	[lbf/in^2]	
X1	1.46	20.7	0.32	4.55	Fail !
X2	1.01	14.36	0.32	4.55	Fail !
YA	1.41	20.05	0.32	4.55	Fail !
YB	3.37	47.9	0.32	4.55	Fail !
YC	3.23	45.94	0.32	4.55	Fail !
YD	1.5	21.3	0.32	4.55	Fail !

Observations: As occured between A1 and A2, the figure 4.6.1.9 illustrates in case B2 the use of polymer mesh reduces areas on which the maximum seismic

stresses is above the admissible wall stresses. In case B2 the difference between the maximun seismic stresses and the admissibles wall stresses in red areas of the walls goes from 9.81 lb/in^2 to 43.35 lb/in^2., which is 1 lb/in^2 lower than range in B1. Although the seismic analysis using SMAM generated more areas than case A2 on which the maximum seismic stresses is above the admissible stresses, these analysis, SAM and SMAM, are not comparable beween each other due to being rooted with different analytical conditions.

Maximum displacement in superior wall border
0,74 [cm]

4.6.3 Analysis C: AS model with basal restriction to rotation and vertical displacement, with springs to restrict horizontal displacement, using SAM according to NCh 433 of.96.

Before designing the BSI components, this section first describes how forces act in the frictional system by comparing both the Seismic force F without exceeding the frictional force and the Seismic force F exceeding the frictional force.

As was reviewed in section 4.2.1 of this chapter, the friction layer produces a reaction force (Ff) equal to the seismic force, in the opposite direction, formed by the vertical force (Vf) times the friction coefficient (μ). This force reaches a size equal to the structural weight above the friction layer times the friction coefficient as shown in following formula.

$$Ff = Vf \times \mu$$

Ff: Maximum friction force [Tonf].

Vf: Vertical force above friction layer [Tonf].

μ: Friction coefficient [Tonf].

Therefore, to activate the base seismic isolator necessarily the seismic force needs to exceed the friction force, generating the sliding effects of the foundation wall as result. Therefore, the total force results in the difference between the seismic force and the friction force.

Case 1: Seismic F does not exceed the friction force.

The seismic force gets increased without exceeding the friction force. The foundation wall is not affected by displacements. Therefore, the structure receives the total seismic force and the base isolator is not activated yet as the Figure 4.6.3.1 shows.

Figure 4.6.3.1 Representative graph case 1. Seismic force is lower than the friction force .
Source: SM creation based on reviewed literature.

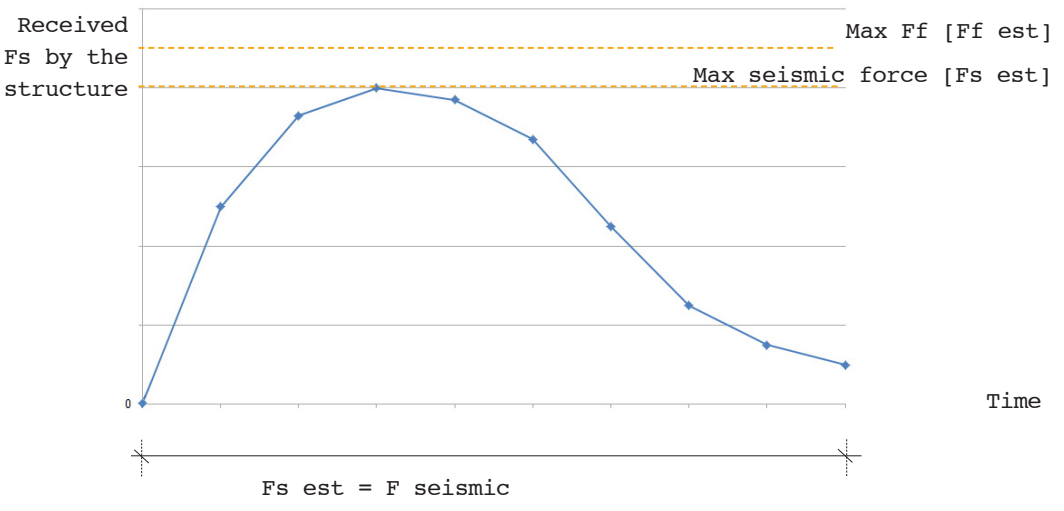

Case 2: Seismic F exceeds the friction force.

The seismic force gets increased exceeding the friction force in a period of time, generating the sliding effect between the footing and the foundation wall. Therefore, the structure receives the difference between the total seismic force and the maximum friction force in this period of time, activating base seismic isolator as the Figure 4.6.3.2 shows.

Figure 4.6.3.2 Representative graph case 2. Seismic force exceeds the maximum friction force in a period of time.
Source: SM creation based on reviewed literature.

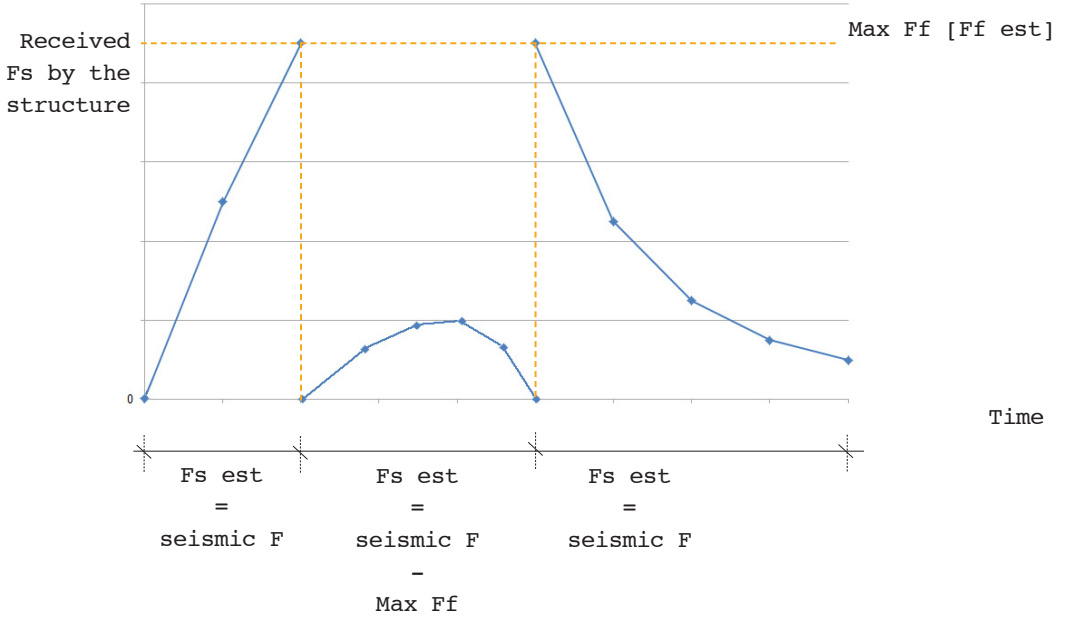

• Dissipated force calculus and the X frictional layer percentage reduction resulted from Seismic Method.

In this case, SAP 2000 provides Qx qnd Qy according to summatory of basal reaction in X and Y. This values is employed to determine Rx and Ry basal seismic stress reduction, which is used to define the scale factor in Load cases.

Table 4.6.3.3: Analysis C, force calculus
Source: Appendix 2

	Symbol	formula	Value	Unit
Seismic weight	**P**		69.3	[Tonf]
Friction coefficient	**Fc**		0.202	
Maximum friction force	**Fd**	P x Fc	14	[Tonf]
X basal seismic stress without isolator	**Qx**		16.95	[Tonf]
Y basal seismic stress without isolator	**Qy**		16.95	[Tonf]
X basal seismic stress with isolator	**QX**	Max (Fd,Qy)	16.95	[Tonf]
Y basal seismic stress with isolator	**QY**	Max (?,Qy)	16.95	[Tonf]
X basal seismic stress reduction by isolator	**Rx**	Qx-Fd	2.951	[Tonf]
X basal seismic stress reduction by isolator	**Rx**	Rx/Qx	0.174	%
Y basal seismic stress reduction by isolator	**Ry**	Qy -Fd	2.951	[Tonf]
Y basal seismic stress reduction by isolator	**Ry**	Ry/Qy	0.174	%

Assign the scale factor in SAP2 000 according to friction coefficient

P building weight 63.9 [Tons] X **Fc** fiction coefficient of gravels 0,202

Qx or Qy ∑ reaction forces in X and Y 16.952 [tons] − **Fd** Maximun friction force 14 [tons] = **Rx or Ry** Basal seismic stress reduction with SBI 2,952 [Tons]

Rx or Ry Basal seismic stress reduction with SBI 2,952 [Tons] / **Qx or Qy** Basal seismic stress reduction without SBI 16,95 [Tons]

Rx or Ry Seismic stress reduction 17.4%

100 % − 17% = **83%**

Case 2: Friction dynamic force (fdF)

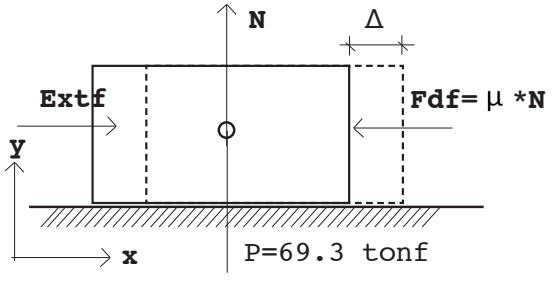

- **Dimension calculus of the steel pipe component in the re-centering system**

Table 4.6.3.4
Analysis C, steel pipe calculus
Source: Appendix 2

	Symbol	formula	Value	Unit
Steel pipe	n		18	
Seismic force per steel pipe	Fs/n	[Max (Fd,Rx,Ry)]/n	0.778	[Tonf]
Yield limit	Fy		2400	[Kgf/cm^2]
Stress	V	0.45 x Fy	1080	[Kgf/cm^2]
Required steel area	A	1000 x (Fs/n)/V	0.72	[cm^2]

18 steel pipes are placed on the footing wall. They should size 1" diameter or 1.47 [cm^2] and thickness of 2 mm as shown in table 4.6.3.4.

- **Dimension calculus for the rubber-ring component in the re-centering system.**

Table 4.6.3.5
Analysis C, rubber ring calculus
Source: Appendix 2

	Symbol	formula	Value	Unit
Rubber donut-ring	n		18	
Seismic force in each rubber donut-ring	Fs/n	[Max (Fd,Rx,Ry)]/n	0.778	[Tonf]
Rubber height	h		5	[cm]
Rubber width	w		1	[cm]
Rubber section subjected to pressure	A	h x w	5	[cm^2]
Compressing strength	Rc		85	[Kgf/cm^2]
Required compressive strength	C	1000 x (Fs/n)/A	155.5	[Kgf/cm^2]
Rubber thickness	e	5 x C/Rc	9.149	[cm]

- **Dimension calculus of the "k" spring component in the re-centering system**

Table 4.6.3.6
Analysis C, k calculus
Source: Appendix 2

	Symbol	formula	Value	Unit
Modulus of Elasticity	**E**		300	[Kgf/cm²]
Seismic force in the rubber	**Fs**	[Max (Fd,Rx,Ry)]/n	0.778	[Tonf]
Rubber height	**A**		5	[cm²]
Compressed rubber section	**Ps**	Fs x 1000/ A	155.5	[Kgf/cm²]
Relative deformation	**dr**	h x w	0.518	%
Deformation	**d**	Ps / E	4.74	[cm]
Model spring	**K**	1000 x Fs/d	163.9	[Kgf/cm]

Figure: Rubber without deformation
Source: SM creation base on dimention calculus of k spring component.

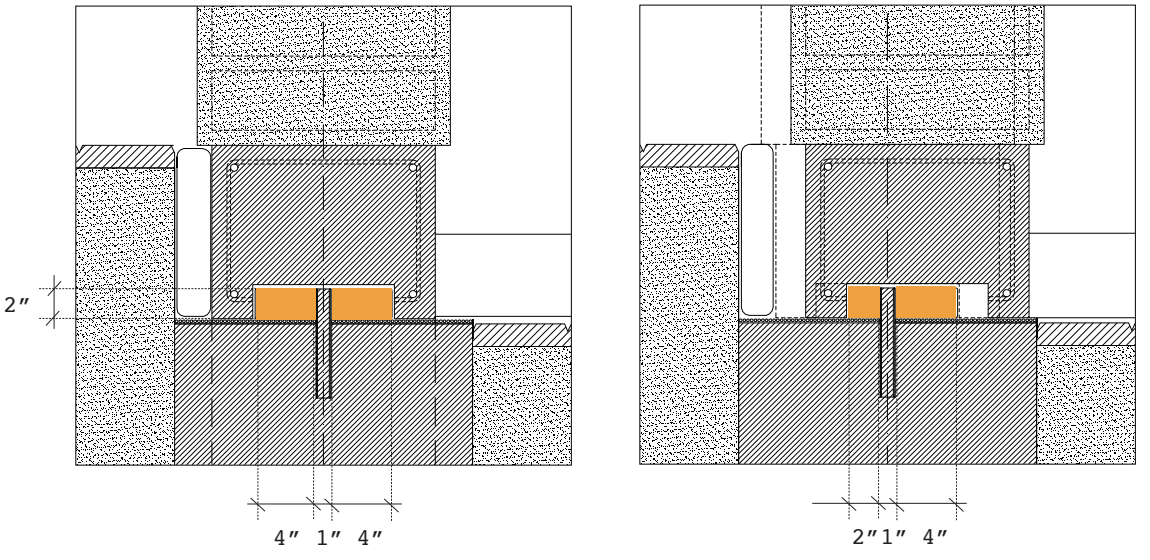

C.1 AS without polymer mesh and with SBI using SMAM.

In this case, the BSI dissipates part of the seismic force, therefore, in both direction, X and Y axis, the seismic force is reduced. As was shown

in figure 4.6.3.2, the most critical period occurs right before the isolator starts working, the period in which the structure is subjected to a seismic force of 14 [Tonf]. In this case, the maximum seismic stresses are reviewed using a model similar to Case A.1, but **the seismic force** applied in the model **is reduced from 33900 lb [16.95 Tonf] to 28000 lb (14 Tonf).** which is P of 69.3 [tonf] times Fc of 0.202 [tonf] shown in table 4.6.3.3. **Thus, the seismic force is diminished in about 17.5%.**

Maximum displacement in superior wall border
0,73 [cm]

Figure 4.6.3.7: SAP 2000 models case C1, showing X and Y axis forces. In red the wall stresses above admissble.
Source: Appendix 2

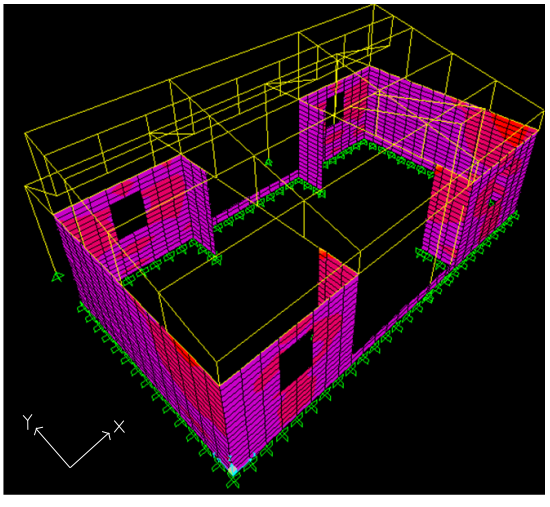

Stress strenght model in X axis

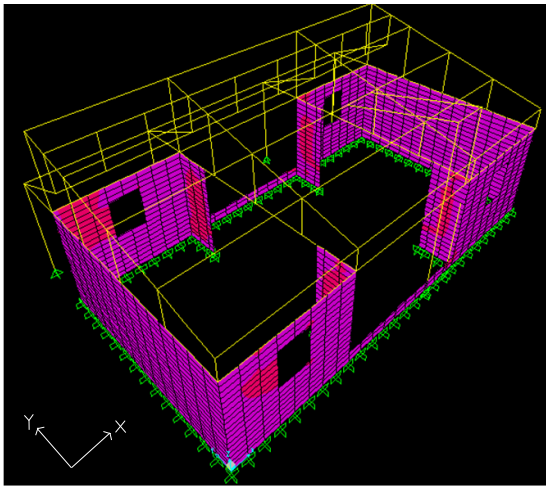

Stress strenght model in Y axis

Table 4.6.3.8: Case C1 comparison between maximum seismic stresses and admissible.
Source: Appendix 2

Wall axis	Maximum seismic stresses		Admissible wall stresses		Result
	[Kgf/cm²]	[lbf/in²]	[Kgf/cm²]	[lbf/in²]	
X1	0.65	9.25	0.255	3.62	Fail !
X2	0.68	9.67	0.255	3.62	Fail !
YA	0.85	12.09	0.255	3.62	Fail !
YB	1.83	26.03	0.255	3.62	Fail !
YC	1.84	26.17	0.255	3.62	Fail !
YD	0.8	11.38	0.255	3.62	Fail !

Observations: Figure 4.6.3.7 shows that in case C1 the areas on which the seismic stresses are above the admissible wall stresses are less than those shown case A2, indicating that the SBI works and generates less damaged area than modeled case A2. The results' breakdown in Table 4.6.3.8 confirms this difference. In case A2 by only using polymer mesh this difference goes from 6.45 [lb/in²] to 26.65 [lb/in²], whereas in C1 by only employing the SBI this difference goes from 5.63 lb/in² to 22.55 lb/in².

Figure 4.6.3.9: SAP 2000 models case C2, showing X and Y axis forces. In red the wall stresses above admissble.
Source: Appendix 2

C.2 AS with polymer mesh and SBI using SAM.

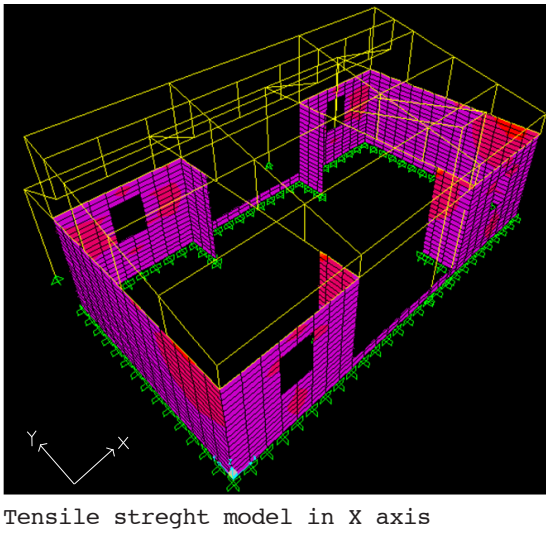

Tensile streght model in X axis

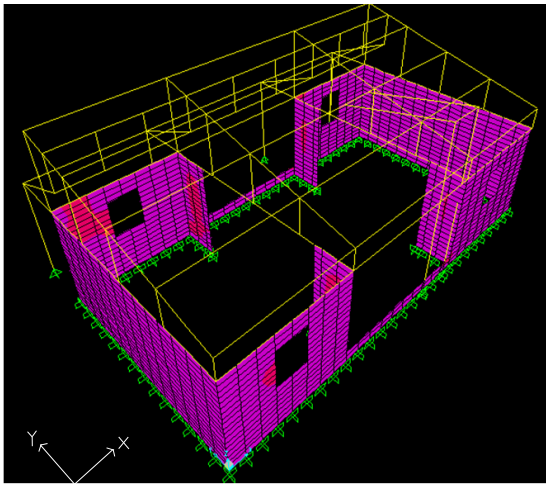

Tensile streght model in Y axis

Table 4.6.3.10: Case C2 comparison between maximum seismic stresses and admissible.
Source: Appendix 2

Wall axis	Maximum seismic stresses		Admissible wall stresses		Result
	[Kgf/cm²]	[lbf/in²]	[Kgf/cm²]	[lbf/in²]	
X1	0.65	9.25	0.32	4.55	Fail !
X2	0.68	9.67	0.32	4.55	Fail !
YA	0.85	12.09	0.32	4.55	Fail !
YB	1.83	26.03	0.32	4.55	Fail !
YC	1.84	26.17	0.32	4.55	Fail !
YD	0.8	11.38	0.32	4.55	Fail !

Observations: As occured between case A1 and A2, and between cas B1 and B2, in this case the use of polymer mesh also reduces the admissible wall stresses in the AS with SBI from the previous analysis. Thus, in C1 this difference goes from 5.63 lb/in² to 22.55 lb/in², whereas in C2 this range goes from 4.77 lb/in² to 21.66 lb/in². Althouth the areas where the admissible wall stesses are below the the maximum seismic stesses still remains, this case represents the most favorable situation of the AS subjected to sesimic motion in comparisont to the previous modelings, which is illustrated in wall comparison graphs in section 4.6.5 of this research.

4.6.4 Analysis D: AS model with basal restriction to rotation and vertical displacement, with springs to restrict horizontal displacement, using SMAM according to NCh 433 of.96.(View SAP 200 steps described in Appendix 2)

• Dissipated force calculus and the X frictional layer percentage reduction from Seismic Method.

Table 4.6.4.1: Analyis D, force calcuclus.
Source: Appendix 2

	Symbol	formula	Value	Unit
Seismic weight	p		69.3	[Tonf]
Friction coefficient	CF		0.202	
Maximum friction force	Fd	P x Fc	14	[Tonf]
X basal seismic stress without isolator	Qx		8.5	[Tonf]
Y basal seismic stress without isolator	Qy		11.2	[Tonf]
X basal seismic stress with isolator	QX	Max (Fd,Qy)	14	[Tonf]
Y basal seismic stress with isolator	QY	Max (?,Qy)	11.2	[Tonf]
X basal seismic stress reduction by isolator	Rx	Qx-Fd	-5.499	[Tonf]
X basal seismic stress reduction by isolator	Rx	Rx/Qx	0.647	%
Y basal seismic stress reduction by isolator	Ry	Qy -Fd	-2.799	[Tonf]
Y basal seismic stress reduction by isolator	Ry	Ry/Qy	-0.25	%

In each axis the seismic force is smaller than the friction isolator force, therefore, the seismic base isolator is not activated. This case shows the same result as those analysed in cases B1 and B2, thereby, there is not the need to repeat the analysis.

• Dimension calculus for the steel pipe component in the re-centering system according to Figure 3.2.2.4

Table 4.6.4.2: Analysis D, steel pipe calculus.
Source: Appendix 2

	Symbol	formula	Value	Unit
Steel pipe	n		18	
Seismic force per pipe	Fs/n	[Max (Fd,Rx,Ry)]/n	0.778	[Tonf]
Yield limit	Fy		2400	[Kgf/cm^2]
Stress	V	0.45 x Fy	1080	[Kgf/cm^2]
Required steel area	A	1000 x (Fs/n)/V	0.72	[cm^2]

18 steel pipes are considered to be placed on the footing wall. They should size 1” diameter or 1.47 [cm^2] and thickness of 2 mm

Table 4.6.4.3
Analysis D, rubber-ring calculus
Source: appendix 2

•Dimension calculus for the rubber-ring component in the re-centering system.

	Symbol	formula	Value	Unit
Rubber donut-ring	n		18	
Sesimic force per rubber donut-ring	Fs/n	[Max (Fd,Rx,Ry)]/n	0.778	[Tonf]
Rubber height	h		5	[cm]
Rubber width	b	Fs x 1000/ A	1	[cm]
Rubber section subjected to pressure	A	h x w	5	[cm²]
Compressing strength	Rc	Ps / E	85	[Kgf/cm²]
Required compressing strength	C	1000 x Fs/d	155.5	[Kgf/cm²]
Rubber thickness	e		9.149	[cm]

18 steel pipes are required to be covered with 4" thickness rubber ring donut or 10 [cm].

4.6.5 Analysis of maximum stresses that go beyond admissible wall stresses in representative walls and the damaged wall area analysis.

Stresses of walls X1, YA, and YB are compared in bar graph of Figures 4.6.5.2 using SAM and 4.6.5.3 employing SMAM. However, the comparison highlights SAM results, which suit the NCh 433.Of96 Chilean Code.

Figure 4.6.5.1
Architecture plan with selected axis.
Source: SM creation

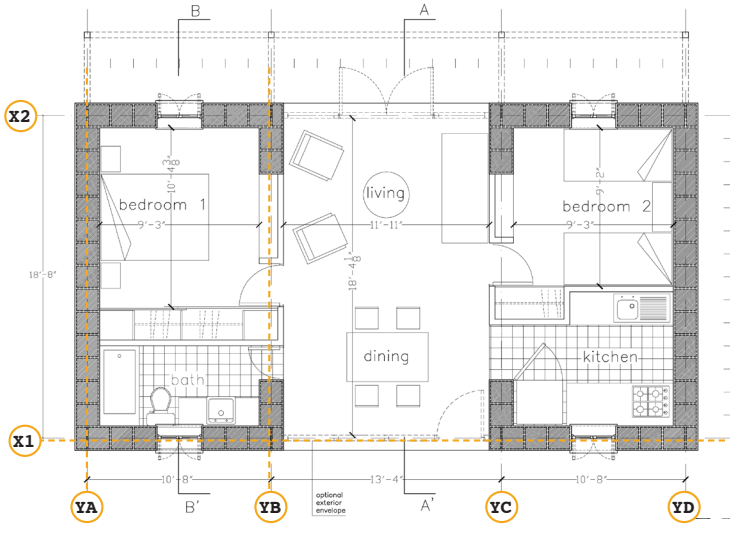

Observations:

• Studied walls using SAM are represented in Fifure 4.6.5.2. This illustrated that all walls reduce their stresses from case A1 to C2 in a

Figure 4.6.5.2: Stresses that go beyond admissible in wall for studied cases A1, A2, C1, and C2 using Static analysis method.
Source: SM creation based on appendix 2.

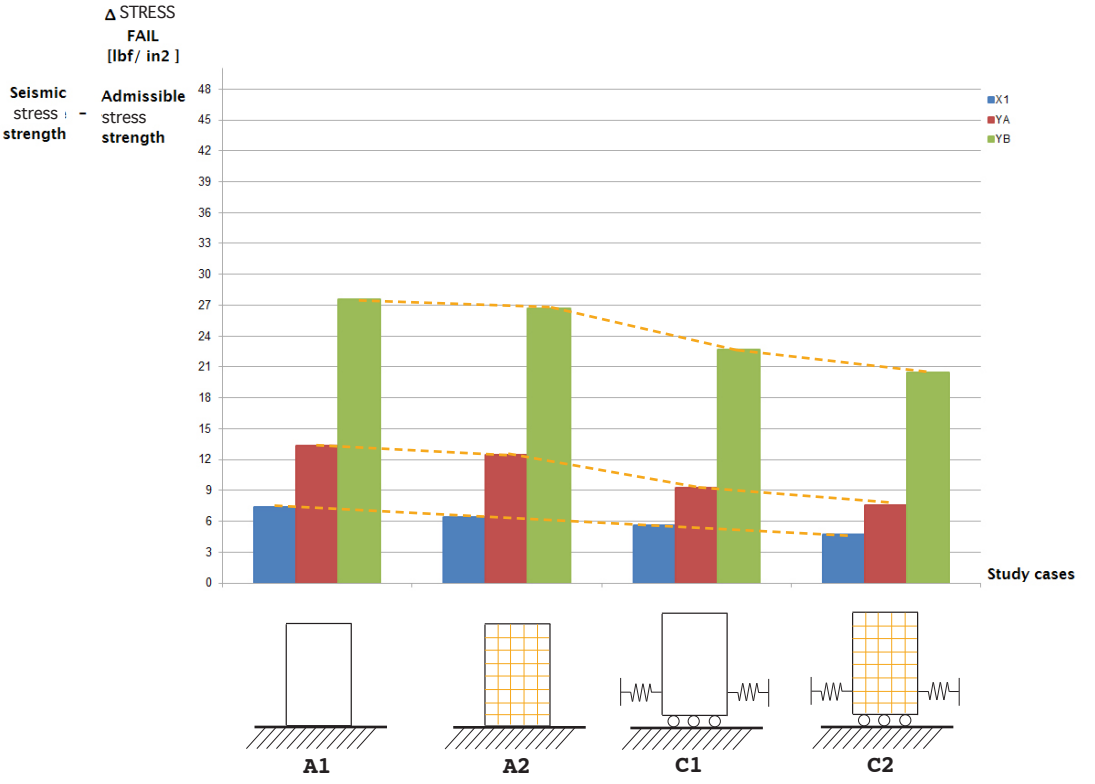

Figure 4.6.5.3: stresses that go beyond admissible in wall for studied cases A1, A2, C1, and C2 using Spectral modal analysis method.
Source: SM creation based on appendix 2.

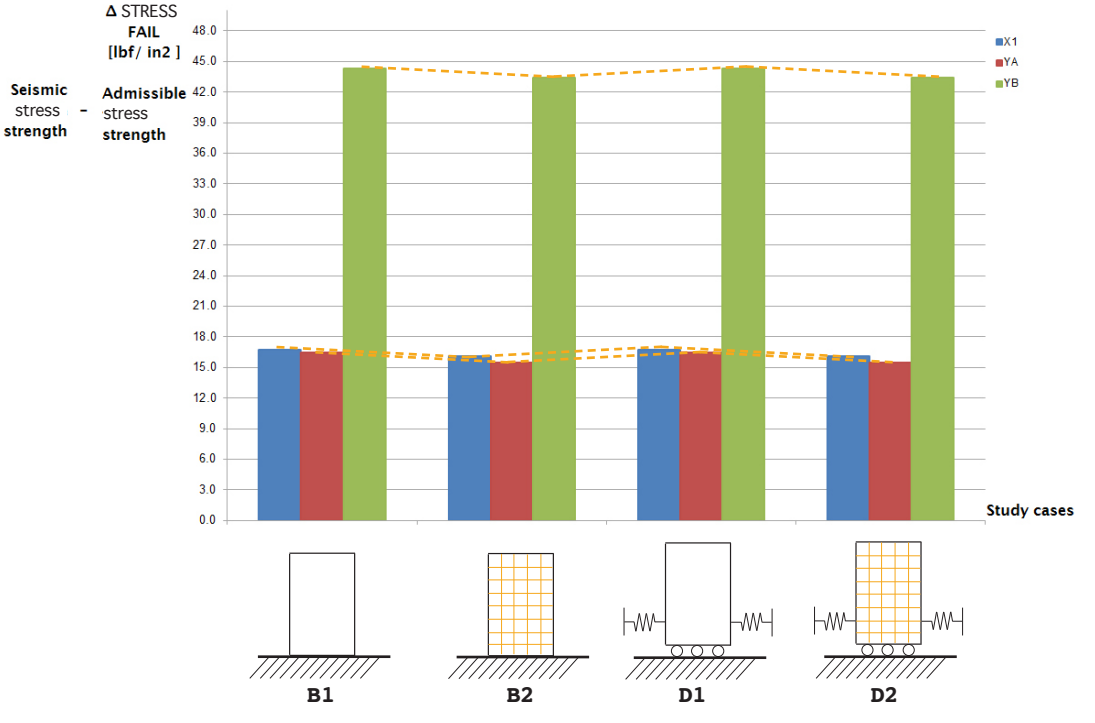

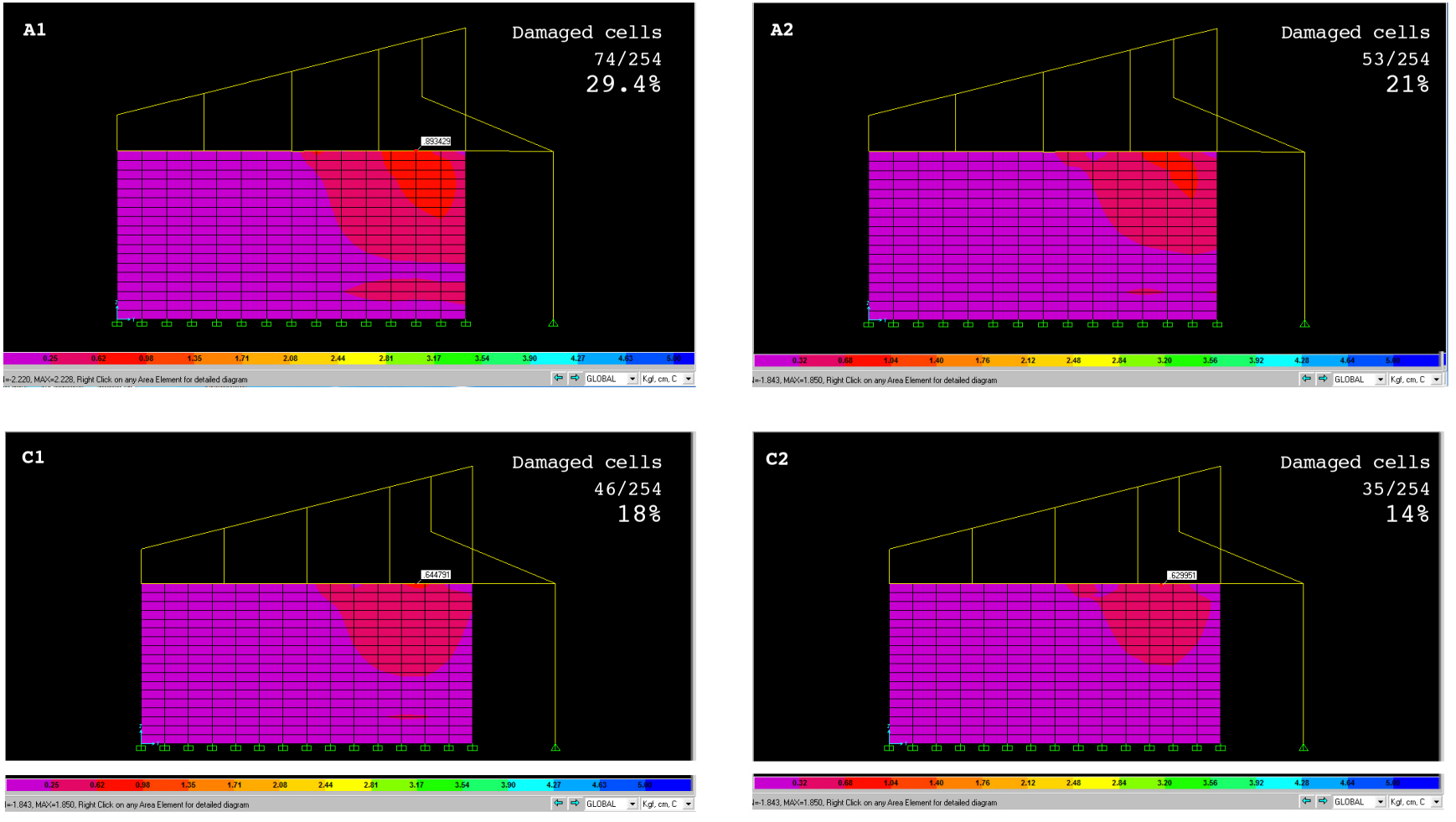

Figure 4.6.5.4: Diagrams of damage in wall X1 using SAM. violet represents areas without damages and red area with damages.
Source: SM creation based on Appendix 2.

range of 3 to 5 [lbf/in^2].

• Wall X1 in case C2 has the smallest difference between the maximum seismic stresses and the admissible wall stresses. This wall reaches a difference in C2 of 4.5 [lbf/in^2] from the baseline un-reinforced specimen in A1 with a difference of 7.5 [lbf/in^2].

• The biggest reduction of stresses in walls between two consecutive cases is given in walls YA and YB between case A2 and C1, achieving 5 [lbf/in^2] of stress reduction.

• In contrast, the minimum reduction occurs in walls YA and YB between cases A1 and A2, and between cases C1 and C2, where the stresses are only reduced in about 1.5 [lbf/in^2].

• The diagrams of SAM in wall X1 shown in Figure 4.6.5.4, determines that in case A1 (AS with foundation wall and without reinforcement systems or SBI) the seismic force damages 30% of the wall area.

• The same diagram of the wall X1 illustrates that by only using polymer mesh in case A2 the total damaged area dropS down to 21%. Also, by only employing the SBI in case C1 18% of the wall area suffers damages. In consequence, by only using the SBI the damage area generated in the wall by the seismic force is reduced by about 11.4%

• Studied walls using SMAM with Ro=1 are represented in Figure 4.6.5.3. By acknowledging that SMAM is a proposal study not required by NCh 433.Of96 Chilean Code. Graphs show that cases B1/B2 and D1/D2 reached the same seismic stresses because the seismic base isolator is not activated. Therefore, the analysis with seismic base isolator using SMAM requires using a friction coefficient smaller than 0.2 (pebble friction coefficient)

4.7 Cost analysis

In this section the cost analysis (1) evaluates construction expenses between models A1, A2, C1 and C2 as shown in Table 4.7.1, 4.7.2, 4.7.3, and Fig-

ure 4.7.4. Also, with the aim to determine if Case C2 can be presented as an economic alternative for affordable housing units in Chile and other regions with similar conditions, the cost analysis (2) compares C2 to other three units that use different envelope materials and suit the same layout and thermal design code required for housing units in Bio Bio VIII Region a shown Table 4.7.5 and Figure 4.7.6.

Cost analysis 1:

Case 1: Adobe structure “without” polymer mesh and with rigid foundation wall.

Case 2: Adobe structure “with” polymer mesh and rigid ring foundation wall.

Case 3: Adobe structure “without” polymer mesh, “with” seismic base isolator.

Case 4: Adobe structure “with” polymer mesh seismic base isolator.

The cost estimation for each model considers the following conditions:

• The total gross area is 645 ft^2 (60 m2). This

means that the total cost is computed considering the incremented area that would increase the capital value over the time as was reviewed in section 2.3.2.

• Detailed construction cost is only estimated to envelope materials in group A.

• According to Boetsch and Becon SA group B can be estimated using a global cost that goes from 50% to 65% of the total cost. This group includes construction components like interior walls, plumbing fixtures, light package, appliances and floor covering, among others interior building components.

• Study cost “Modulo basico de adobe reforzado con geomalla” by Rodriguez and Walker (2009) is used for referencing cost and items included in construction group A.

• Reference of material costs and building hour wages are sourced in building material suppliers in Chile like Homecentre and independent built dwelling projects. Nevertheless, the final cost of estimated items depends on the local availability.

• Reference costs in study of Ozden (2006) are considered to the SBI components scrap tire rubber.

Table 4.7.1: Breakdown of construction cost in four study cases
Source: SM creation

Group A components	Construction component	Unit	quantity (foot or feet)	quantity (meters)	Unit value	Case 1 [A1]	Case 2 [A2]	Case 3 [C1]	Case 4 [C2]
Preliminary works	Preliminary works	global		1	361	361	361	361	361
	Excavation and level settings	ft3,m3	766.8	21.6	26	562	562	562	562
Footing	Footing (18" width and 23" height)	ft3,m3	766.8	21.6	155	3348	3348	3348	3348
Foundational wall	Foundation wall (16" width and 12" height)	ft3,m3	766.8	21.6	137	2959	2959	2959	2959
	Foundational wall mold	ft2,m2	852	24	51	1224	1224	1224	1224
Seismic base isolator	"L" steel rebars (1"x1")	feet,ml	230.4	72	1.5			108	108
	Steel pipes	piece, pieza	18	18	6			108	108
	Gravel layer (6mm to 8mm)	ft2, m2	173.34	16.2	1.5			24.3	24.3
	Teflon layer (2mm)	ft2, m2	154.08	14.4	6			86.4	86.4
	Scrap tire rubber donuts	piece, pieza	18	18	20			360	360
	Tin hat (4" diameter)	piece, pieza	18	18	1.3			23.4	23.4
	wall base moister isolation layer	ft2,m2	140	13.05	3.02	39	39	39	39
Adobe wall	Adobe wall (16" width and 83" height)	ft2,m2	888.1	83	8	664	664	664	664
	Exterior and interior mud Stucco (2")	ft2,m2	888.1	83	4	332	332	332	332
Slab	Polished concrete slab	ft2,m2	449.4	42	29	1218	1218	1218	1218
Roofing	roof-structural trusses (5"x1" pine timber)	piece, pieza	4	4	43	172	172	172	172
	roof-decking (4" pine timber)	ft2,m2	665.54	62.2	20	1244	1244	1244	1244
	roof-roofing (USB panel + earth)	ft2,m2	665.54	62.2	30.3	1885	1885	1885	1885
Polymer mesh reinforcement (PM)	Reinforcement polymeric mesh (TENSAS)	m2 or ft2	1776.2	166	5		830		830
	Reinforcement connectors	m2 or ft2	888.1	83	2		166		166
	Reinforcement Sup.ring beam (4" x4" timber)	ml or feet	129.92	40.6	14.65		594.79		594.79
Windows and door	Timber-framed window	pza or piece	4	4	180	720	720	720	720
	Timber-framed door	pza or piece	2	2	320	640	640	640	640
	Glazings	ft2,m2	295	27.8	40	1112	1112	1112	1112
	Doorknobs and others fittings	pza or piece	2	3	55	165	165	165	165
Paintings	Paintings-exterior	ft2,m2	1257.571	117.53	5.45	641	641	641	641
	Paintings-interior	ft2,m2	1136.875	106.25	4.8	510	510	510	510
	Paintings-strips	ft2,m2	256.8	24	3.5	84	84	84	84
Delivery	Delivery- materials	kg	66138	30000	0.02	600	600	600	600
Group B components						18000	18000	18000	18000
Total						**36479.4**	**38070.2**	**37189.5**	**38780.3**
%						100	104	102	106

Table 4.7.2: Comparison cost summary of four study cases
Source: SM creation

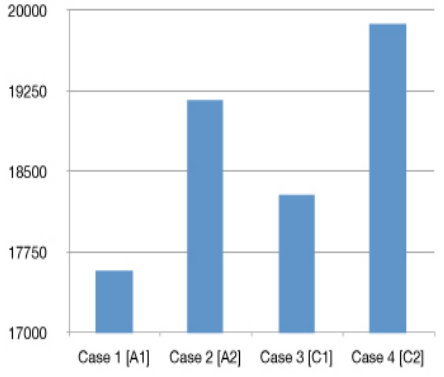

Table 4.7.3: Percentages of construction items in Case 4
Source: SM creation

C1: AS with only SBI	Total ($US)	%
Group A		
Preliminary works	923	2.4
Footing	3348	8.9
Foundational wall	4183	11
Seismic base isolator	710	1.88
Base moister isolation	39	0.00001
Adobe wall	996	2.6
Slab	1218	3.2
Roofing	3301	8.7
Sup. beam reinforcement	595	1.6
Windows and door	2637	7.0
Paintings	1235	3.3
Delivery materials	600	1.6
Group B	18000	48
	37784	100

Figure 4.7.4: Percentages of construction items in Case C1
Source: SM creation

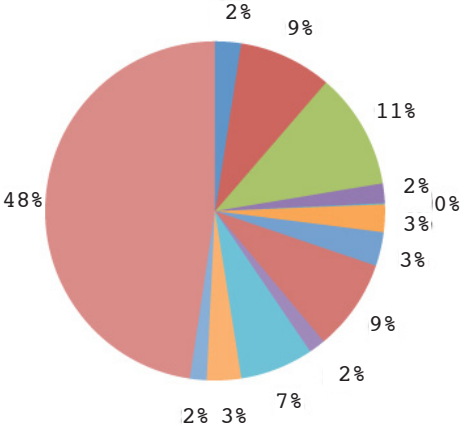

Nevertheless, this component eventually can be resourced locally.

Observation:

• The listed construction components in Table 4.7.1 shows that by employing polymer mesh the total construction cost of the adobe dwelling with no reinforcement system increases by 4%, whereas by only employing the SBI the total cost of the adobe unit augments 2%. In addition, by combining both systems, the total construction cost increase 6%, from an un reinforced adobe structure.

The summary breakdown of construction cost of C1 shown in Table 4.7.3 and Figure 4.7.4 reveal that the SBI accounts with 2% of the total expenses. Therefore, by implementing the SBI the total construction cost would be significantly lower than the expenses used

to include other alternatives of seismic base isolators that have both functions diffusing seismic force and re-centering the superstructure reviewed in section 2.2. Thus, the proposed SBI cost is lower than the friction roller bearing, the friction pendulum bearing, the elastomeric bearing, the self centering strut, the steel dumper, and the fluid dumper.

Cost analysis 2:

Case C1 is compared to three other housing units with different envelope construction settings: the 4" reinforced brick with 2" of isolation, the structural isolation panels (SIP), and the light steel frame (LSF). These three cases meet both the proposed dwelling layout design and the thermal design code required for residential units in Climate zone 4 MINVU (2006), OGUC 4.1.10.

• Table 4.7.6 illustrates that the total cost of

Table 4.7.5: Comparison cost summary between C1 and three other dwelling units made out different envelope materials
Source: SM creation

	Wall unit cost 10.7 sf,1m2 ($US)	Total Wall ($US)	Total A ($US)	Total B ($US)	Total ($US)	Unit cost 10.7 sf or 1m2 ($UF)
Adobe A1 (with only PM)	12	1035	18479	18000	36479	794
Adobe C1 (with only SBI)	21	1746	19190	18000	37190	810
4" reinforced brick with 2" insolation	38	4180	22258	18000	40258	876
Structural isolated panels (SIP)	46	5060	23138	20000	43138	939
Light steel frame (LSF)	48	5280	23358	20000	43358	944

Figure 4.7.6: Comparison cost summary between C1 and three other dwelling units made out different envelope materials
Source: SM creation

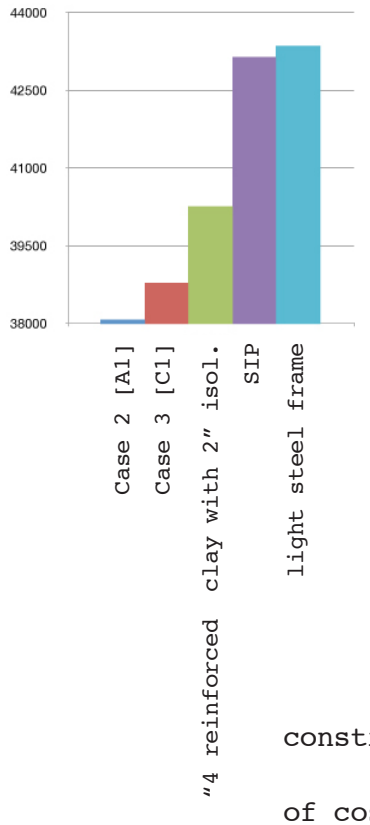

Thus, C1 cost is 14.2% lower than the total cost used to build the dwelling unit with light steel frame system, 13.8% lower than employing SIP system, and 8% lower than using the 4" reinforced brick with 2" of isolation.

• The total cost of C1 also suits the required conditions to apply for governmental funds reviewed in section 2.3.1. The total construction cost for case C1 is within the range of costs to apply for housing funds type FSV, which covers units that cost up to US 43625 $ (900 UF). If C1 is implemented in rural areas, the program SHR could fund up to US$ 22.400 (420 UF), which is 50% of the total construction cost estimated in the adobe dwelling. Range of costs to apply for housing funds type FSV, which covers units that cost up to US$ 4,3625 (900 UF). If C2 is implemented in rural areas, the program SHR could fund up to US$ 22,400 (420 UF), which is 50% of the total construction

cost estimated in the adobe dwelling.

Ultimately, by combining the results of the static analysis method developed in section 4.6 and the cost analysis reviewed in section 4.7, there exist conditions to argue that the AS with BSI modeled in case C1, might suit a better ratio cost&funtion than the A2, the AS with polymer mesh. This means that by only implementing the SBI the AS experiences less stresses, generates less area of damages, and is less pricy than the AS protected only with polymer mesh.

4.8 Local and broad implications

This section attempts to determine the consequences of installing the SBI in the current context of Chile and other part of the globe on which seismic activities coincide with the adobe architecture. The assumption of these effects use data given by the report of damage in Chile PRTM (2010) reviewed in section 1.0 and conclusion content presented in static analysis method developed in section 4.6.5.

The PRTM (2010) mentions that from a total dam-

aged dwellings in urban and rural areas of 135,433 (100%), 50,576 (27%) were completely destroyed, 47,936 (37%) had major damages, and 36,921 (36%) suffered minor damages. In addition, PRTM uses the same Macro-seismic scale classification of damages employed by the USGS and European 1998 (EMS-98). These are:

Minor to Moderate damages:

From cracks in stucco to cracks in sev eral walls

Collapse of chimney

Major damages:

Structural damages

Structure can withstand by itself

Table 4.8.1: Seismic damages in dwellings in F2010 with unaffected people estimation.
Source: SM creation base on PRTM (2010) presented in section 1.0

Dwelling Tipology	Total destruction	Major damages	Minor damages	Total
Costal	7,931	8,607	15,384	31,922
Urban adobe	26,038	28,153	14,869	69,060
Rural adobe	24,538	19,783	22,052	66,373
SERVIU	5,489	15,015	50,955	71,459
Privated	17,448	37,356	76,433	131,237
total	81,444	108,914	179,693	370,051

affected

135,433 dwellings
460,472 people

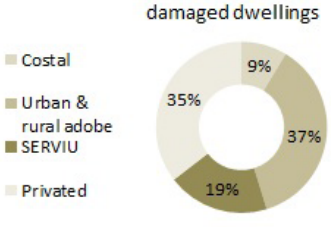

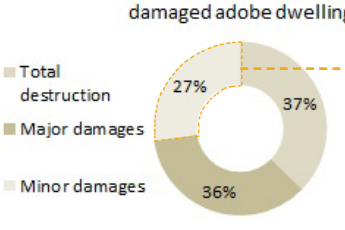

unaffected

36,921 dwellings
125,900 people

Big cracks in some or several walls

Collapse of chimney

Total destruction:

Severe structural damages

Structure can not withstand by itself

Several walls collapse.

In addition, the analysis of damaged areas in the A1,A2, C1, and C2 using SAM reviewed in section 4.6.5, reveals that although in all four cases the adobe structure suffers major damages in area of the wall, confirmed by the stresses differences analysis, in Case C1 this area is reduced in about 14% from un-isolated or un-reinforced structure. Therefore, it is possible to argue that by using SBI the total reported adobe dwellings with minor damages, 36,921 (36%), had had remained without damages after the earthquake F2010 as shown Figure 4.8.1. Also, if 3.41 is the average number of people assigned for ordinary households in Chile according to CASEN survey (2011) 125,900 people living in adobe structures had not being affected by the seismic force from the past earthquake F2010. By using the same

scenery, the SBI might also reduce the number of destroyed adobe dwellings of 50,576 (37%), remaining some of them within the major damages classification.

Because the BSI considers material that can be easily found in any recycled material deposit of developing nations, the risk of material availability is significantly reduced compared to other affordable solutions, such as the polymer mesh, which generally has no local availability.

Although sizes and composition of adobe blocks are different in each territory the construction process described in following section 4.9 is globally used in all adobe territories. This is taken into consideration to determine the installation process of the SBI. Thus, instead of modifying the traditional process to build the footing and foundation wall, the proposed SBI aggregates steps as described in the section 4.9.

4.9 Installation process

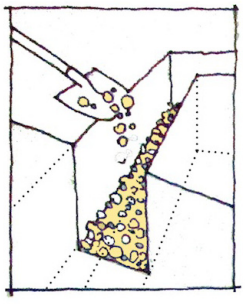

Diagram:SM creation

1.Dig the trench out and place pebble layer

The 18" (45 cm) width and 30" (76 cm) height trench is dug out, which is the form of the footing. Then, lay dow a layer of pebbles and stones in the bottom of the trench.

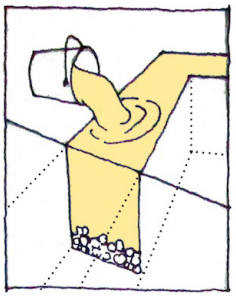

Diagram:SM creation

2.Build the footing wall

Construct the footing wall with concrete H-25 based on dimensions shown in section 3.2.4. Lay horizontally "L" steel rebars in borders before pouring the last inch of concrete. This will act as the boundary for the gravel layer that will be placed of top of the footing wall. Make sure to finish the foundation wall with a flat top level

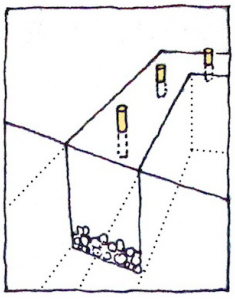

Diagram:SM creation

3. Place steel pipes (re-centering system)

The 17" height,1"ø,and 2mm thickness recycled steel pipe is placed in the top of the footing as shown foundation plans in section 3.2.4. The steel pipe is buried 12" (30 cm) height before the footing concrete dry. Make sure that the the steel pipe is vertically located.

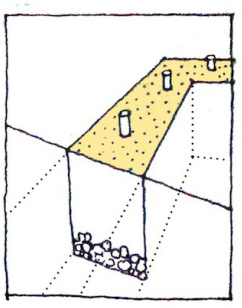

Diagram: SM creation

4. Pebble layer (frictional system)

The pebble layer is placed on top of the footing, employing coarse sandy mix with small stones with (between 6mm to 8 mm), smooth or sharp edges.

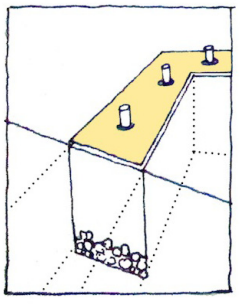

Diagram: SM creation

5. Teflon layer (frictional system)

On top of the gravel layer the 18" [40 cm] width teflon layer is located. This component avoids the pebble layer that gets mixed with the concrete of the foundation wall once this has been poured.

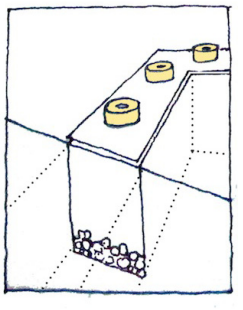

Diagram: SM creation

6. Rubber donut-ring (re-centering system)

2" high recycled car tire rubber bands are placed around the steel pipe until reaching a width of 4" [10cm]. Bands are glued together using based-polyurethane adhesive.

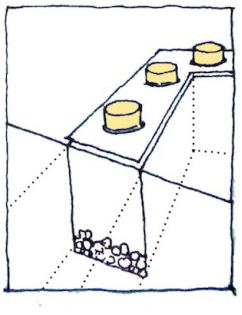

Diagram: SM creation

7. Place Tin hat (re-centering system)

Cut painting tin with diameter of 4" [10cm] covers the steel pipe and the recycled car tire rubber. The painting tin acts as a hat to avoid the re-centering system being affected when the concrete for the foundation wall is poured.

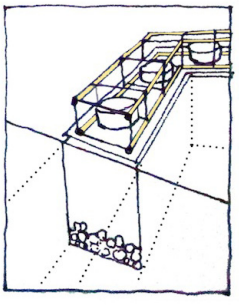

Diagram:SM creation

8. Install steel rebars.

The basket that reinforce the foundation wall is located in the center of the wall axis, directly on top of the teflon layer, confined the re-centering components. The basket is formed by four steel re-bars separated by stirrups.

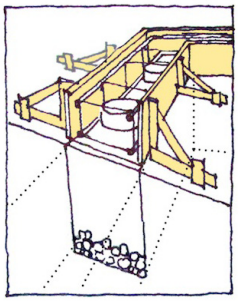

Diagram:SM creation

9. Set the shuttering (wood forms)

1 foot height by 1'4" width shuttering is set directly on top of the Teflon layer, enclosing the rubber donut and the rebar. This must be solidly braced against ground surface to prevent movement when the concrete is poured. To avoid bulging, shuttering should also be thick enough. Wood forms are usually set by using 1½ inch thick lumbers, wood sheathings, or plywood, braced about every 6 feet.

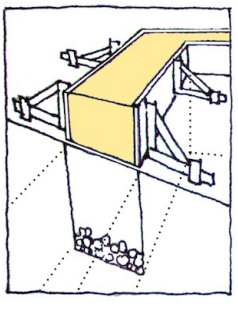

Diagram:SM creation

10. Build the foundation wall and locate the polymer mesh.

10-A: The H-25 concrete is poured into the shuttering until reaching 1' height. A peace of Polymer mesh located before the last layer of concrete is

poured. To prevent air pockets the concrete should be properly tamped into the shuttering.

10-B: Adjust polymer mesh and finish foundation wall

In case polymer mesh is required to reinforce adobe wall, concrete must be powdered until reaching 8 inches height. Then, the "U" shape [350 kgf/m] stress strength polymer mesh is placed and concrete is powdered to complete the 1' height foundation wall.

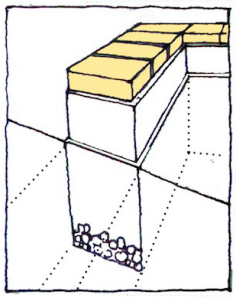

Diagram:SM creation

11. Build adobe wall:

Once the foundation wall is finished the adobe wall is built on top of it according to bouilding patterns described in section 1.8.2 of this research.

Conclusions

A. Seismic analysis in SAP 2000 using the static analysis method:

1. The seismic analysis for adobe architecture only considers the static analysis method and the Ro value is not given. Ro value is not established in the NCh 433.Of96 Chilean Code for adobe architecture. Therefore, this research proposed Ro value = 1. Thus, there exist differences between the static analysis method and the spectral modal analysis method.

2. Although the NCh 433.Of96 Chilean Code do not require the time history analysis for adobe architecture, this evaluation would be considered in a 3rd evaluation to determine dynamic responses of the AS through direct numerical integration of the dynamic equilibrium equation. This analysis could define peak responses by statistical means such as the SRSS and the CQC rules.

3. Although the seismic analysis reveals that the four cases (A1, A2, C1, and C2) do not pass the seismic simulation, the SBI reduces the seismic

force in walls and dynamic displacements, exclusively in those cases where the friction force is shorter than the maximum seismic stresses. In this case the force drops down in 17.5%, from 33,900 lb [16.95 Tonf] to 28,000 [14 Tonf].

4. To guarantee successful function of the SBI, the friction layer needs to provide the minimum friction coefficient of 0.2. Thus, the superstructure reaches displacement between the footing and the foundation wall, resulting in release of energy.

5. The analysis of stresses shown from section 4.6.1 to 4.6.4, on which the maximum wall stresses and the admissible wall stresses are compared, revealed first that in case C1 the SBI effectible works generating less difference of stress than A2, which only uses polymer mesh. In case A2 this difference goes from 6.45 [lb/in^2] to 26.65 [lb/in^2] whereas in C1 this value goes from 5.63 [lb/in^2] to 22.55 [lb/in^2].

6. The analysis of damaged wall areas in the wall

developed in section 4.6.5 reveals that by only using the SBI this area is reduced in about 11.4%, which is 3% lower than by using only polymer mesh.

7. The spectral modal analysis method of the effects of seismic forces in the adobe structure without polymer mesh and base seismic isolator in case D1 and D2 is not necessary. This is because the SBI is not activated. The case is equal to the case without seismic base isolator B1 and B2, with and without polymer mesh.

8. 18 steel pipes are proposed to re-center the superstructure. Each pipe will be 1" diameter and 2 mm thickness, covered by a 4" [10 cm] recycled car tire rubbers.

B. Cost:

1. By only employing the SBI the total cost of the AS unit augments 2%, where that by only using polymer mesh the total cost rises 4%.

2. The total cost of C1 is 2% lower than A2, 14.2% lower than the total cost used to build the dwelling unit out of light steel frame system, 13.8% lower than employing SIP system, and 8% lower than using the 4" reinforced brick with 2" of isolation.

3. The total cost of C1 also suits the required conditions to apply for governmental funds type FSV, which covers units that cost up to US$ 43,625 (900 UF). the program SHR could fund up to US$ 22,400 (420 UF) if this adobe dwelling is located in rural areas, which is 50% of the total construction cost estimated in the adobe dwelling.

4. Local availability of building materials would limit the implementation of the proposed seismic base isolator. However, selected materials such as the recycled steel pipe or the care tire rubber might be easily found in local disposals.

C. Combination seismic and cost analysis

1. Ultimately, by combining the results of the static analysis method developed in section 4.6 and

the cost analysis reviewed in section 4.7, there exist conditions to argue that case C1, the AS with BSI, might suits a better ratio cost&funtion than A2 by employing polymer mesh. This means that by only implementing the SBI the AS experiences less stress, generates less area of damages, and is less pricey than the AS protected only with polymer mesh.

2. Local and broad implementation:

The analysis of damaged areas in the wall developed in section 4.6.5 reveal that by only using the SBI this area is reduced in about 11.4%. Therefore, it is possible to argue that by using SBI the total adobe dwellings with minor damages surveyed in last earthquake in Chile, 36921 (36%), would remain without damages. By implementing the SBI also some of total destroyed adobe dwellings of 50576 (27%), would remain within major damages group of classification.

D. Installation process v/s modeling

1. Construction settings were used to built 1/2

scale physical modeling of the SBI. This modeling proves that the SBI installation process does not alter typical construction steps globally used for all the adobe territories to build the foundation wall, footing, and the adobe wall. This condition allows to argue that the SBI might have the potential to easely be implemented in developing countries, with relative low cost for mitigating seismic failure in adobe architecture involving community participation.

***

Image: Seismic base isolator in traditional adobe units in Chile.
Source: SM creation base on image from Technical team Cobquecura work shoop school 2010

BIBLIOGRAPHY

Adán, L., & Urbina, S. (2007). Arquitectura formativa en San Pedro de Atacama Estudios Atacameños. *Arqueología y Antropología Surandinas*, *34*, 7–30.

AIS Colombian government. (no date). *Manual para la rehabilitación de viviendas de construidas en adobe y tapia pisada*. Colombia.

Almazán, J. L., & De la Llera, J. C. (2002). Analytical Model for Structures with Frictional Pendulum Isolators. *Earthquake Engineering ans Structural Dynamics*, *31*(305-332).

Aravena, A., & Iacobelli, A. (2012). *Elemental, Incremetal housing and parcipatory design manual* (Universidad Catolica.). Germany: Hatje Cantz Verlag.

Arumala, J., & Gondal, T. (2007). Compressed Earth Building Blocks For Affordable Housing. *RICS, Georgia Tech and the contributors*.

Asquith, A., & Vellinga, M. (2006). *Vernacular architecture in the Twenty-first century: Theory, education, and practice*. NY USA: Taylor and Francis Group.

Astroza, M. (n.d.). Efectos de los terremotos en las obras civiles. Departamento de Ingeniería Civil -FCFC, Universidad de Chile.

Baron, A. M. (1984). Tulor: Posibilidades y limitaciones de un ecosistema. *Revista Chungará Universidadd de Tarapacá*, *17*(16), 149 –159.

Bengoa, J. (1996). *Historia del pueblo Mapuche (Siglos XIX y XX)* (3rd ed.). Santiago, Chile: Ediciones Sur. coleccion estudios Historicos.

Blondet, M., Villa, G., Brzev, S., & Rubiños, A. (2011). *Earthquake-Rssistant Construction of adobe buildings: A tutorial* (2nd ed.). EERI/IAEE World Housing Encyclopedia.

Blondet, M., Villa, G., & Loaiza, C. (2002). Comportamiento de vovendas de adobe sometidas a terremoto.

Cabrerizo, C. (2010). Técnica y cultura técnicas constructivas en tierra cruda en el valle central de Chile. VI y VII Región. *Seminario Universidad de Chile*, 42 –51.

CDT. (2012). *Evaluación de Daños y Soluciones para Construcciones en Tierra Cruda: Manual de Terreno*. Corporación de Desarrollo Tecnológico, CDT.

Christocpouls, C., Filiatrault, A., & Folz, B. (2002). Seismic response of Self-Centering Hysteretic SDOF System. *Earthquake Engineering ans Structural Dynamics*.

Concha, M. (1966). Establecimientos humanos en el altiplano chileno. *Estudios Geográficos*.

Universidad de Chile.

Cortes, M. (n.d.). *Www.marcelocortes.cl*. architecture.

Cuadra, C., Karkee, M., Ogawa, J., & Rojas, J. (2004). Preliminary investigation of earthquake risk to Inca's architectural heritage. 13th World Conference on Earthquake Engineerings.

De Jongh, V. W. (2009).

De Sensi, B. (2003). Terracruda, La Diffusione Dell'architettura Di Terra (Soil, Dissemination of Earth Architecture).

Diana Comte, D. (n.d.). *CFG: Terremotos: Usos y Abusos*. Facultad de Ciencias Físicas y Matemáticas, Universidad de Chile, Stgo, Chile.

Dowling, D., Samali, B., & Li, J. (2005). An Improved means of reinforcing adobe walls-external vertical reinforcement. *Pontificie Universidad Catolica de Peru, PUCP*, *19*(16).

Edminster, A. V. (2009). *The energy free homes for a small planet*.

Enokela, O., & Alada, P. (2012). Strength analysis of coconut fiber stabilazer earth for farm structures. *d Alada P.O (2012). Strength analysis of coconut fiber stabilazer earth for farm structures. Department of Agricultural and Environmental Engineering, University of Agriculture Makurdi-Nigeria*.

Evison, F. (n.d.). Seismic hazard assessment in continental areas, in Proceedings International Symposium on Continental Seismicity and Earthquake prediction. *Seismological Press, Beijing, China*, 751–762.

Fundacion Jofre. (n.d.). fundacion Jofre. *Www.fundacionjofre.cl*. architecture.

Ginells, W. ., & Tolles, L. (No date). Seismic stabilization of historic adobe structures. *Journal of the America Institute of conservation (JAIC) US*, *39*(1).

Guerreiro, L., & Branco, M. (2006). The use of passive seismic protection in structural rehabilitation. *Progress in Structural Engineering and Materials*, *8*(4), 121–132.

Haesebrouck, L., & Michiels, T. (2011). *Improving durability of adobe: A case study for Cuenca, Ecuador*. Katholieke University Leuven.

Heathcote, K. (n.d.). The thermal performance of earth buildings. *Sydney. Australia.*, *63*(523), 117–126.

Heredia, E., Bariola, J., Neumann, J., & Mehta, P. (1988). Improving the moister resistance of

adobe structures.

Houben, H., & Hubert, G. (1993). *Earth Constructions: A comprehensive Guide*. London, UK: Intermediate Technology.

Hussain, S., Lee, D., & Retamal, E. (On line). Viscous damping for base isolated strutures.

INE Chile. (1996). *Norma Chilena Of 96: Diseño sismico de edificios*. Chile: Instituto Nacional de Normalizacion (INE).

INE Chile. (2010). *Norma Chilena 1537: Diseño estructural – Cargas y sobracargas*. Chile: Instituto Nacional de Normalizacion (INE).

Jerome, P. (2000). The use of lime plasters for waterproofing and decoration of mud brick buildings in Yemen (pp. 144–149). Torquay, UK.

Jorquera, N. (2010). Los daños al patrimonio constrido en tierra luego del terremoto de Chile 2010. Mitos y verdades del comportamiento de las estructuras de terra. Presented at the VII Congreso de Tierra en Cuenca de Campos, Valladolid, 2010.

Karmelic, L. (2009). *Estudio descriptivo de los inmuebles patrimoniales construidos en tierra cruda que forman parte del inventario de patrimonio cultural inmueble de Chile*. Facultad de Arquitectura, Urbanismo y Paisaje. Universidad Central, Santiago, Chile.

Kelly, J., & Konstantinidis, D. (2011). *Mechanism of Rubber bearings for seismic and vibration isolation*. WILEY.

Koshkin, & Shirkévich. (1975).

Lertwattanaruk, P., & Choksiriwanna, J. (2011). The Physical and Thermal Properties of Adobe Brick Containing Bagasse for Earth Construction. *Faculty of Architecture and Planning, Thammasat University*.

Martins, T., & Varum, H. (no date). Adobe's Mechanical Characterization in Ancient Constructions: The Case of Aveiro's Region. *Civil Engineering Department, University of Aveiro*.

Mehta, D. (2007). *On Conservation and Development: The Role of Traditional Mud Brick Firms in Southern Yemen*. Columbia University, Graduate School of Architecture, Planning and Preservation.

Milani, P., & Paradiso, M. (2010). *Analisys, consideraciones y propuestas para la reconstrucción*.

Italy: Edition Medina.

Minke, M. (2006). *Building with Earth; Design and technology of sustainable design*. Germany: Birkhäuser – Publishers for Architecture.

MINPLA Chile. (2010). *Plan de reconstrucción terremoto y maremoto del 27 de febrero del 2010. Resumen ejecutivo*.

MINPLA Chile. (2011). *Encuesta de Caracterización Socioeconómica Nacional, CASEN*. Retrieved from www.minvu.cl

MINVU Chile. (2009a). *Resolución Exenta No2070. Aprueba Itemizado Técnico de Construcción para Proyectos del Programa Fondo Solidario de Vivienda, para el Sistema de Subsidio Habitacional Rural y para el Programa de Protección del Patrimonio Familiar*. Santiago, Chil: MINVU Chile. Retrieved from www.minvu.cl

MINVU Chile. (2009b). *Decreto Supremo No47, (V. y U.) de 1992. D.O. de 13.04.09 OGUC*. Santiago, Chile. Retrieved from www.minvu.cl

MINVU Chile. (2009c). *Decreto Supremo No174, (V. y U.) de 2005. D.O. de 09.02.06 Reglamenta Programa Fondo Solidario de Vivienda*. Santiago, Chile. Retrieved from www.minvu.cl

MINVU Chile. (2009d). *Decreto Supremo No145, (V. y U.) de 2007. D.O. de 09.10.07 Nuevo Regla- mento del Sistema de Subsidio Habitacional Rural*. Santiago, Chile. Retrieved from www.minvu.cl

MINVU Chile. (2009e). *Resolución Exenta No0504 (V. y U.).Listado Oficial de Soluciones Constructivas para Acondicionamiento Térmico*. Santiago, Chile. Retrieved from www.minvu.cl

MINVU Chile. (2012). *Manual de Aplicacion de reglamentacion Termica OGUC 4.1.10* (Article 49.). Santiago, Chile: MINVU Chile. Retrieved from www.minvu.cl

MINVU Chile. (n.d.-a). *Ampliacion de superficie para vivienda social*. Chile: MINVU Chile, Comite Tecnico DICTUC. Retrieved from www.minvu.cl

MINVU Chile. (n.d.-b). *Anteproyecto de Normua Tecnica NTM 002. Estructuras: Proyecto de intervencion structural deconstrucciones patrimoniales en tierra*. Chile: MINVU Chile Comité tecnico. Retrieved from www.minvu.cl

MINVU Peru. (2008). *Refuerzo de Geomalla en Edificaciones de Adobe* (Anexo 1.). Chile:

MINVU Chile Comité tecnico.

MINVU-Ditec Chile. (n.d.). *Resolución Exenta No0860 (V. y U.).Listado Oficial de Soluciones Constructivas para Acondicionamiento Acústico*. Chile: MINVU Chile, Comite Tecnico DICTUC. Retrieved from www.minvu.cl

Mojsilovic, N., Page, A., & Simundic, G. (n.d.). Masonry wallette with damp-proof course membrane subjected to cyclic shear: an experimental study. *Expanded Academic ASAP. University of Newcastle and the ETH Zurich*.

Morris, J., & Booysen, Q. (2000). Earth Construction in Africa. Strategies for sustainable Built Environment. *Petoria*.

Nwankwor, N. (2008). Justification for the Combination of Organic and Inorganic Stabilizers to Stabilize Traditional Earth Materials (Mud) for Quality and Capacity Utilization in Africa. *Terra*.

Oates, D. (1990). Innovations in mud-brick: Decorative and structural techniques in Ancient Mesopotami. *Department of Civil Engineering. Meddle East Technical University.*, *21*, 388–406.

OSGS. (n.d.). United State geological Survays (OSGS). Seismic activity. Retrieved from http://earthquake.usgs.gov/earthquakes/world/10_largest_world.php

Ozden, B. (2006). *Low- cost seismic base isolation using scrap tire pad (STP)*. Middle East Technical University Department of Civil Engineering, Ankara, Turkey.

PUC. (2009). *Design Guide for Energy Efficient Affordable Housing* (Vol. 333).

Pumpelly, R. (1908). Explorations in Turkestan. *Washington, USA*.

Rael, R. (2009). *Earth Architlecture*. NY, US: Princeton Architecture Press. Retrieved from http://www.eartharchitecture.org/

Reitherman, R. (n.d.). *Earthquakes and Engineers: An International History*. Reston, VA: ASCE Press.

Rodriguez, A., & Walker, H. (2009). Expediente técnico: Módulo básico de adobe reforzado con geomalla Zona de costa. Pontificia Universidad Católica del Perú (PUCP). Retrieved from https://www.sheltercluster.org

šolc, V. (2011). Casa Aymara en el Enquelga. *Revista Mapuches, Chungará, Chile*.

Teter, T. E., Kent, & Liu, R. C. (1964). *Use of Stabilized earth block in farm constructions*. Agriculture research service.

Tolles, E., Leroy, E., Edna E, E., & Williams, G. (2002). Guías de planeamiento e ingeniería p la estabilización sismorresistente de estructuras históricas de adobe. *Los Angeles: The Ge Conservation Institute*.

UNESCO. (n.d.). Chair Earth Architecture. Architecture. Retrieved from http://craterre.org

APPENDIX 1

PROCESS STEPS FOR SEISMIC ANALYSIS USING SAP 2000

OVERVIEW: the steps described in this section were used to analyze the modeling created for the following cases using SAP 2000:

Case 1:

Adobe structure without polymer mesh rigid and with foundation ring wall using SAM.

Case 2:

Adobe structure with polymer mesh and foundation ring wall using SMAM.

Case 3:

Adobe structure without polymer mesh and with seismic base isolator using SAM.

Case 4:

Adobe structure with polymer mesh and seismic base iso lator using SMAM.

These cases are used for simulations with and without polymer mesh because the use of polymer mesh only increments the admissible stress of the wall, but it does not increase the seismic force, given by the modelings.

Case 1: Adobe structure without polymer mesh rigid and with foundation ring wall using SAM.

Step 1: Define Units

In bottom-right corner specify a set of units.

Step 2: Define Materials

Define => Materials => Add new materials => assign properties of adobe, concrete, and timber according to values given by literature

review. Make sure that set of units does not change.

Step 3: Define Sections

1.3.1 Define section of footing wall and adobe wall:

Define => Section properties => Area Sections => Add New Section => assign section properties selecting appropriate material.

1.3.2 Define section of frames:

Define => Section properties => Frame Sections => Add New Property => assign section properties selecting appropriate material.

Step 4: Define Grids

Grids are defined according to architecture.

Define => Coordinate Systems/Grids => select Global and Modify/Show Systems.

Step 5: Modeling

Assign walls and sections to the grid according to architecture.

Step 6: Restrain conditions for joints

Select joints on the modeling. Joins should be restrained in those cases “without” seismic isolator (Displacement and rotation limitations)

Select join elements on the modeling => Assign => Joint => Restrains => Select 6 degree of freedom.

Step 7: Assign loads status

Define status of loads: Dead loads (DL), live-loads (LL), Seismic force in X (SX), and seismic force in Y (SY)

1.7.1 Define Load Patterns =>

DL: Add New Load Pattern => (Name) DEAD => (Type) DEAD =>

(Self Weight Multiplier)1

LL: Add New Load Pattern => (Name) LL => (Type) LIVE =>

(Self Weight Multiplier)0

SX: Add New Load Pattern => (Name) SX => (Type) OTHER =>

(Self Weight Multiplier)0

SY: Add New Load Pattern => (Name) SY => (Type) OTHER =>

(Self Weight Multiplier)0

1.7.2 Define Load Cases =>

Add New Load Case => (Name) DEAD => (Type) Linear Static

Add New Load Case => (Name) MODAL => (Type) Modal

Add New Load Case => (Name) SC => (Type) Linear Static

Add New Load Case => (Name) SX => (Type) Linear Static

Add New Load Case => (Name) SY => (Type) Linear Static

Step 8: Define load combinations

Seismic mass= DL + 0.25*LL

C1 = DL + LL

C2X = DL + LL + SX

C2Y = DL + LL + SY

C3X = DL + SX

C3Y = DL + SY

Define Load Combinations => Add New Combo

Step 9: Assign loads

In each load status weighs should be assigned according to report. Select component of the modeling => Assign => Frame Loads => Distributed => Select load pattern, direction and dimensions.

Step 10: Run seismic simulation

Analyze => Run Analysis => Run Now

Step 11: Check P, Qx, and Qy

P: seismic weight

Qx: basal rupture by seismic force in axis X

Qy: basal rupture by seismic force in axis Y

Display => Show Table => ANALYSIS RESULTS => Structure Output => Base Reactions

In same window select in right menu Select Load Cases => select seismic weight, Sx, and Sy.

Finally click on OK below.

Review P: OutputCase Text “Seismic Weight” and column GlobalFZ

Review Qx: OutputCase Text “Sx” and column GlobalFX

Review Qy: OutputCase Text “Sy” and column GlobalFY

Step 12: Check deformations

Select superior joints on the modeling in the adobe walls.

Display => Show Table => ANALYSIS RESULTS => Joint Output => Displacement => Joint displacement.

In same window select Select Load Cases => select Sx and Sy.

Finally click on OK below.

To review maximum deformation in X, search for the highest absolute value in column U1.

To review maximum deformation in Y, search for the highest absolute value in column U2.

Step 13: Check value of stresses

From the the model select blocks in the wall that want to be verified.

=> Display => Show Table => ANALYSIS RESULTS => Element Outputs

=>Area Output => Table: Element Stresses - Area Shells.

In same window select in right menu Select Load Case => select Sx, Sy.

Finally click on OK below.

To check stresses look at column S12Top.

Step 14: Check value of stresses.(with color representation).

Select bottom Show/forces/stresses.

=> Shell => select Case/Combo Name (Sx o Sy, from which want to be visualized)

In same window select in right menu:

Component types => Shell Stresses.

Output Type => Visible face.

Components => S12

Finally click on OK below.

Case 2: Adobe structure with polymer mesh and foundation ring wall using SMAM

Step 1 to Step 6 are the same than those used in Case 1.

Step 6B: Assign acceleration spectrum

Access text file with periods and accelerations, computed according to report in Chapter IV. They are needed to design spectrum of acceleration graphs.

Define => Function => Response Spectrum.

=> Choose Function Type to Add => From File => Click to => Add New Function.

=> Function name: SISMO => Value are: Period vs Value.

=> Browse: Select file

Finally click on OK below.

Step 7: Assign loads status

Define status of loads: Dead loads (DL), live-loads (LL), Seismic force in X (SX), and seismic force in Y (SY)

7.1 and 7.2: Define Load Patterns and Load Cases as Case 1

After these are defined:

Load case Type => Choose Response Spectrum

Loads Applied: Load Type: Accel

Load name: U1

Function: SISMO

Scale Factor: 1/R* (use report content)

Add and finally click OK.

Add New Load Case => (Name) SY => Modify/Show Load Case.

Load Case Type => Choose Response Spectrum

Loads Applied: Load Type: Accel

Load Name: U2

Function: SISMO

Scale Factor: 1/R* (use report content)

Add and finally click OK.

Step 8 to 14: These steps are the same than those used in Case 1.

Case 3: Adobe structure without polymer mesh and with seismic base

isolator using SAM.Modeling steps in SAP 2000

Step 1 to Step 5: are the same as those used in Case 1

Step 6: Restrain conditions (RC) for joints and definition of Scale factor(SC) for dissipated force

RC: Spring are located exclusibly in rubber locks.

Select joints on the modeling. where is desired to located springs.

Joints should be restrained in those cases “with” seismic isolator (Vertical displacement and rotation limitations)

Select joint elements on the modeling => Assign => Joint => Restrains => Select 4 degree of freedom. (leave free displacements in 1 and 2)

After this select joints which use seismic locks and locate displacement springs. (use report content)

Assign => Join => springs => Spring stiffness => assign spring values in translation 1 and translation 2.

SF: Define => Load Case => Sx (y Sy) => Modify/Show Load Case => Scale Factor.

Maximum friction force Fd 14 [tons] results of “P” times Fc where “P” is seismic weight 63.9 [tons] and “Fc” gravel friction coefficient [0.202]

Seismic stress reduction Ry 2,952 [tons] results of basal stress Qx or Qy (-) Maximum friction force Fd 14 [tons] where Q 16.9 [tones] is sumatory of reaction forces in X and Y for static analysis.

Seismic stress reduction 17.4% is result of basal sesimic stress “with” isolator 2.951 [Tons] divided by basal seismic stress “without” isolator 16.95 [Tones].

Ultimately, Scale factor 83% results of 100% - 17,4% = 83% aprox.

Step 7 to 14: These steps are the same as those used in Case 1.

Case 4: Adobe structure with polymer mesh and seismic base isolator using SMAM.

Modeling steps in SAP 2000:

Step 1 to Step 5 are the same as those used in Case 2.

Step 6: Restrain conditions (RC) for joints and definition of Scale factor(SC) for dissipated force as shown in Case 3.

Select joints on the modeling. Joins should be restrained in those cases “with” seismic isolator (Vertical displacement and rotation limitations)

Select joint compoments on the modeling => Assign => Joint => Restrains => Select 4 degree of freedom. (leave free displacements in 1 and 2)

After this select joints which use seismic locks and locate displacement springs. (use report content)

Assign => Joint => springs => Spring stiffness => assign spring values in translation 1 and translation 2.

Step 6B: Assign acceleration spectrum.

Access text file with periods and accelerations, computed according to report in Chapter IV. They are needed to design spectrum of acceleration graphs.

Define => Function => Response Spectrum.

=> Choose Function Type to Add => From File => Click to => Add New Function.

=> Function name: SISMO => Value are: Period vs Value.

=> Browse: Select file

Finally click on OK below.

Step 7: Assign loads status

Define status of loads: Dead loads (DL), live-loads (LL), Seismic force in X (SX), and seismic force in Y (SY)

7.1 and 7.2: Define Load Patterns and Load Cases as Case 1

After these are defined:

Load case Type => Choose Response Spectrum

Loads Applied: Load Type: Accel

Load name: U1

Function: SISMO

Scale Factor: 1/R* (use report content)

Add and finally click OK.

Add New Load Case => (Name) SY => Modify/Show Load Case.

Load Case Type => Choose Response Spectrum

Loads Applied: Load Type: Accel

Load Name: U2

Function: SISMO

Scale Factor: 1/R* (use report content)

Add and finally click OK.

Step 8 to 14: These steps are the same than those used in Case 1.

***

APPENDIX 2

CERTIFICATION LETTER OF AUTHOR CONTENT

Dear Committee and the Graduate Student Service and Progress (GSSP)
University of Minnesota
321 Jhonston Hall, 101 Pleasant St, SE
Minneapolis, MN 55455

Issue: **Content author "MEMORIA EXPLICATIVA DE CALCULO: Analisis de uso en vivienda de adobe".**
The content presented in Chapter IV has been fully elaborated by Sebastian Mery and Rodrigo Bravo according to following content list:

Mery's author content:
- Definition of physics concepts for the seismic analysis.
- Propose seismic analysis effects of four cases of adobe dwelling units.
- Propose analysis of effects of using seismic base isolator in adobe dwelling units with/without seismic reinforcement of polymer mesh.
- Seismic base isolator component definition, formed by a friction layer force dissipator and the another component to limit lateral displacements.
- Design and material components of the seismic base isolator.
- Establish the use of Peruvian seismic code design Anexo 1" Norma técnica de Perú, with the aim to complement seismic analysis.
- Material properties presentation according to reviewed literature.
- Design, architecture, diagrams of the adobe prototype.
- Design, tables, and diagrams of the seismic analysis.
- Static analysis method observations and conclusions.

Bravo's author content:
- Implementation of Spectral modal analysis method according to NCh 433 of 96 Mod 2009.
- Engineering criteria used in the seismic analysis based on national and international seismic design code.
- Modeling and computing seismic diffusor using Hook elastic law.
- Modeling analysis results.
- Spectral modal analysis method conclusions.

Bravo/Mery's author content:
- SAP 2000 modeling implementation.
- Implementation of Static analysis method according to NCh 433 of 96 Mod 2009.

Sebastian Mery
ID: 12.005.513-5
Graduate in Architecture
Universidad Central

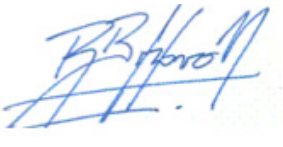

Rodrigo Bravo
ID: 13.466.717-6
Graduate in Engineering
University of Chile

April 2013

ESTUDIO ESTRUCTURAL

MEMORIA EXPLICATIVA DE CALCULO

"Análisis de uso de aisladores sísmicos en viviendas de adobe"

FEBRERO 2013

Estudio Estructural *María Luisa Santander N° 568* *email: rbn.ingeniero@gmail.com*

MEMORIA EXPLICATIVA DE CÁLCULO

ANÁLISIS DE USO DE AISLADORES SÍSMICOS EN VIVIENDAS DE ADOBE

1.- GENERALIDADES

El presente informe es un registro de los criterios, desarrollo, resultados y conclusiones del análisis del efecto del uso de aisladores sísmicos en viviendas sociales de adobe en Chile. Además, se propondrá un diseño de aislador sísmico.

Este estudio contempla analizar el comportamiento sísmico de 4 viviendas sociales de adobe (espesor de muros de 40 cm + 2,5 cm de revoque por cada cara), de 1 piso sin diafragma rígido y con cerchas de techo de pino, ante solicitaciones sísmicas. Se analizarán los siguientes casos:

Caso 1: Estructura de adobe sin geomalla con fundación corrida.
Caso 2: Estructura de adobe con geomalla con fundación corrida.
Caso 3: Estructura de adobe sin geomalla con disipador sísmico.
Caso 4: Estructura de adobe con geomalla con disipador sísmico.

El análisis sísmico se hará con el Método Estático y Análisis Espectral, considerando un suelo de baja resistencia mecánica (suelo tipo E, según NCh 433.Of1996 Mod 2009 con D.S.61) ubicado en la zona sísmica 3, correspondiente a la zona costera de Chile, que es la que está sometida a las mayores solicitaciones sísmicas.

Fig.1 Imagen de la vivienda de adobe con techo de madera.

Estudio Estructural *María Luisa Santander N° 568* *email: rbn.ingeniero@gmail.com*

Fig.2 Imagen de la vivienda de adobe con techo de madera.

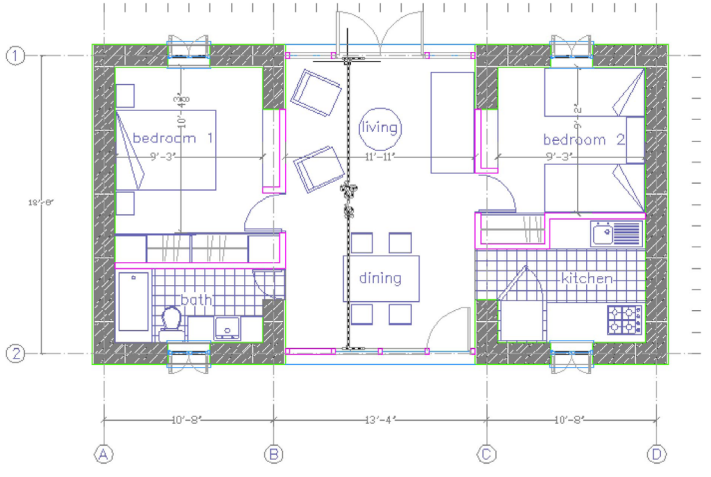

Fig.3 Imagen de la planta de la vivienda.

Se propondrá el uso de aisladores sísmicos, para analizar el efecto que tendrá sobre los muros de adobe con y sin geomalla. Para esto se utilizará una capa de fricción intermedia entre la fundación corrida de la estructura y su sobrecimiento, utilizando topes sísmicos que limiten el desplazamiento lateral de la estructura ante solicitaciones dinámicas.

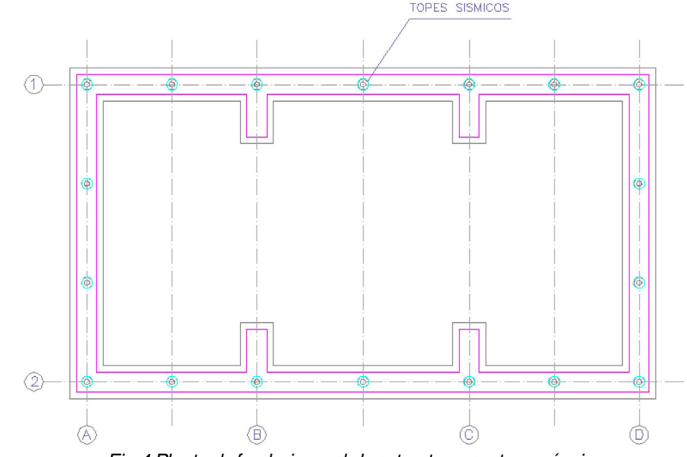

Fig.4 Planta de fundaciones de la estructura con topes sísmicos.

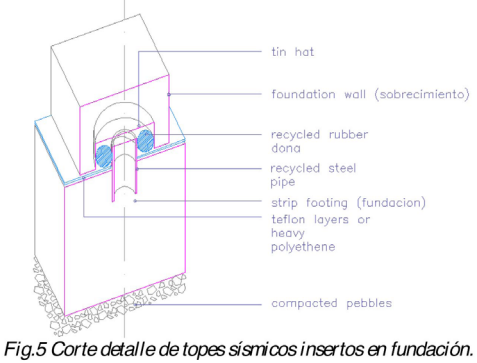

Fig.5 Corte detalle de topes sísmicos insertos en fundación.

Estudio Estructural María Luisa Santander N° 568 email: rbn.ingeniero@gmail.com

2.- NORMAS

El análisis se ciñe a las normas pertinentes del Instituto Nacional de Normalización de Chile, en especial a la norma sísmica NCh433of.96 MOD2009.

- Norma NCh1537 of.2009 Cargas permanentes y sobrecargas.
- Norma NCh432 of. 71 Cálculo de la acción del viento.
- Norma NCh1198-2006 - Madera - Construcciones en madera – Calculo.
- Norma NCh429.of.57 Hormigón Armado – I Parte.
- Norma NCh430.of.61 Hormigón Armado – II Parte.
- Norma Técnica de Perú, E.080 "Adobe" y su Anexo N°1 "Refuerzo de Geomalla en Edificaciones de Adobe".

3.- MATERIALES A UTILIZAR

A continuación se detallan las propiedades de los materiales a utilizar:

-*Techo*: ***Teja muslera***.

Peso = 64 [Kgf/m^2].

-*Cerchas de techo de madera*: ***Pino***.

Densidad = 750 [Kgf/m^3].
E = 8.000 [MPa] (módulo de elasticidad).
Fy = 9.6 [MPa] (fluencia).

-*Muros de 40 cm de espesor*: ***Adobe***.

Densidad = 1.600 [Kgf/m^3].
E = 200 [MPa] (módulo de elasticidad).
Resistencia a la compresión = 0.75 [MPa].
Resistencia al corte = 0.025 [MPa].

-*Refuerzos muros de adobe*: ***Geomalla***.

Resistencia mínima a la tracción = 350 [Kgf/m].
Resistencia mínima estimada al corte = 0.007 [MPa] (colocada en ambas caras de un muro de adobe).

-*Sobrecimiento y Fundaciones*: ***Hormigón armado***.

Densidad Hormigón Armado= 2.540 [Kgf/m^3].

Tipo de hormigón = H-25
E = 25.300 [MPa] (módulo de elasticidad).
f'c = 20 [MPa] (Resistencia a la compresión).

Tipo de acero de refuerzo = A630-420H.
f'y = 420 [MPa] (fluencia).

-*Capa de fricción entre fundación y sobrecimiento*: ***Gravilla***.

Coeficiente de fricción = 0,202.

-*Topes sísmicos anclados a fundación*: ***Acero estructural***.

Tipo de acero estructural = A37-24ES.
f'y = 240 [MPa] (fluencia).

-*Capa alrededor de tope sísmico (absorbe desplazamientos laterales)*: ***Goma (neumático reciclado)***.

Módulo de compresión = 30 [MPa].
Resistencia a la compresión (5 cm de espesor) = 8.5 [MPa].

4.- CARGAS Y SOBRECARGAS VERTICALES

Para el cálculo y diseño de los elementos se consideran los siguientes tipos de carga:

- Peso propio de la estructura.
- Peso de tejas musleras: 64 [Kgf/m^2].
- Sobrecarga de techo: 39 [Kgf/m^2] (con disminuciones según NCh1537of.2009)*.
- Acción del viento sobre la estructura**.
- Acción del sismo sobre la estructura.

**La NCh1537 propone una SC=100 [Kgf/m^2] ponderado por los coeficientes de reducción de 0,93 por área tributaria y 0,42 por pendiente de techo, ponderando un coeficiente de 0,39 que se pondera a la SC de techo (ver Tabla 3 NCh1537of.2009).*
***La Normativa nacional propone usar una carga de 70 [Kgf/m^2] (NCh432 Tabla 1) para estructuras de 4 [m] de altura ubicadas en campo abierto ponderado por el factor por pendiente de techo (NCh432 - Anexo A – Fig. 10): 1,2sen(ang del techo) – 0,4.*

Estudio Estructural María Luisa Santander N° 568 email: rbn.ingeniero@gmail.com

Con este modelo se obtendrán las solicitaciones de corte sobre los muros de adobe. Luego se verificaran resistencia de los muros ante estas solicitaciones para los casos con y sin geomalla (casos 3 y 4).

D) Modelo de estructura de adobe con restricciones basales al giro y al desplazamiento vertical, correspondiente al uso de disipadores sísmicos. Se colocarán resortes para el desplazamiento horizontal, representativos de los topes sísmicos. Se aplicará análisis sísmico con el Método Modal Espectral según NCh433 y con el criterio de Ro=1. Se estimará la disminución de esfuerzos sísmicos por la capa de fricción, según el método estatice del modelo C, y se le aplicará esta reducción en la aceleración basal, lo que se debiese traducir en una disminución de solicitaciones sísmicas en la estructura.

Con este modelo se obtendrán las solicitaciones de corte sobre los muros de adobe. Luego se verificaran resistencia de los muros ante estas solicitaciones para los casos con y sin geomalla (casos 3 y 4).

6.- DESARROLLO

6.1 Parámetros de los Análisis por Métodos Estático y Modal Espectral.

Estimación del peso sísmico (P):

$$P = CM + 0{,}25*SC$$

CM: Carga Muerta [Kgf].
SC: Sobrecarga [Kgf].

- **<u>Método Estático</u>**

$$\mathbf{F_{sismica\ en\ X} = F_{sismica\ en\ Y} = Q_O = corte\ basal = C*I*P}$$

C: Coef. Sísmico. [sin unidad].
I: Factor de importancia. [sin unidad].
P: Peso sísmico de la estructura. [kgf].

5.- ANÁLISIS SÍSMICO (METODOLOGÍA DE ANÁLISIS)

Se modeló la estructura con el software de elementos finitos SAP2000, con las cargas y materiales antes descritos. Se realizaron 4 modelos para analizar los casos descritos en el punto 1 del presente documento.

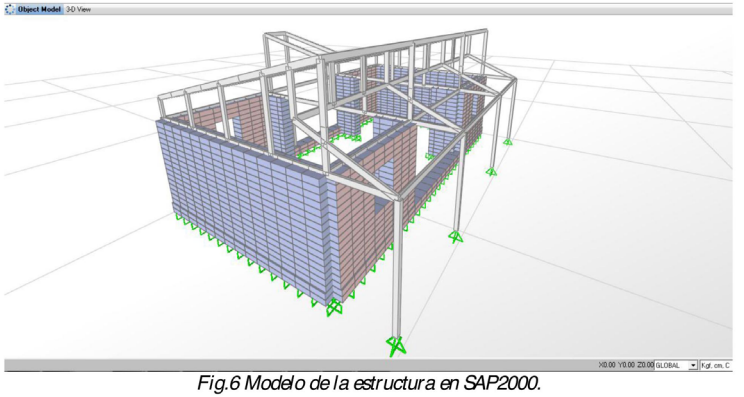

Fig.6 Modelo de la estructura en SAP2000.

Para el análisis sísmico se seguirá las estipulaciones y criterios de la norma sísmica de Chile, correspondiente a la NCh 433.Of1996 Mod 2009 con D.S.61. En este documento, se establece que para estructuras de adobe, el análisis sísmico aplicable es el correspondiente al Método Estático, ya que para el Método de Análisis Modal Espectral no se entregan valores de Ro para el adobe.

El análisis sísmico por el Método Estático, simula las solicitaciones sísmicas en la estructura, a través de la aplicación de fuerzas "estáticas" horizontales (en cada sentido de análisis para sismo en X e Y) equivalentes a un porcentaje del peso de la estructura.

El análisis sísmico por el Método Modal Espectral, simula las solicitaciones sísmicas sobre la estructura, a través de la aplicación de un espectro de aceleraciones en la base de la estructura.

A modo de propuesta se realizará un Análisis Modal Espectral considerando el valor de Ro que nos entregue mayores aceleraciones

basales, que corresponde a Ro = 1, valor solo requerido para este método y no para el Método Estático:

Espectro de aceleraciones: $$S_a = \frac{IA_0\alpha}{R^*}$$

Factor de amplificación: $$\alpha = \frac{1+4{,}5\left(\frac{T_n}{T_o}\right)^p}{1+\left(\frac{T_n}{T_o}\right)^3}$$

Factor de reducción R*: $$R^* = 1 + \frac{T^*}{0{,}10\,T_o + \frac{T^*}{R_o}}$$

***Sa**: Aceleración espectral de diseño.* [m/s^2].
***I**: Coeficiente relativo a la importancia, uso y riesgo de falla de la estructura.* [sin unidad].
***A$_o$**: Aceleración efectiva máxima del suelo.* [m/s^2].
α: Factor de amplificación de la aceleración efectiva máxima. [sin unidad].
***T$_n$**: Período de vibración del modo n.* [s].
***T$_o$**: Parámetro que depende del tipo de suelo.* [sin unidad].
***p**: Parámetro que depende del tipo de suelo.* [s].
***R***: Factor de reducción de la aceleración espectral, calculado para el período del modo con mayor masa traslacional equivalente en la dirección de análisis.* [sin unidad].
***T***: Período del modo con mayor masa traslacional equivalente en la dirección de análisis.* [s].
***R$_o$**: Factor de modificación de la respuesta estructural para el Método Modal Espectral.* [sin unidad].

Con lo cual se concluye que el valor de Ro = 1 es el que entrega el menor factor de reducción, lo que se traduce en un espectro de aceleraciones mayor, que es la situación que buscamos, para ser un análisis conservador por utilizar el valor más desfavorable.

Se estudiarán los siguientes casos:

Caso 1: Estructura de adobe sin geomalla con fundación corrida.
Caso 2: Estructura de adobe con geomalla con fundación corrida.
Caso 3: Estructura de adobe sin geomalla con disipador sísmico.
Caso 4: Estructura de adobe con geomalla con disipador sísmico.

Para esto se realizarán 4 modelos, los cuales se describen a continuación junto a su aplicación en los casos descritos anteriormente:

A) Modelo de estructura de adobe con restricciones basales al desplazamiento y al giro, aplicando análisis sísmico con el Método Estático según NCh433.

Con este modelo se obtendrán las solicitaciones de corte sobre los muros de adobe. Luego se verificaran resistencia de los muros ante estas solicitaciones para los casos con y sin geomalla (casos 1 y 2).

B) Modelo de estructura de adobe con restricciones basales al desplazamiento y al giro, aplicando análisis sísmico con el Método Modal Espectral según NCh433 y con el criterio de Ro=1.

Con este modelo se obtendrán las solicitaciones de corte sobre los muros de adobe. Luego se verificaran resistencia de los muros ante estas solicitaciones para los casos con y sin geomalla (casos 1 y 2).

C) Modelo de estructura de adobe con restricciones basales al giro y al desplazamiento vertical, correspondiente al uso de disipadores sísmicos. Se colocarán resortes para el desplazamiento horizontal, representativos de los topes sísmicos. Se aplicará análisis sísmico con el Método Estático según NCh433. Se colocarán fuerzas horizontales de sentido opuesto a las fuerzas sísmicas, de modo tal que sea representativa del efecto de la capa de fricción, lo que se debiese traducir en una disminución de solicitaciones sísmicas en la estructura.

Para el coeficiente sísmico C utilizaremos el valor más desfavorable que corresponde al C_{max} entregado por la norma.

Considerando R=2 para el adobe (Tabla 5.1 NCh 433) y según Tabla 6.4 NCh 433:

$$C_{max} = 0,9 * S*Ao / g$$

S: Parámetro que depende del tipo de suelo. [sin unidad].
g: Aceleración de gravedad = 9,8 [m/s^2].

Consideremos un suelo de baja resistencia, de manera tal que sea representativo para gran parte de Chile, correspondiente a un suelo tipo E, y considerando zona sísmica 3 (zona costera de Chile), la cual tiene mayores aceleraciones basales:

S = 1,3
Ao = 0,4g (aceleración efectiva)

⇨ **C_{max} = 0,47**.

⇨ **I = 1,0** (vivienda privada, Tabla 6.1 NCh433).

- **<u>Método Modal Espectral</u>**

El análisis sísmico por el Método Modal Espectral, simula las solicitaciones sísmicas sobre la estructura, a través de la aplicación de un espectro de aceleraciones (Sa) en la base de la estructura, para lo cual ingresaremos al modelo de SAP2000 (*Define -> Functions -> Response Spectrum*), una tabla con los valores del espectro de aceleración según el tipo de período:

Espectro de aceleración Sa: $$S_a = \frac{IA_0\alpha}{R^*}$$

Factor de amplificación: $$\alpha = \frac{1+4,5\left(\frac{T_n}{T_o}\right)^p}{1+\left(\frac{T_n}{T_o}\right)^3}$$

Factor de reducción: $$R^* = 1 + \frac{T^*}{0,10\,T_o + \frac{T^*}{R_o}}$$

Del modelo se obtienen los siguientes períodos de mayor masa traslacional en cada eje principal:

T^*_X = 0,144326 [s].
T^*_Y = 0,001211 [s].

A continuación se muestran los demás parámetros para obtener el espectro de aceleraciones (según la NCh433 y D.S.61):

Factores del suelo			Factores Zona			Factores tipo de estructura		
Tipo	E		Zona	3		Categoria	A	
S	1.30		A_0	0.4		R	2	
T_0	1.20	[s]	Constantes			R_0	1	
T'	1.35	[s]	g	9.8	[m/s]	I	1	
n	1.80							
p	1.00							

Con lo cual se obtiene el espectro de aceleraciones representado en el siguiente gráfico:

Gráfico 1 "Espectro de aceleraciones en el eje X para la estructura a analizar según el método Modal Espectral."

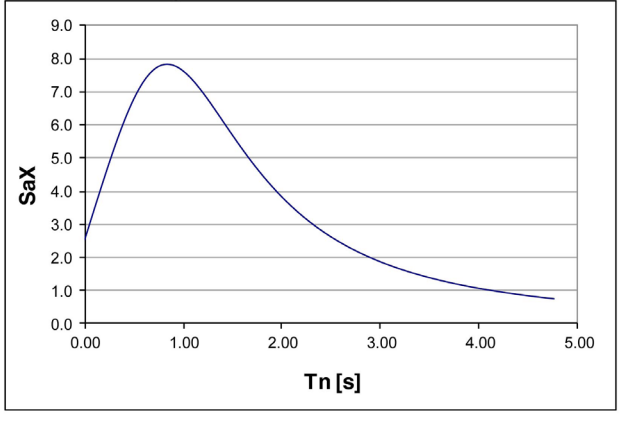

Techo eje A y D = (130 + 0,25*63,5) * 0,47 = 69 [Kgf/m]
Techo eje B y C = (293 + 0,25*143) * 0,47 = 155 [Kgf/m]
Techo corto = (39.6 + 0,25*19,33) * 0,47 = 21 [Kgf/m]
Muros de adobe = (1.600*1,35*0,45) * 0,47 = 457 [Kgf/m] (*)

(*) Se considera que solo la mitad superior de la altura del muro de adobe aporta a masa sísmica, ya que la mitad inferior del muro descarga directamente al suelo.

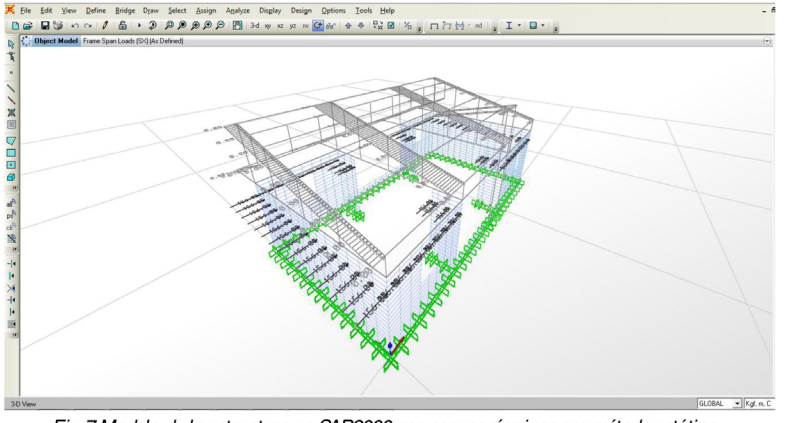

Fig.7 Modelo de la estructura en SAP2000 con cargas sísmicas por método estático.

Desplazamiento máximo en borde superior muro de adobe = 0,9 [cm].

A.1) Caso 1: Estructura de adobe sin geomalla con fundación corrida (análisis por método estático).

Tabla 1 "Tensiones internas por solicitaciones sísmicas y tensiones admisibles del adobe sin geomalla"

EJE MURO	TENSIÓN SOLICITANTE MAX [Kgf/cm2]	TENSIÓN ADMISIBLE [Kgf/cm2]	RESISTENCIA
A	1.02	0.25	FALLA !!!
B	2.2	0.25	FALLA !!!
C	2.22	0.25	FALLA !!!
D	0.96	0.25	FALLA !!!
1	0.78	0.25	FALLA !!!
2	0.81	0.25	FALLA !!!

Gráfico 2 "Espectro de aceleraciones en el eje Y para la estructura a analizar según el método Modal Espectral."

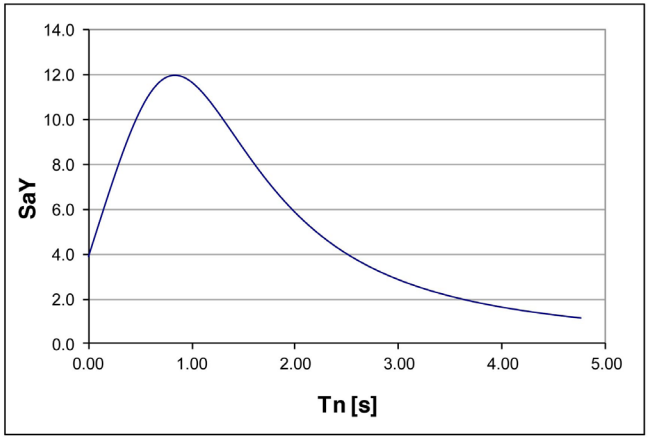

Estos gráficos corresponde al espectro de aceleraciones en el eje X e Y, que se ingresa a SAP2000, el cual toma la estructura con N grados de libertad dinámicos y transforma en N estructuras de un grado de libertad, que son los N modos de vibración de la estructura. Cada modo de vibrar posee un período distinto, y para cada modo, el programa considera la masa asignada y aplica la aceleración del grafico correspondiente para cada período de vibrar. Posteriormente, el programa superpone los efectos de cada modo de vibrar y los combina para tener una respuesta única, para cada dirección del sismo.

6.2 Modelos en SAP2000

A) Modelo de estructura de adobe con restricciones basales al desplazamiento y al giro, aplicando análisis sísmico con el Método Estático según NCh433.

C = 0,47 (Coeficiente sísmico).

Fsismica = Peso sísmico * C

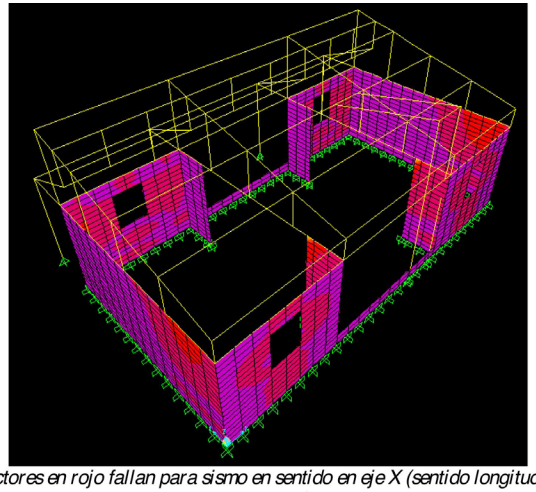

Fig.8 Sectores en rojo fallan para sismo en sentido en eje X (sentido longitudinal de la estructura).

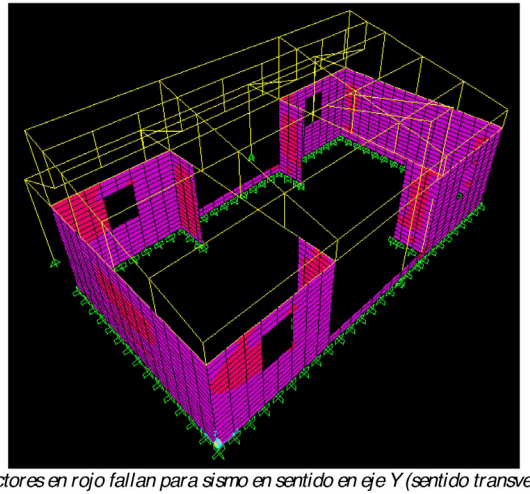

Fig.9 Sectores en rojo fallan para sismo en sentido en eje Y (sentido transversal de la estructura).

A.2) Caso 2: Estructura de adobe con geomalla con fundación corrida (análisis por método estático).

Tabla 2 "Tensiones internas por solicitaciones sísmicas y tensiones admisibles del adobe con geomalla"

EJE MURO	TENSIÓN SOLICITANTE MAX [Kgf/cm2]	TENSIÓN ADMISIBLE [Kgf/cm2]	RESISTENCIA
A	1.02	0.32	FALLA !!!
B	2.2	0.32	FALLA !!!
C	2.22	0.32	FALLA !!!
D	0.96	0.32	FALLA !!!
1	0.78	0.32	FALLA !!!
2	0.81	0.32	FALLA !!!

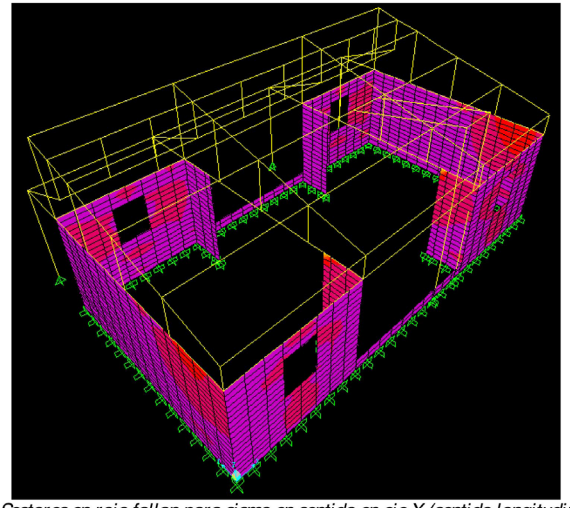

Fig.10 Sectores en rojo fallan para sismo en sentido en eje X (sentido longitudinal de la estructura).

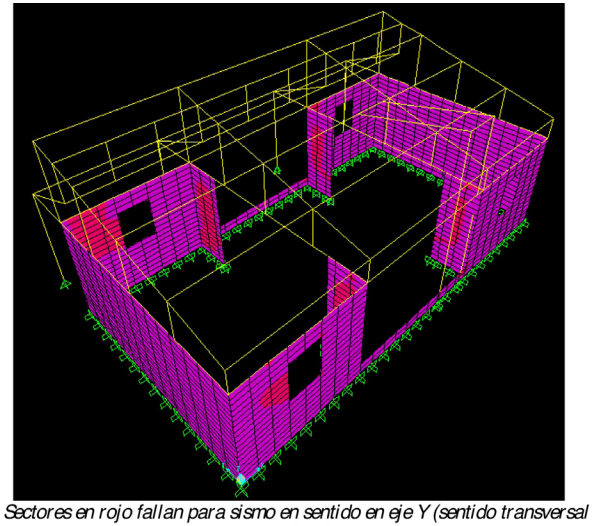

Fig.11 Sectores en rojo fallan para sismo en sentido en eje Y (sentido transversal de la estructura).

B) Modelo de estructura de adobe con restricciones basales al desplazamiento y al giro, aplicando análisis sísmico con el Método Modal Espectral según NCh433 y con el criterio de Ro=1.

Desplazamiento máximo en borde superior muro de adobe = 0.74 [cm].

B.1) Caso 1: Estructura de adobe sin geomalla con fundación corrida (análisis por método modal espectral).

Tabla 3 "Tensiones internas por solicitaciones sísmicas y tensiones admisibles del adobe sin geomalla"

EJE MURO	TENSIÓN SOLICITANTE MAX [Kgf/cm2]	TENSIÓN ADMISIBLE [Kgf/cm2]	RESISTENCIA
A	1.41	0.25	FALLA !!!
B	3.37	0.25	FALLA !!!
C	3.23	0.25	FALLA !!!
D	1.5	0.25	FALLA !!!
1	1.46	0.25	FALLA !!!
2	1.01	0.25	FALLA !!!

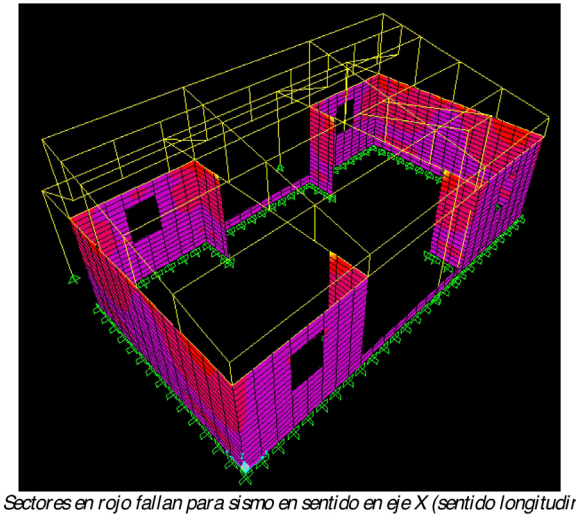

Fig.12 Sectores en rojo fallan para sismo en sentido en eje X (sentido longitudinal de la estructura).

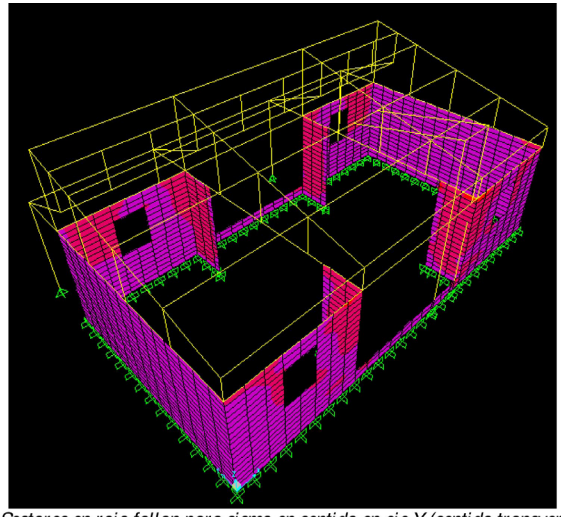

Fig.13 Sectores en rojo fallan para sismo en sentido en eje Y (sentido transversal de la estructura).

B.2) Caso 2: Estructura de adobe con geomalla con fundación corrida (análisis por método modal espectral).

Tabla 4 "Tensiones internas por solicitaciones sísmicas y tensiones admisibles del adobe con geomalla"

EJE MURO	TENSIÓN SOLICITANTE MAX [Kgf/cm2]	TENSIÓN ADMISIBLE [Kgf/cm2]	RESISTENCIA
A	1.41	0.32	FALLA !!!
B	3.37	0.32	FALLA !!!
C	3.23	0.32	FALLA !!!
D	1.5	0.32	FALLA !!!
1	1.46	0.32	FALLA !!!
2	1.01	0.32	FALLA !!!

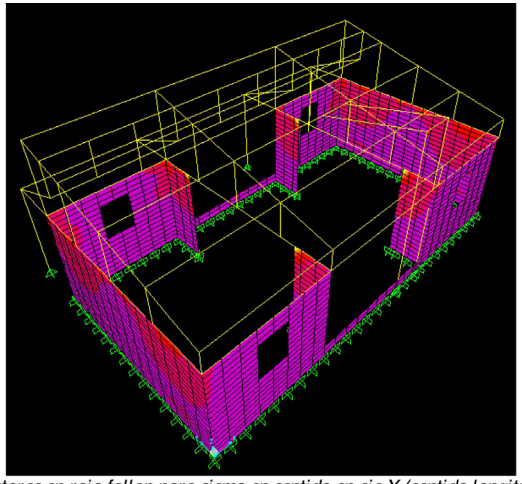

Fig.14 Sectores en rojo fallan para sismo en sentido en eje X (sentido longitudinal de la estructura).

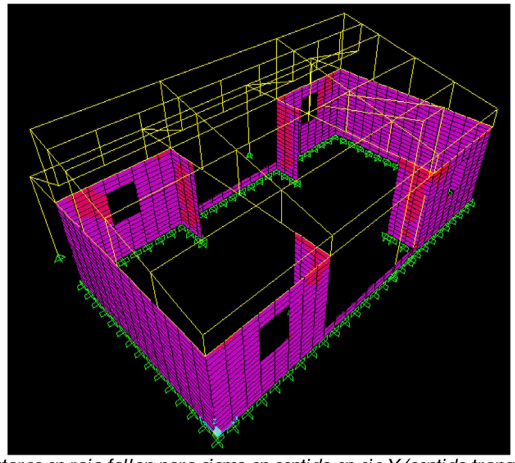

Fig.15 Sectores en rojo fallan para sismo en sentido en eje Y (sentido transversal de la estructura).

C) *Modelo de estructura de adobe con restricciones basales al giro y al desplazamiento vertical, con resortes para el desplazamiento horizontal, aplicando análisis sísmico con el Método Estático según NCh433.*

En cada caso, se debe verificar si el disipador trabaja o no. Se verifican estos 2 casos:

Caso 1) La Fuerza Sísmica no supera la fuerza de roce de la capa de fricción.

La capa de fricción genera una fuerza por reacción a la fuerza sísmica, de igual tamaño y sentido opuesto, hasta un tamaño igual al peso sobre la capa multiplicado por el coeficiente de roce del material utilizado como capa de fricción:

$$F_{fr} = F_v \times \mu$$

F_{fr}: Fuerza de fricción máxima. [Tonf].
F_v : Fuerza vertical sobre capa de fricción. [Tonf].
μ: Coeficiente de roce de la capa de fricción. [sin unidad].

Para que trabaje el disipador sísmico, necesariamente la fuerza sísmica debe superar la fuerza de roce de la capa de fricción, de manera tal que haya deslizamiento, con una fuerza total igual a la diferencia entre la fuerza sísmica y la fuerza por roce. Es por esto que se debe verificar en cual de los 2 casos se encuentra el caso a analizar:

Caso 1) La Fuerza Sísmica no supera la fuerza de roce de la capa de fricción.

La fuerza sísmica comienza y va en aumento, sin superar la fuerza de fricción, por lo cual no ocurre deslizamiento entre cimiento y sobrecimiento, por lo cual la estructura recibe por completo la fuerza sísmica. Es decir, *no trabaja el disipador sísmico*.

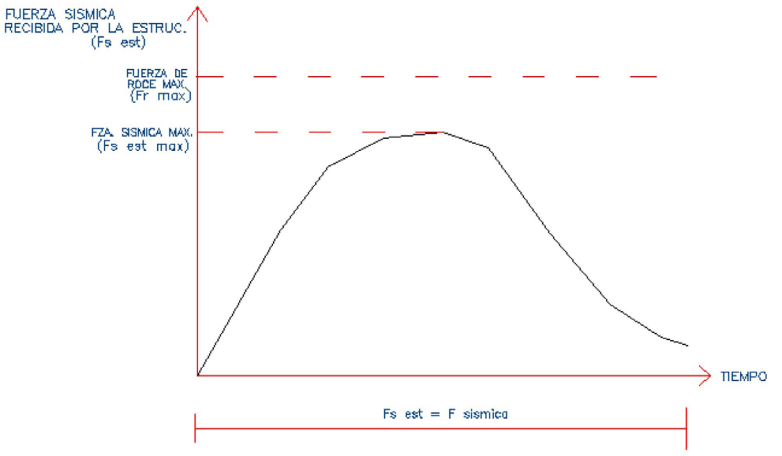

Fig.16 Gráfico representativo del caso 1: La acción de la fuerza sísmica es menor a la fuerza de roce de la capa de fricción (el disipador no alcanza a actuar).

Caso 2) La Fuerza Sísmica supera en un momento la fuerza de roce de la capa de fricción.

La fuerza sísmica comienza y va en aumento, y en un tramo de tiempo superar la fuerza de fricción, lo que provoca deslizamiento entre cimiento y sobrecimiento, por lo cual la estructura recibe en ese tramo la diferencia entre la fuerza sísmica y la fuerza de roce máxima. En este tramo *trabaja el disipador sísmico*.

Estudio Estructural María Luisa Santander N° 568 email: rbn.ingeniero@gmail.com

Calculo de tubos de acero para topes sísmicos basales

Considerando 18 topes sísmicos (según Fig. 4 del presente documento):

n	18		n° topes sismicos
Fs/n	0.778	[Tonf]	Fuerza sismica en cada tope
Fy	2400	[Kgf/cm2]	Fluencia acero
V	1080	[Kgf/cm2]	Resistencia al corte
A	0.72	[cm2]	Area de acero requerida

⇨ **18 tubos de acero de 1" de diámetro y 2 mm de espesor (área = 1,47 cm2).**

- *Calculo de espesor de gomas (que envuelven a los tubos de acero) para topes sísmicos basales*

n	18		n° topes sismicos
Fs/n	0.778	[Tonf]	Fuerza sismica en cada tope
h	5	[cm]	Altura goma
b	1	[cm]	Ancho goma
A	5	[cm2]	Seccion de goma a compresion
Rc	85	[Kgf/cm2]	Resistencia a la compresion (e=5cm)
C	155.5	[Kgf/cm2]	Compresion solicitante
e	9.149	[cm]	Espesor capa

⇨ **Envolver los tubos de acero con un espesor de 10 cm de goma.**

- *Calculo del resorte k de desplazamientos horizontales para el modelo en SAP2000.*

E	300	[Kgf/cm2]	Modulo de Elasticidad
Fs	0.778	[Tonf]	Fuerza sismica en goma
A	5	[cm2]	Seccion de goma a compresion
Ps	155.5	[Kgf/cm2]	Presión sobre goma
dr	0.518	%	Deformacion relativa al espesor
d	4.744	[cm]	Deformacion
K	163.9	[Kgf/cm]	Resorte modelo

C.1) Caso 3: Estructura de adobe sin geomalla con disipador sísmico (análisis por método estático).

Para este caso (equivalente para el caso sin y con geomalla) el disipador sísmico trabaja, por lo cual la fuerza sísmica disminuye en ambos sentidos. La situación más crítica de la estructura es el momento antes de que comience a trabajar el disipador sísmico, que es para una fuerza sísmica de 14 [Tonf]. Verificaremos las tensiones solicitantes sobre el adobe, con un modelo semejante al del caso A.1) de este informe, pero disminuyendo la fuerza sísmica de 16.95 [Tonf] a 14 [Tonf]. Es decir, *las fuerzas sísmicas sobre la estructura disminuyen un 17%.*

Desplazamiento máximo en borde superior muro de adobe = 0,73 [cm].

Tabla 5 "Tensiones internas por solicitaciones sísmicas y tensiones admisibles del adobe sin geomalla"

EJE MURO	TENSIÓN SOLICITANTE MAX [Kgf/cm2]	TENSIÓN ADMISIBLE [Kgf/cm2]	RESISTENCIA
A	0.85	0.25	FALLA !!!
B	1.83	0.25	FALLA !!!
C	1.84	0.25	FALLA !!!
D	0.8	0.25	FALLA !!!
1	0.65	0.25	FALLA !!!
2	0.68	0.25	FALLA !!!

Estudio Estructural *María Luisa Santander N° 568* *email: rbn.ingeniero@gmail.com*

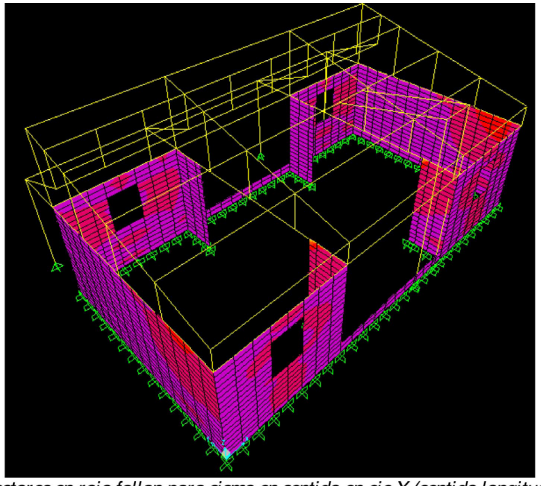

Fig.18 Sectores en rojo fallan para sismo en sentido en eje X (sentido longitudinal de la estructura).

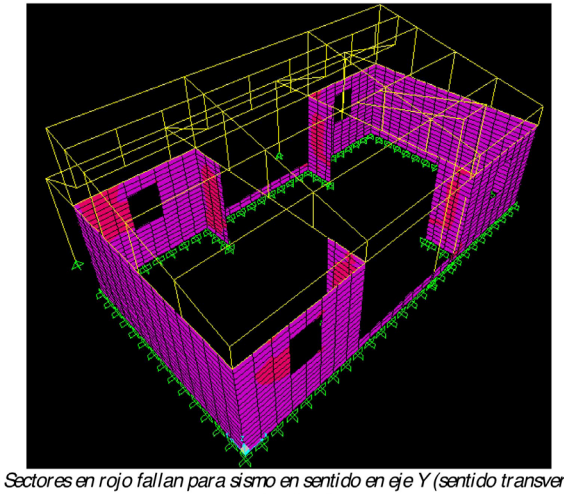

Fig.19 Sectores en rojo fallan para sismo en sentido en eje Y (sentido transversal de la estructura).

C.2) Caso 4: Estructura de adobe con geomalla con disipador sísmico (análisis por método estático).[d]

Tabla 6 "Tensiones internas por solicitaciones sísmicas y tensiones admisibles del adobe con geomalla"

EJE MURO	TENSIÓN SOLICITANTE MAX [Kgf/cm2]	TENSIÓN ADMISIBLE [Kgf/cm2]	RESISTENCIA
A	0.85	0.32	FALLA !!!
B	1.83	0.32	FALLA !!!
C	1.84	0.32	FALLA !!!
D	0.8	0.32	FALLA !!!
1	0.65	0.32	FALLA !!!
2	0.68	0.32	FALLA !!!

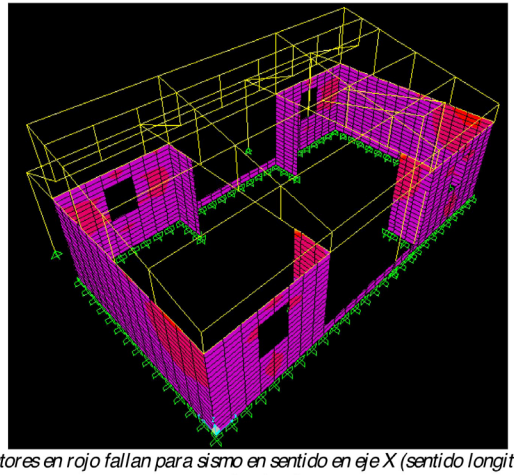

Fig.20 Sectores en rojo fallan para sismo en sentido en eje X (sentido longitudinal de la estructura).

Estudio Estructural *María Luisa Santander N° 568* *email: rbn.ingeniero@gmail.com*

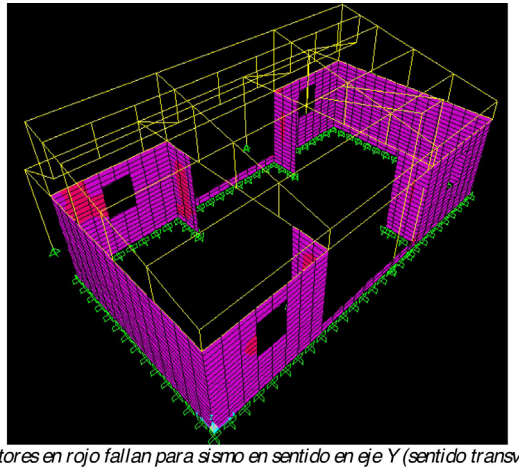

Fig.21 Sectores en rojo fallan para sismo en sentido en eje Y (sentido transversal de la estructura).

D) Modelo de estructura de adobe con restricciones basales al giro y al desplazamiento vertical, con resortes para el desplazamiento horizontal, aplicando análisis sísmico con el Método Modal Espectral según NCh433 y con el criterio de Ro=1.

- *Calculo de fuerza disipada y % de reducción por capa de fricción (para análisis por método modal espectral)*

P	69.3	[Tonf]	Peso sismico
CF	0.202		Coeficiente de friccion
Fd	14	[Tonf]	Fuerza max de capa de fricción
Qx	8.5	[Tonf]	Corte Sismico basal en X sin disipador
Qy	11.2	[Tonf]	Corte Sismico basal en Y sin disipador
QX	14	[Tonf]	Corte Sism. basal en X con disipador
QY	11.2	[Tonf]	Corte Sism. basal en Y con disipador
Rx	-5.499	[Tonf]	No alcanza a actuar el disipador
Rx	-0.647	%	No alcanza a actuar el disipador
Ry	-2.799	[Tonf]	No alcanza a actuar el disipador
Ry	-0.25	%	No alcanza a actuar el disipador

⇨ **Fuerza sísmica, en cada eje, es menor que la fuerza de roce del disipador, por lo cual no alcanzan a trabajar los disipadores sísmicos. Es decir, tenemos los mismos casos que los analizados en B.1) y B.2) del presente informe, por lo cual no es necesario repetir análisis de estos casos.**

- *Calculo de tubos de acero para topes sísmicos basales*

Considerando 18 topes sísmicos (según Fig. 4 del presente documento):

n	18		n° topes sismicos
Fs/n	0.778	[Tonf]	Fuerza sismica en cada tope
Fy	2400	[Kgf/cm2	Fluencia acero
V	1080	[Kgf/cm2	Resistencia al corte
A	0.72	[cm2]	Area de acero requerida

⇨ **18 tubos de acero de 1" de diámetro y 2 mm de espesor (área = 1,47 cm2).**

- *Calculo de espesor de gomas (que envuelven a los tubos de acero) para topes sísmicos basales*

n	18		n° topes sismicos
Fs/n	0.778	[Tonf]	Fuerza sismica en cada tope
h	5	[cm]	Altura goma
b	1	[cm]	Ancho goma
A	5	[cm2]	Seccion de goma a compresion
Rc	85	[Kgf/cm2	Resistencia a la compresion (e=5cm)
C	155.5	[Kgf/cm2	Compresion solicitante
e	9.149	[cm]	Espesor capa

⇨ **Envolver los tubos de acero con un espesor de 10 cm de goma.**

Estudio Estructural *María Luisa Santander N° 568* *email: rbn.ingeniero@gmail.com*

7.- CONCLUSIONES

- Existen diferencias entre el análisis sísmico realizado por el método estático y por el método modal espectral. La normativa chilena actual no establece un parámetro de Ro que permita el uso del análisis modal espectral en estructuras de adobe. En este informe se propuso utilizar un valor Ro = 1.
- El uso de aisladores sísmicos demuestra una disminución en las solicitaciones sísmicas en muros de adobe y en los desplazamientos dinámicos, exclusivamente en los casos en que la fuerza de roce por capa de fricción es menor que las solicitaciones sísmicas.
- Para garantizar que los disipadores sísmicos trabajen, es necesario contar con una capa de fricción que tenga el menor coeficiente de roce, que para este caso es de al menos de 0,12. Así la estructura alcanzará a tener deslizamiento entre sobrecimiento y cimiento, lo que se traduce en liberación de energía sísmica.
- Para el caso de análisis sísmico por Modal Espectral en estructura con disipadores, no es necesario realizar análisis ya que los disipadores sísmicos no trabajan (es igual que el caso sin disipador con y sin geomalla).
- Se propone usar 18 topes sísmicos basales, compuestos por tubos de acero de 1" de diámetro y 2mm de espesor. Estos elementos deben estar recubiertos por goma de neumático de 10 cm de espesor.
- Una vez comprobada la eficacia, a nivel de análisis teórico, se recomienda realizar una evaluación de costos comparativa que permita establecer la conveniencia de realizar viviendas en:

  -Estructura de adobe con fundación tradicional, con espesores de muros que permitan resistir solicitaciones sísmicas.
  -Estructura de adobe con fundación tradicional, con espesores de muros menores al utilizar geomalla, de manera tal que los elementos estructurales resistan solicitaciones sísmicas.
  -Estructura de adobe, con o sin geomalla, con disipador sísmico, que permita disminuir las solicitaciones sísmicas y sus efectos en los muros de adobe.

Febrero 2013.

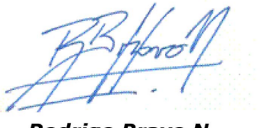

Rodrigo Bravo N
INGENIERO CIVIL ESTRUCTURAL
UNIVERSIDAD DE CHILE

Estudio Estructural *María Luisa Santander N° 568* *email: rbn.ingeniero@gmail.com*